Techno-economic Assessment of Algae Conversion to Biofuels

Ndumiso Sweet-man Duma

BSc Chemical Engineering (University of the Witwatersrand, Johannesburg)

This dissertation is submitted in partial fulfilment of the academic requirements of Master of Science in Chemical Engineering

School of Engineering

College of Agriculture, Engineering and Science

University of KwaZulu Natal

Howard College Campus

Durban, South Africa

March 2023

Supervisor: Prof Amir H. Mohammadi

Co-supervisor: Prof Manimagalay

Chetty

PREFACE

The research contained in this dissertation was completed by the candidate while based in the Discipline of Chemical Engineering, School of Engineering of the College of Agriculture, Engineering and Science, University of KwaZulu-Natal, Howard College Campus, Durban, South Africa. The research was financially funded by the University of Kwa-Zulu Natal: Strategic Funds and Fee Remission as well as supervisor's cost centre.

The contents of this work have not been submitted in any form to another university and, except where the work of others is acknowledged in the text, the results reported are due to investigations by the candidate.

_____

Signed: Prof Amir H. Mohammadi

Date: 7 July 2022

_____

Signed: Prof Manimagalay Chetty

Date: 7 July 2022

DECLARATION - PLAGIARISM

I, Ndumiso Sweet-man Duma, declare that:

1. The research reported in this thesis, except where otherwise indicated, is my original research.
2. This thesis has not been submitted for any degree or examination at any other university.
3. This thesis does not contain other persons' data, pictures, graphs or other information, unless specifically acknowledged as being sourced from other persons.
4. This thesis does not contain other persons' writing, unless specifically acknowledged as being sourced from other researchers. Where other written sources have been quoted, then:

a. Their words have been re-written, but the general information attributed to them has been referenced

b. Where their exact words have been used, then their writing has been placed in italics and inside quotation marks and referenced.

5. This thesis does not contain text, graphics or tables copied and pasted from the Internet, unless specifically acknowledged, and the source being detailed in the thesis and in the References sections.

Signed

……

ACKNOWLEDGEMENTS

I wish to express my utmost gratitude to the following individuals for whom this research would not have been possible:

- Prof Amir H. Mohammadi (supervisor) and Prof. Manimagalay Chetty (co-supervisor). Thank you for the guidance throughout the project, holding me accountable and motivating me when it seemed impossible. Your inputs have been invaluable throughout the project. Professor Amir H. Mohammadi for contributing towards funding my studies through his research grant.
- Mr. Preyothen Nayager (IT Supervisor), for his dedication every month, to activate Aspen Plus, which was the core software for this project.
- My parents, for their support for the duration of this research. This one is for you and the generations to come.
- My friends for their encouraging words every time I shared about the project. I appreciate your understanding when I could not show up at times, and your efforts to make my journey more enjoyable.
- Finally, and most importantly, I would like to acknowledge God, for whom I constantly drew strength.

ABSTRACT

One of the most promising biomasses for the production of biofuels is microalgae. This is because microalgae have a high growth rate and a high CO_2 capture ability when compared to other biomasses. Furthermore, biofuels produced from microalgae are deemed eco-friendly due to their low sulphur content, superior lubricating efficiency, and non-toxicity nature. As opposed to carbon-based fuels, biofuels are viable alternatives with the potential to meet the increasing demand for energy (Jafari & Zilouei, 2016). Because of its potential of being inexhaustible and a low-cost renewable energy carrier, biofuels research has increased (Akobi *et al*., 2016).

This research investigated the thermochemical and biochemical conversions for producing algal biofuels on a technical, economic, and environmental basis. The primary feed considered was wet algal biomass with a 20 wt%. Each investigated process was simulated on Aspen Plus ® v12. The processing units considered for the thermochemical conversion on Aspen Plus were hydrothermal liquefaction (HTL) for depolymerization, hydrotreating for removing contaminants by using H_2, and hydrocracking for removing contaminants by using a high-activity catalyst and H_2. The primary processing units considered for the biochemical conversion simulation included pre-treatment where dilute sulphuric acid is fed, conditioning with the assistance of dilute ammonia, fermentation with the aid of S. cerevisiae, purification, and finally, anaerobic digestion of the production of biogas.

The process properties for the investigated conversion methods were obtained through mass and energy balance calculations. The thermochemical conversion had a mass ratio of 0,39 and an energy efficiency of 47,45%. The biochemical conversion had a mass ratio of 0,98 and an energy efficiency of 73,11%.

The processes were both optimized using the Aspen Energy Analyzer (AEA). The thermochemical simulation had a 23,56% energy savings and a 17,3% carbon emissions reduction. The base case simulation for the biochemical conversion had no design alternatives to improve the heat exchanger network (HEN).

The fixed capital investment (FCI) for the thermochemical conversion was 18,3% lower than for the biochemical conversion. The internal rate of return (IRR) for the thermochemical method was 27,36% and 29,61% for the biochemical conversion. The economic evaluation was completed using the discounted cash flow analysis. Both the thermochemical and biochemical processes were profitable. The thermochemical method had a discounted payback period of 7,2 years (break-even point at seven years five months) and seven years (break-even point at six years ten months) for the biochemical method.

The environmental impacts of both processes were evaluated using OpenLCA. Typically, OpenLCA employs the cradle-to-gate approach. The assessment used the Agribalyse v3.0.1 database, and the LCIA method used was the ReCiPe 2016 midpoint (H) method and the CML-IA baseline method. The thermochemical method was the more sustainable method. The global warming impact was 42,25% less, the human toxicity was 41,46% less, and the freshwater aquatic ecotoxicity was 38,3% lower than the biochemical method. The investigation is summarized in the Table 0-1 below:

Table 0-1 : Summary of the processes studied.

	Thermochemical Conversion	Biochemical Conversion
Objective 1: Process synthesis		
Feed	Wet algal biomass with 20 wt%	Wet algal biomass with 20 wt%
Process sections	1. HTL (depolymerisation) 2. Hydrotreating (removal of contaminants with H_2) 3. Hydrocracking (removal of contaminants with high activity catalyst and H_2	1. Pre-treatment with dilute H_2SO_4 2. Conditioning with dilute NH_3 3. Fermentation with *S. cerevisiae* 4. Purification (via beer distillation column, rectification column, molecular sieve adsorption unit 5. Anaerobic digestion
Objective 2: Mass and energy balances		
Process simulation	Reactors: R-301, R-310Y, R-350Y used RYield model.	Reactors: R-101 (pre-treatment), R-102 (conditioning), R201 (seed growth), R-202 (fermentation) used RStoic, and R-501 (anaerobic digestor), R-502 (anaerobic digestor) used RYield
	Purification; T-301, T-320, T-330, T-350 used Radfrac model.	Purification; T-301, T-302, T-303 used Radfrac
Mass ratio	0,39	0,98
Energy intensity (MJ/kg)	-172,79	-70,68
Energy ratio	0,39	0,7286
Energy efficiency %	47,45	73,11
Objective 3: Heat integration		
Power requirement (MW)	2,54	0,73
Heat requirement (MW)	19,68	-68,1

Available energy saving (MW)	15 620	59 950
Available carbon emissions savings (kg/hr)	1 836	13 536
Energy saving %	23,56	No design alternatives from AEA to improve HEN.
Greenhouse gases reduction	17,3	No design alternatives from AEA to improve HEN.
Objective 4: Economic Analysis		
Equipment cost (R)	453 721 525,35	428 691 192,54
FCI (R)	2 367 160 592,35	2 898 328 107,68
TCI (R)	2 840 592 710,82	3 477 993 729,21
Manufacturing (R)	7 037 479 644,51	5 749 146 874,99
Revenue (R)	7 678 981 722,85	4 714 240 208,37
NPV(R)	1 344 301 784,18	2 223 983 071,52
IRR %	27,36	29,61
Objective 5: Life Cycle Assessment		
Global warming (kg CO_2 eq)	7,53	13,04
Human toxicity (kg 1,4-DB eq)	3,77	6,44
Fresh water aquatic ecotoxicity (kg 1,4-DB eq)	2,9	4,7

TABLE OF CONTENTS

LIST OF FIGURES

LIST OF TABLES

LIST OF ABBREVIATIONS

ACCE : Aspen Capital Cost Estimator

AD : Anaerobic Digestion

AEA : Aspen Energy Analyzer

ATP3 : Algae Testbed Public-Private Partnership

CBP : Consolidated Bioprocessing

CFD : Cash Flow Diagram

COM : Cost of Manufacturing

DAP : Diammonium Phosphate

DHA : Docosahexaenoic Acid

DMC : Direct Manufacturing Cost

EPA : Eicosapentaenoic Acid

FAME : Fatty Acid Methyl Esters

FCI : Fixed Capital Investment

FMC : Fixed Manufacturing Cost

FOC : Fixed Operating Costs

GE : General Expenses

HRT : Hydraulic Retention Time

HTL : Hydrothermal Liquefaction

IRR : Internal Rate of Return

LCA : Life Cycle Assessment

LCI : Life Cycle Inventory

LCIA : Life Cycle Impact Assessment

MARCS: Modified Accelerated Recovery Cost System

NPV : Net Present Value

NREL : National Renewable Energy Laboratory

ODP : Ozone Layer Depletion

OLR : Organic Loading Rate

PBR : Packed Bed Reactor

PMI : Process Mass Intensity

PSRK : Predictive SRK

PVR : Present Value Ratio

SARS : South African Revenue Services

SCWG : Supercritical Water Gasification

SHF : Separate Hydrolysis and Fermentation

SSCF : Simultaneous Saccharification and Co-Fermentation

SSF : Simultaneous Saccharification and Fermentation

TCI : Total Capital Investment

VOC : Variable Operating Cost

CHAPTER 1: INTRODUCTION

1.1 Background and motivation

There has been widespread concern over using fossil fuels in producing electricity as it has been the primary energy source for years. On a global scale, technologies that make energy continue to rely majorly on fossil fuels, and due to the demand, this resource is rapidly depleting. In contrast, its prices continue to rise (Jafari & Zilouei, 2016). This is not the only concern for governments, researchers, and industries. As energy consumption continues to grow, carbon dioxide emissions, which contribute to global warming, are increasing (Akobi *et al*., 2016). This is primarily due to the transportation and combustion of fossil fuels. The issues mentioned above necessitate research on alternative sources of clean energy.

Over the past decade, there has been extensive literature on the production of renewable fuels as an environmentally viable alternative source of renewable energy (Baêta *et al*., 2016). Biofuels are an excellent alternative because they do not contain sulphur and harmful gas emissions; they are abundant and can potentially reduce landfills. As a result, research initiatives aimed at producing carbon-neutral products and renewable research were developed. This included the research on first-generation renewable fuels, which are derived from terrestrial plants such as maize, sugarcane, rapeseed, and sugar beet. However, the research raised concerns about food market strain, water scarcity, and the demolition of forestry.

An increased interest in the utilization of lignocellulosic materials such as bagasse, wood, and herbaceous renewable organic matter for the production of biofuels due to their availability, renewability, affordability, and their richness in sugars arose. Lignocellulosic materials are converted through bioprocesses, which include fermentation and or anaerobic digestion (Waldron, 2014). However, these second-generation biofuels derived from lignocellulosic materials raised concerns over competing land use (Brennan & Owende, 2010).

Currently, research efforts have been placed on third-generation renewable fuels, which are explicitly deduced from microalgae. These biofuels are regarded as technically viable alternative energy sources as they do not require land, do not require large amounts of water, and cannot cause strain on the food market. Microalgae have simple growing requirements but can produce, over short periods, large amounts of lipids, carbohydrates, and proteins (Brennan & Owende, 2010).

This project aims to study the conversion of microalgae to renewable fuels such as biodiesel, bioethanol, and biogas on a comparative technical and economic basis. This will be done by conducting a thorough literature review on the investigated processes, thereby determining the

process configurations. Thereafter, process modelling, and simulation will be performed, including mass and energy balance calculations. Finally, a process economic analysis will be performed to determine the viability of producing biofuels from microalgae, and factors that significantly affect process economics will be chosen.

1.2 Problem statement

Fossil-based fuels have contributed significantly to global warming and played a considerable part in increasing greenhouse gas emissions. Plant-based fuels are widely accepted as an interesting fuel type that produces less net gas emission, which increase with an increase in population, demand, and transportation use. However, using third-generation biofuels with the primary feedstock being microalgae is even more advantageous because it does not take up land or require large amounts of water to grow. Literature on techno-economic assessments of algal biofuels exists but remains limited. Most studies either focus on one type of biofuel, mostly biodiesel (jet fuel), or bioethanol, but a comprehensive comparative assessment of the different processes is scarce.

1.3 Research Aims and Objectives

1.3.1 Research Aims

The overall aim of this study is to investigate whether the conversion of algae to biofuels such as biomethane, bioethanol, biohydrogen, and biodiesel is a sustainable and viable investment option. Furthermore, a comparative techno-economic and life cycle assessment for each process is aimed to be conducted.

1.3.2 Research Objectives

The primary objectives for the research are outlined below.

Objective 1: Determine the various processing routes to produce biofuels from algae through chemical, biochemical, and thermochemical conversion methods (see Chapter 2, Chapter 5.3).

Objective 2: Determine the process properties for each process (i.e., mass ratios, energy ratios, and energy efficiencies) through mass and energy balances (see Chapter 5.4).

Objective 3: Determine the maximum heat recovery of each process through heat integration (see Chapter 5.6).

Objective 4: Determine which biorefinery is economically feasible through equipment sizing and economic analysis for each process simulated (see Chapter 5.5, 5.7).

Objective 5: Determine the environmental impact of biofuels production from algae for each process using life cycle assessment methods (see Chapter 5.8).

Objective 6: Determine through techno-economic analyses the most sustainable solution for implementation (see Chapter 5.9).

1.4 Thesis Layout

Chapter 1 highlights the background of biofuels and algae and outlines the need for such an investigation. Furthermore, the aims and objectives of the research are detailed for the reader to have a comprehensive understanding of the investigation.

Chapter 2 focuses on the literature behind the production of biofuels from algae. The aim is to comprehensively review the available process options and highlight the potentials and concerns of each option. Operating conditions are highlighted, which will subsequently inform the project's process selection and simulation stage. Finally, the feedstock, algae, and biofuels produced are highlighted with their current potential and challenges.

Chapter 3 details the methodologies and materials used to model the different processes, perform economic assessments, and conduct a life cycle assessment for each process investigated.

Chapter 4 outlines in great length the details that will be used for the process designs for this research. The selection of suitable technology will be discussed. The process descriptions and detailed block flow diagrams will be touched on. Furthermore, the process simulation assumptions used to model the processes investigated will be highlighted.

Chapter 5 presents the investigation findings and discusses in length the conclusions of mass and energy balances, equipment sizing, heat integration, economic analysis, and life cycle assessment. Contrasts will be made for the investigated processes.

Chapter 6 final conclusions of the study will be drawn and recommendations for future work will be highlighted.

CHAPTER 2: LITERATURE REVIEW

2.1 Introduction

The purpose of this literature review is to survey previous studies on the production of biofuels using algae as the primary feedstock. Initially, this chapter highlights the current state of biofuels on a global scale, the energy mix in South Africa, and the accessibility of algae in South Africa. Following that, the research reviewed the different conversion methods for algal biofuels, such as thermochemical, biochemical, and chemical. Additionally, the study highlighted techno-economic assessments and life cycle analyses from past and most recent studies. Finally, the study discussed the challenges and prospects of algal biofuels. This chapter is critical as it highlights the literature data that will be imperative in the designing and evaluating stages of the study.

2.2 Biofuels

Renewable resources such as wind, solar, biomass, geothermal, and hydrogen play a considerable part in the future of global energy demand (Pandey, 2008). There are various reasons why renewable fuels are essential technologies in both industrialized and developing countries. These reasons include enhancing energy security, environmental benefits, energy access, and socioeconomic issues in developing countries (economic development of rural societies and rural diversification), foreign exchange savings (Pandey, 2008), the formation of local environmental and health benefits (Gheewala, Damen & Shi, 2013).

Biofuels are essential in combating climate change by offering an efficient solution to reducing carbon emissions (Neste, 2016). One of the most significant sources of carbon emission is traffic. With growing population numbers and economies advancing, more people will drive, thus increasing carbon emissions (Demırbas, 2017). Therefore, using clean, non-toxic renewable fuels will be a great solution to many environmental challenges that fossil-based fuels bring.

The global population is anticipated to rise to 8,5 billion in 2030, to 9,7 billion in 2050, and to further rise to 11,2 billion by 2100 (UnitedNations, 2019). Emerging markets are projected to have 4,4% GDP by 2023 (WorldBank, 2021), in 2042, they are projected to overtake advanced economies, and in 2050 will contribute about 60% of the global GDP (WorldBank, 2021). With both a growing global population and emerging economies, energy consumption is expected to increase substantially (Neste, 2016).

The utilization of residue and waste obtains the need for a circular economy as raw material for producing renewable fuels. Biofuels are, therefore, the solution to the intractable waste problems and the result of making the most out of valuable, scarce natural resources, which is essential for future generations (Neste, 2016).

Investing in biofuels has the potential to boost the growth of the economy. New job opportunities emanate in cultivating and harvesting renewable organic material, plant operation, transportation and handling, equipment manufacturers, and maintenance crews. In addition, farmers will experience a new source of income from energy by-products (Demırbas, 2017). The high global demand for energy, projected to rise by 84%, will help the economy of developing countries that choose to increase investment in biofuels (SGBiofuels, 2016).

2.3 Energy in South Africa

2.3.1 Coal in South Africa

Among 53 African nations, South Africa is the biggest consumer of energy. This is primarily due to the country's extensive and growing industrial sector and population. In 2012, about 31% of the total primary energy consumption was ascribed to South Africa (Pradhan & Mbohwa, 2014). Data from (Enerdata, 2019) shows that the industrial sector consumes 49% of the energy, while the residential sector consumes about 22%, and the services sector consumes the remaining 18%. This data has been consistent since 2016.

Coal remains a critical component of the South African energy mix strategy, with plans by the government to add 1,500 GW of coal-based power capability by 2030. This is estimated to contribute 59% to the nation's overall mix of energy sources. (Phillips, 2021) revealed that in 2020, South Africa topped the G20 coal reliance list with 86% of the nation's electricity derived from coal, which is relatively high compared to the global average of 34%. Although, it is essential to highlight that the government has plans to champion the advancement of carbon capture and storage technologies to address environmental responsibility by the sector (Fawthrop, 2019).

As the energy industry currently accounts for approximately 80% of all the greenhouse emissions generated by the nation, for which 50% results in liquid fuel production and electricity, the government also plans on aggressively focussing on renewable options such as wind and solar power for power generation. This will be achieved by adding 14,400 MW of wind power capabilities, 2,500 MW from hydropower, and 6,000 MW from solar power (Fawthrop, 2019). This is evident in the data for 2020, which showed a growth in wind and solar and a record fall of 4% in coal power (Phillips, 2021).

The tough challenge South Africa faces is that it is already struggling to decarbonise its coal-heavy grid (Phillips, 2021) successfully. Any further investment into coal generation could potentially lead to more problems.

2.3.2 Biofuels production in South Africa: Application and Advancement

In most Southern African countries, biofuels are in their early stage of development, with the most implementations at a small to medium scale. The commercialisation and widespread implementation of several well-developed biofuels technologies is hindered by a dearth of cost competitiveness with non-renewable fuels. South Africa is the most developed in Southern Africa regarding renewable fuel production with numerous small-scale biogas plants, industrial-scale plants utilising biogas, and strategies to establish biogas as a transport fuel (Herbert Lee Stafford *et al*., 2019). (Blanchard *et al*., 2011) prognosticated that the contribution of biofuels to South Africa's fuel supply would be at least 2 % by 2013, and according to (Pradhan & Mbohwa, 2014), the country's contribution to global production was much less than 0.01 %. Figure 2-1 shows a summary of manufacturing sites that have been licensed for biofuels production in South Africa.

Name	Type (feedstock)	Capacity (million litres/year)	Location
Arengo 316P. Ltd.	Ethanol (sorghum)	90	Cradock, Eastern Cape
Mabele Fuels	Ethanol (sorghum)	158	Bothaville, Free State
Ubuhle Renewable Energy	Ethanol (sugarcane)	50	Jozinin, KZN
E10 Petroleum Africa CC	Ethanol	4.2	Gauteng, Germiston
Rainbow Nation Renewable Fuels Ltd.	Biodiesel (soybean)	288	Port Elizabeth, Eastern Cape
Phyto Energy	Biodiesel (canola)	>500	Port Elizabeth, Eastern Cape
Exol Oil Refinery	Biodiesel (WVO)	12	Krugersdorp, Gauteng
Basfour 3528 P. Ltd.	Biodiesel (WVO)	50	Berlin, Eastern Cape

Figure 2-1: Biofuel production in South Africa (Pradhan & Mbohwa, 2014)

In 2014, South Africa implemented the biofuel blending mandates of 5% for biodiesel and 2-10% for bioethanol. Though this is possible for local companies to meet, (Arndt, Henley & Hartley, 2019) predicted that within ten years of the implemented blending mandates, the demand for bioethanol in South Africa would increase to 300 and 1400 million litres. Furthermore, if South Africa introduced the use of flexible-fuel cars, the desire for biofuel would expand to approximately 3 billion litres. In addition, South Africa’s commitment to the adopted mandatory blending mandates remains unclear as it has not commenced since its implementation (Herbert

Lee Stafford *et al*., 2019), (Henley & Fundira, 2019). However, according to (Brand South Africa, 2013), eight companies were granted provisional licences to produce biodiesel or bioethanol.

2.3 Algae in South Africa

Algae in Africa is an underexploited bioresource but is slowly growing its legs as countries like South Africa have initiated various algal biotechnology research groups. Additionally, the research in South Africa, in particular, has run numerous pilot-scale trials. The interest has led to the development of the Algae Testbed Public-Private Partnership (ATP3) for further large-scale trials (Jones, 2016).

Due to South Africa's optimal climate conditions, the country is capable of being a competitive producer of algal products. The government has plenty of non-arable lands which can be utilized for algal production (Jones, 2016). Unlike crops, which require a great deal of water supply, a negative for a water-scarce country, algae have lower requirements. Commercial aquaculture operations in South Africa annually grow over 2 000 tonnes of green seaweed Ulva. On an annual basis, over 6 000 tonnes of large brown algae, also known as kelps, are harvested for use in agriculture, aquaculture, and colloid extraction. In addition, there is active research in South Africa focusing on a variety of algae for drug discovery and the production of biofuels (Bolton & Victor, 2018).

2.4 Microalgal biomass as biofuel feedstock

Microalgae are one of the most critical renewable organic material sources, known to contain high proteins, carbohydrates, enzymes, minerals, and vitamins. In addition, microalgae lack lignin, making them suitable for various conversion technologies. When compared to terrestrial crops, microalgal biomass has the potential to generate 30-100 times more energy per hectare (Raheem *et al*., 2015). Moreover, some microalgal biomass contains considerably higher oil and protein concentrations than crops (Jones, 2016). Its versatility, simple cultivation system, and inexpensiveness have made microalgae be promising biomass that can replace fossil fuels completely (Raheem *et al*., 2015), (Tiwari & Kiran, 2018).

Microalgae are characterized by their rapid growth and typically grow on liquid media but are not dependent on a freshwater supply (Hossain *et al*., 2020). As a result of high photosynthetic levels and growth rates, they are used to produce a plethora of biofuels that are highly biodegradable and nontoxic (Tiwari & Kiran, 2018). The carbohydrate content present can be used to produce bioethanol, the algal oil can be employed to generate biodiesel, and the residual biomass can produce biomethane, fuel oil, or fuel gas. Apart from its ability to produce diverse biofuels, microalgae can produce various value-adds such as therapeutics, protein supplements, biocontrol agents, eicosapentaenoic acid (EPA), fertilizers, nutraceuticals, animal feed, docosahexaenoic acid (DHA), therapeutics, and aquaculture.

The utilisation of microalgae can also reduce greenhouse gas emissions considerably because they have high carbon dioxide sequestering efficacy or carbon assimilating efficiency (Chen *et al*., 2015), making carbon capturing and storage possible while microalgae grow and are harvested. Another positive of using microalgae for biofuels production is that it does not require arable land to grow, unlike agricultural crops (Hossain *et al*., 2020). As microalgae are readily adaptable, it can be facilitated through genetic or metabolic engineering or synthetic biology to generate high yields (Tiwari & Kiran, 2018).

2.5 Biofuels derived from microalgae

2.5.1 Biodiesel

Biodiesel is a non-poisonous biodegradable alternative fuel to petrodiesel attained from renewable resources such as algae, soybean, yellow grease, jatropha, canola, and Pongamia (Papavinasam, 2014). It has a comparable engine performance and combustion properties similar to petroleum diesel fuel (Viswanathan, 2017), but can also reduce sulphur and particulate matter emissions (Tiwari & Kiran, 2018).

There are two ways biodiesel from algae can be produced, either through direct transesterification or a two-step process of initially extracting lipids and then later transesterification. Direct transesterification is considered the faster and more cost-effective option of the two methods. However, for the effective production of biodiesel, microalgae strains with high lipid content and growth rate have to be selected (Tiwari & Kiran, 2018).

2.5.2 Biomethane

Biomethane or biogas production occurs when organic matter is converted through anaerobic digestion. Through anaerobic digestion, biogas is produced, which contains 50-70 % methane, 30-40% carbon dioxide, and a trace of other impurities such as hydrogen sulphide, ammonia, siloxanes, and water vapour (Ardolino *et al*., 2021). The biogas produced then has to be upgraded using techniques such as membrane separation, chemical absorption, or water scrubbing, for which (Ardolino *et al*., 2021) concluded that membrane separation has the best performance. Biomethane is flexible and an easy-to-store fuel that can be employed in processes that require natural gas without altering any settings on equipment (Urban, 2013). Nearly all types of renewable sources can be used to produce biomethane, even wet biomass, which is not used for most renewable fuels (Molino, Iovane & Migliori, 2016).

Contrary to contemporary microalgal biodiesel production, which requires the selection of high lipid-containing strains, for biomethane production, any microalgal species or residual biomass is utilized (Xin *et al*., 2016). A study by (Ramos-Suárez & Carreras, 2014) evaluated the use of Scenedesmus spp., residual biomass, for biomethane production. The study found that residual biomass produces a higher biomethane yield than raw biomass. The production of biomethane

from microalgal biomass is of interest because of its efficiency. Algal biomass production per hectare is approximated to be 5-30 times higher than that of terrestrial crops (Connelly, 2014).

2.5.3 Biohydrogen

Biohydrogen is a carbon-free fuel that is considered a valuable alternative energy carrier as it can combat pressing emissions from fossil fuels. In addition, this fuel type has attractive ecological features and powerful energy explosion (Show, Yan & Lee, 2019). Though biohydrogen can be derived from biogas through anaerobic digestion, the most economical method for its production is through the gasification of microalgae (Show, Yan & Lee, 2019). However, (Saratale *et al*., 2019) pointed out that fermentation is the most sustainable and environmentally friendly method. The study further suggested that its efficiency requires enhancement, and the production costs require a significant reduction. The cost of fermentation can be reduced by utilizing third-generation biomass such as microalgae.

2.5.4 Biosyngas

Biosyngas is derived from the gasification of microalgae in the presence of oxygen, air, or water vapour. The resulting products include hydrogen, methane, water, carbon dioxide, ashes, and other hydrocarbons (Tiwari & Kiran, 2018). Biosyngas is a flexible product as it can be used in energy production and as a transportation fuel when upgraded to biomethane (Labriet, 2013).

2.5.5 Bioethanol

Bioethanol is a valuable alternative to fossil fuel-derived transportation fuel. Though it can be generated from sugar and starch-containing plants, much research is focused on its production from its forestry and agricultural waste (Parachin, Hahn-Hägerdal & Bettiga, 2019). Typically, bioethanol production occurs in four processes; (1) pre-treatment and separation of cellulose, hemicellulose, and lignin, (2) production of fermentable sugars through hydrolysis, (3) conversion of sugars to ethanol through anaerobic fermentation, (4) the separation and purification of ethanol through distillation (Anyanwu *et al*., 2018).

Cellulose and hemicellulose contained in microalgae can be hydrolysed with new technologies to produce sugars, ultimately forming bioethanol. Using microalgae as a feedstock is beneficial as microalgal cells contain considerable amounts of polysaccharides. Like other biofuels, bioethanol production from microalgae is promising but needs more development for a full-scale production system (Tiwari & Kiran, 2018).

2.6 Elemental composition and Biochemistry of Algae

Algae are described as organisms that are unicellular, microscopic, and photosynthetically grown. These organisms consume sunlight, water, and carbon dioxide to generate considerable quantities of proteins, lipids, and carbohydrates in a short stretch of time. Generally, algae are found in a

wide range of aquatic systems (López-Gómez & Pérez-Rivero, 2019), such as oceans, lakes, water streams, or freshwater. Still, they can also be found in unexpected places like tree trunks, hot springs, and animal fur.

Algae is categorized into microalgae (filamentous) and microalgae (phytoplankton). Macroalgae are further classified into red, green, and brown seaweed. On the other hand, microalgae are classified into diatom, green algae, golden algae, and blue algae. Typically, algal biomass consists of 20-50% protein, 17-57% carbohydrate, and 9.5-42% lipid (Raheem *et al*., 2015). The elemental and composition compositions and higher heating values of some of the most common microalgae are summarized in Figure 2-2 (Chen *et al*., 2015).

Materials	Elemental analysis (wt%)					Composition (dry-ash-free, wt%)				HHV (MJ kg^{-1})
	C	H	N	O	S	Protein	Lipid	Carbohydrate	Others[c]	
Chlorella	50.20	7.25	9.30	33.2						21.20
Chlorella vulgaris[a]	45.80	5.60	4.60	38.70		29.00	49.50	19.70	1.8	18.40
Chlorella vulgaris[b]	53.8	7.72	1.1	37.0		6.00	43.00	51.00	0	24.00
Chlorella vulgaris	42.51	6.77	6.64	27.95		41.51	15.67	20.99	21.83	16.80
Chlorella vulgaris	43.90	6.20	6.70	43.30		54.90	15.50		29.6	18.00
Chlorella vulgaris residue	45.04	6.88	9.79	29.42		61.24	5.71	20.34	12.71	19.44
Chlorella sorokiniana CY1 residue						18.81	9.9	35.67	35.62	20.24
Chlamydomonas sp. JSC4 residue						12.18	6.85	35.7	45.27	17.41
Chlamydomonas reinhardtii (wild)	52.00	7.40	10.70	29.80		47.40	18.10		34.5	23.00
Chlamydomonas reinhardtii CW15+	50.20	7.30	11.10	31.40		45.70	22.40		31.9	22.00
Dunaliella tertiolecta	39.00	5.37	1.99	53.2	0.62	61.32	2.87	21.69	14.12	14.24
Hapalosiphon sp.	47.94	7.44	6.45	37.58	0.58					14.75[d]
Nannocloropsis oculata	39.90	5.50	6.20			39.00	20.00	17.00	24	16.80
Nannochloropsis oceanica	50.06	7.46	7.54	34.47	0.47	19.1	24.8	22.7	33.4	21.46
Nannochloropsis oceanica residue	45.24	6.55	11.07	36.58	0.56					18.17
Spirulinaplatensis	46.16	7.14	10.56	35.44	0.74	48.36	13.30	30.21	8.13	20.52
Spirulinaplatensis	45.70	7.71	11.26	25.69	0.75					20.46
Scenedesmus obliquus CNW-N	37.37	5.80	6.82	50.02		30.38	4.66	13.41	51.55	16.10

Figure 2-2: Elemental compositions of common microalgae (Chen *et al*., 2015).

2.7 Microalgae cultivation

Microalgal cultivation is a considerable element that influences lipid production yield, and there are three significant metabolic ways microalgae are cultivated. These include photoautotrophic cultivation, mixotrophic cultivation, and heterotrophic cultivation. Autotrophic cultivation involves closed photobioreactors and open ponds, while heterotrophic cultivation involves fermenters, and the mixotrophic cultivation gains energy by photosynthesis (Rajesh Banu *et al*., 2020).

2.7.1 Photoautotrophic cultivation

2.7.1.1 Open ponds

Open ponds have various shapes and forms and are commonly used in microalgae cultivation. Examples of industrial applications include raceway ponds, circular ponds tanks, and big shallow ponds (Özçimen, Gülyurt & İnan, 2013). The use of open ponds has unneglectable disadvantages. First, the microalgae productivity could be affected by evaporation and contaminants such as bacteria, protozoa, or other microalgae since the pond is open (Veillette *et al*., 2012). Open ponds

are a function of the local climate as the ponds lack control. These ponds are also limited by growth parameters such as light intensity, temperature, dissolved O_2 concentration, and pH. Finally, the construction, maintenance, and operation costs of open ponds are less than photobioreactors and are simpler (Özçimen, Gülyurt & İnan, 2013).

2.7.1.2 Photobioreactors

Photobioreactors are continuous culture systems that can be a flat plate, bubble column, tubular, airlift, and stirred tank. These systems have the potential to reach up to 6,7 g/L of microalgae concentration in fresh or seawater. The advantages of utilizing a photobioreactor are that it can achieve a higher harvesting efficiency, has flexible systems, prevents contamination (Özçimen, Gülyurt & İnan, 2013), has good control on culture parameters such as pH, CO_2 concentration, and a temperature is, a water-saving option (Saad *et al*., 2019). However, photobioreactors have higher capital costs, approximately ten times more than open ponds. Additionally, photobioreactors have overheating problems, biological pollution, scale-up difficulty, and oxygen accumulation.

Other options that have been studied and proved profitable are using both open ponds and photobioreactors. In this process, the production of microalgae is firstly managed in a photobioreactor under regulated temperatures. Secondly, the microalgae are transferred into an open pond for five days (Veillette *et al*., 2012). Flat-plate photobioreactors are the preferred type as they offer high cell density, have low energy consumption, reduction of oxygen increases, high mass transfer capacity, and high photosynthetic efficiency (Özçimen, Gülyurt & İnan, 2013).

2.7.2 Heterotrophic cultivation

Heterotrophic cultivation uses fermenters to generate heterotrophic microalgae. During the conversion, organic carbon sources such as glucose, glycerol, fructose, acetic acid, and galactose acetate are used. The advantage of using these bioreactors is that they can reach high biomass concentrations without rheological challenges. However, this method remains uneconomical (Veillette *et al*., 2012).

2.7.3 Mixotrophic cultivation

Mixotrophic cultivation is the cultivation of microalgae under both photoautotrophic and heterotrophic conditions. This method has a higher growth rate than photoautotrophic and heterotrophic microalgae, and a higher biomass productivity can be expected. However, this technique is uncompetitive to photoautotrophic due to the costs of organic substrates (Zabed *et al*., 2020).

2.8 Microalgae harvesting

Biomass harvesting and processing usually take place during the cultivation period. There are various methods to harvest and dry microalgae. The main techniques include gravity sedimentation, filtration, centrifugation, flocculation, screening, electrophoresis, and flotation (Zabed *et al.*, 2020). In designing an economical bioprocess, selecting a suitable method is vital as harvesting accounts for about 20 to 30% of the total cost for producing biofuels. The harvesting costs make algal cultivation ineffective on a large scale. Above being an expensive process, harvesting is also energy-intensive. This is largely attributed to the low density of algal cells in the growth medium and the cells being in a suspension state (Veeramuthu & Ngamcharussrivichai, 2021).

Sedimentation in the context of microalgae from ponds involves the use of gravity force to settle suspended solids or particles in a fluid. This method is economical and straightforward, but the solids suspended in the fluid have to be incompressible, which is contrary to the nature of *Chlorella sp* and *Scenedesmus sp*. Nevertheless, sedimentation is a viable option if it is improved with flocculation (Özçimen, Gülyurt & İnan, 2013).

Another method used for harvesting microalgae is flocculation. The commonly used flocculants in this method are $FeCl_3$, $Fe_2(SO_4)_3$, and $Al_2(SO_4)_3$. The use of flocculants on negatively charged microalgae incites coagulation. Filtration is one of the most aggressive methods to collect algae. Examples of the types of filtrations include dead-end, pressure filter, ultrafiltration, microfiltration, and vacuum filter. This method is uneconomical, especially for microalgae (Özçimen, Gülyurt & İnan, 2013), and the flocculants can contaminate the slurry. On the other hand, it has a higher efficiency than most of the mentioned methods. Figure 2-3 depicts a summary of the advantages and disadvantages of some of the most common harvesting techniques.

Technique	Pros	Cons
Filtration	Low cost, water reuse	Slow, membrane fouling and clogging, limited volume, cell damage
Centrifugation	Rapid, easy, efficient	Very high energy input
Gravity sedimentation	Low cost, potential for water recycling	Slow process, product deterioration, separation depends on cell density
Chemical flocculation	Low cost, low cell damage	Biomass toxicity, no water reuse, inefficient, potential to remove lipids, produces large quantity of sludgethat increases the difficulty to dehydrate the biomass
Dissolved air flotation (DAF)	Low cost, easy application at large scale	Needs flocculants, water reuse and product extraction may be negatively affected
Foam fractionation	Small footprint, no addition of chemicals	Low yield due to inefficient floatation
Ozone fractionation	Small footprint, cell disruption required for extraction occurs simultaneously	Ozone generation is expensive, Loss product
Microstrainers	Easy operation, low cost construction, high filtration ratios	Strongly cell concentration dependant, smaller cells may undergo incomplete removal, difficulty and handling solids fluctuations
Bio-flocculation	High efficiency, no damage to cells	No water reuse, higher energy input than other flocculants
Electrolytic flocculation	High efficiency	High energy input (up to 16KWh/kg biomass), increased temp may damage system, fouling of cathodes
Cross-flow membrane	Water reuse, removal of pathogens, protozoa	Membrane fouling, requirement for frequent use
Submerged membrane microfiltration	Low cost, less shear stress, less membrane fouling than conventional cross-flow	Membrane fouling, scale up potentially has problems

Figure 2-3: Pros and cons of microalgal harvesting techniques (Rawat *et al.*, 2013).

2.9 Extraction technologies

Algal lipids can be classified into polar lipids and non-polar lipids. Polar lipids include phospholipids and glycolipids. Non-polar lipids, eicosanoids, acylglycerols, hydrocarbons, waxes, and fatty acids. The extraction methods for lipids are classified as mechanical, physical, chemical, and enzymatic. Mechanical methods include (i) Homogeniser-high-pressure, High-speed cavitation, Hydrodynamic microfluidiser, Ultrasonic, and (ii) Bead Mill. Physical methods include (i) Decompression, (ii) Microwave, (iii) Freeze-drying, and (iv) Thermolysis. Chemical methods include (i) Solvent (ii) Chelating agent (iii) Supercritical CO_2 (iv) Detergent (v) Antibiotics. Enzymatic methods include (i) Lytic, (ii) Autolysis (iii) Phage. A comparison of some of the common extraction methods used in microalgal biorefinery has been summarised in Figure 2-4.

Sl. No	Method	Lipid extraction efficiency	Efficiency rating[a]	Cost involved	Energy requirement	Remarks
1	Use of organic solvents such as chloro-form/methanol, hexane, and ether	Extraction efficiency depends on the species used, volume of the extractor, reaction time, sample volume, moisture content, types of lipids present, and in case of solvent-based methods, choice of the solvents, solvent ratios, etc	Moderate	High due to the use of solvents. Re-use may help save some costs but again an energy-intensive process	Energy intensive	Fire, health, and environmental hazards; regulatory issues
2	Pressurized solvent extraction		High	High because of cumulative costs incurred by use of solvent as well as use of pressurized nitrogen	Energy intensive	Fire, health, and environmental hazards; regulatory issues
3	Isotonic extraction		Moderate-high	High cost of the solvents as the solvents used are synthetic "green" non-volatile solvents	Energy intensive	Less hazardous
4	Supercritical CO_2		High	High cost	Energy-intensive due to use of high pressure	Environmental and safety issues
5	Expeller press		Low-moderate	High cost	Energy intensive	Heat generation and possible damage of the compounds
6	Bead beating		Moderate	Cost-effective	Energy intensive. Reactor should be suitably designed to reduce energy inputs	Difficult to scale up

7	Microwave	Very high	Initial investment and maintenance costs high	Energy demand is too high (also requires energy for cooling)	Easy to scale up, but yet to be standardized at a commercial level
8	Sonication method	High	Initial investment and maintenance costs high	Energy intensive (requires energy for both sonication and cooling)	Poor product quality due to the damage during the process
9	Osmotic shock method	Moderate-high	Low-cost method	Less energy	Requires longer treatment time (not <48 h)
10	Electroporation	Very high	Initial investment and maintenance costs high, but operates at comparatively lower costs	Less energy	Appears promising but detailed pilot-scale studies have to be carried out

Figure 2-4: Comparison of microalgal extraction methods (Medipally *et al*., 2015).

2.10 Conversion technologies for microalgal biofuels production

The production of biofuels such as biodiesel, biohydrogen, bioethanol, and biomethane from photosynthetically grown microalgal biomass can occur through chemical, biochemical, or thermochemical conversion processes. To ensure that biofuel production is economically feasible and resource-efficient, selecting the most suitable conversion technology is essential (Raheem *et al*., 2015).

2.10.1 Thermochemical conversion technologies

The thermal decomposition of organic matter of biomass to produce biofuels is known as the thermochemical conversion. Typically, the biomass is firstly converted to synthetic gas, which is ultimately synthesised into the desired biofuels (Basu, 2018). The conversion can be through gasification, liquefaction, torrefaction (carbonisation), pyrolysis, or direct combustion, as shown in Figure 2-5. For a successful conversion, the biomass is heated with air, steam, or oxygen under controlled conditions.

Thermochemical conversion is the most studied method and is more preferred over chemical and biochemical processes as it is a more straightforward route (Raheem *et al*., 2015). In addition, the conversion requires no additions of chemicals and converts a range of biomass feedstock with a shorter biofuel producing time (Chen *et al*., 2015). A comparison between the various methods is shown in Figure 2-6.

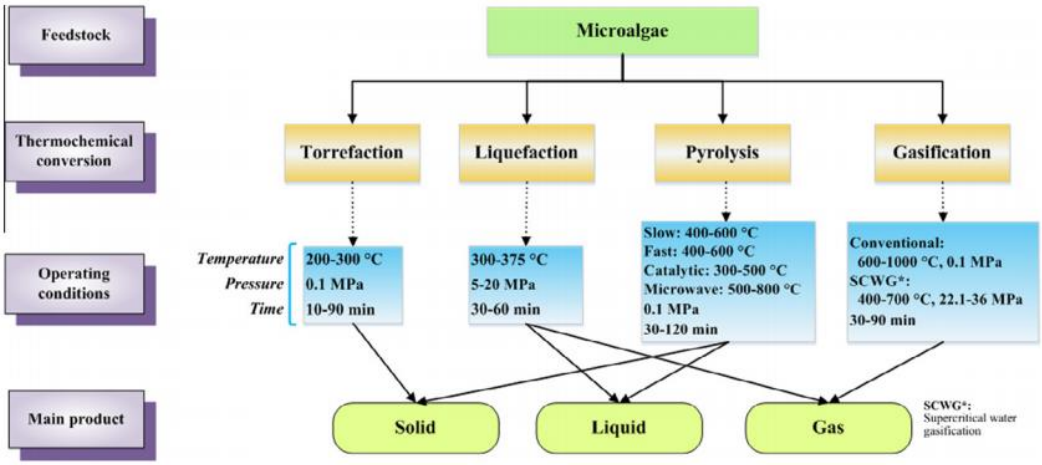

Figure 2-5: A summary of different thermochemical methods for the conversion of microalgae (Chen *et al*., 2021).

Conversion process	Microalgae	Production	Temperature (°C)	Pressure (MPa)	Liquid		Gas	Solid
					Content (% dry wt.)	HHV ($MJ\,kg^{-1}$)	Content (% dry wt.)	Content (% dry wt.)
Gasification	*Spirulina*	N/A	1000	0.101	–	–	64	–
Thermochemical liquefaction	*Botryococcus braunii*	N/A	300	3	64	45.9	–	–
Thermochemical liquefaction	*Dunaliella tertiolecta*	N/A	300	3	42	34.9	–	–
Pyrolysis	*Chlorella prothothecoides*	Heterotrophic	450	0.101	57.9	41	32	10.1
Pyrolysis	*Chlorella prothothecoides*	Phototrophic	450	0.101	16.6	30	–	–
Pyrolysis	*Chlorella prothothecoides*	Phototrophic	500	0.101	18	30	–	–
Pyrolysis	*Chlorella prothothecoides*	N/A	502	0.101	55.3	39.7	36.3	8.4
Pyrolysis	*Microcystis aeruginosa*	Phototrophic	500	0.101	24	29	–	–

Figure 2-6: A comparison between thermochemical conversion methods (Brennan & Owende, 2010).

2.10.1.1 Gasification

The gasification process involves converting organic or fossil-based carbonaceous materials into synthetic gas or clean fuel gases. The conversion occurs at high temperatures (1073,15-1273,15 K). The chemical reactions involved in converting carbonaceous materials entail different processes such as drying, pyrolysis, combustion, and reduction (Raheem *et al*., 2015). Gasification performs best when the moisture content of the biomass is not more than 15%. However, moisture content of up to 40% is acceptable. The higher the moisture content, the decrease in efficiency of the gasifier. There are two branches of the gasification technology of

microalgae that is, conventional and supercritical water gasification (Chen *et al*., 2015). A schematic representation of microalgae gasification is shown in Figure 2-7.

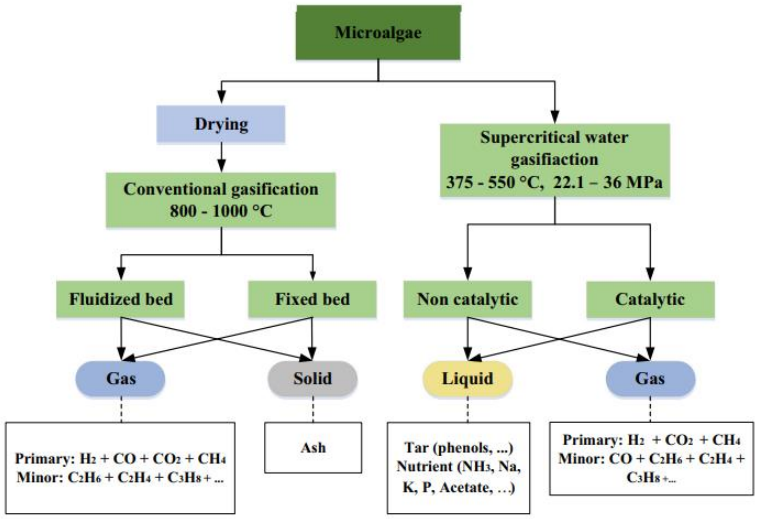

Figure 2-7: A schematic diagram of microalgae gasification (Chen *et al*., 2015)

2.10.1.1 (a) Conventional gasification

Conventional gasification involves the conversion of dry microalgae in the presence of an oxidiser such as oxygen, air, steam or water. The conversion occurs in a partial oxidation environment at a pressure range of 1-10 bar and a temperature range of 1073,15-1273,15 K. The microalgae in a gasifier undergo various reactions, including drying or dehydration, pyrolysis or devolitisation, oxidation or combustion, and reduction or gasification. Other reactions involved in the conversion include the homogenous and heterogeneous water gas shift, methanation reactions, and the Boudouard reaction (Chen *et al*., 2015). The disadvantage of this method is the high heating energy requirement due to the high latent heat of water vaporisation in the drying process. Though the process has been commercialised, it has low thermal efficiency.

2.10.1.1(b) Supercritical water gasification (SCWG)

Supercritical water gasification converts microalgae to gas products above the critical point of water (647,15 K and 221 bar) without drying. The method involves using water as a reaction medium while aiming to break the C-C bonds to produce gases such as methane and hydrogen. This is a promising process in the production of gas fuels using microalgae as it has a higher thermal efficiency (Chen *et al*., 2015). The process is operated at 673,15-773,15 K and 240-360 bar, where catalysts may be utilised. The method produces higher gas yields, energy recoveries, and carbon yields when more elevated temperatures, higher water densities, and longer holding times are used. In addition, the use of homogeneous catalysts (such as NaOH and KOH) or

heterogeneous) has the potential to accelerate the microalgae reaction rates and control the ultimate product distribution (Chen *et al*., 2015). A summary of various studies that have been undertaken for microalgae gasification is shown in Figure 2-8.

Microalgae	Operation conditions			Production	
	Reactor	Temperature (°C)	Agent gas	Performance	Primarily gases composition (vol%)
Nannochloropsis sp. residue	Fixed bed	850	Nitrogen, 650 ml min^{-1}	HHV of gases = 38.3 MJ/kg; 140% T.E.[a]	H_2, CO, CO_2, CH_4, totally 85%
Nannochloropsis gaditana	TGA[b]	850	Ar/steam, Ar: 200 ml min^{-1}		H_2 (46), CO (33), CO_2 (12), CH_4 (<5)
Nannochloropsis oculata residue	Fixed bed	600–850	Steam	42–70% C.C.[c]	H_2 (40–52), CO (<6), CH_4 (~10), CO_2 (32–38)
Spirulina platensis (torrefied pellet)	Fluidized bed	800	Air/steam	Syngas LHV = 5–8 MJ/kg	H_2 (20), CO (35), CO_2 (40), CH_4 (<4) (ER[e] = 0.4)
Spirulina platensis[d] (torrefied pellet)	Fluidized bed	800	Air/steam	Higher MR[f] with higher CO, but fewer H_2	H_2 (19), CO (40), CO_2 (25), CH_4 (8) (ER = 0.4, MR = 7:3)
Spirulina	Fluidized bed	850–1000	O_2: steam = 0.39 ml: 0.25 g (min^{-1})	93–103% C.C.	H_2 (35–48), CO (10–18), CO_2 (31–36), CH_4 (9–11)
Tetraselmis sp.[g]	Fluidized bed	820–885	Air/steam, air: 35 L min^{-1}		H_2 (9), CO (12), CO_2 (13), CH_4 (<2) (at 860 °C)

Figure 2-8: A summary of microalgae gasification investigations at different operating conditions (Chen *et al*., 2015).

2.10.1.2 Pyrolysis

Pyrolysis is another thermochemical process that entails microalgae's heating and thermal decomposition that produces renewable bio-oil, non-condensable gases, and biochar. It is wildly accepted as one of the hottest thermochemical conversion processes and involves thermal cracking (Adeniyi, Azimov & Burluka, 2018). As shown in Figure 2-9, the process occurs in the absence of oxygen or air, between the temperature range 473,15-1023,15 K (Raheem *et al*., 2015) and is normally operated at 1,01 bar. Bio-oil produced from microalgae is more stable than those produced from lignocellulosic biomass and contains compounds such as nitrogenous species and linear hydrocarbons (Raheem *et al*., 2015), (Chen *et al*., 2015).

The yield for this method depends on the microalgae properties, operating conditions, and reaction type. The process would have to be operated at moderate temperatures of 673,15-773,15 K and short residence times of 2-3s (Chen *et al*., 2015) to favour liquid production. At higher temperatures, the gas product yield is higher. When considering the high ash content, pyrolysis is the easiest conversion method. However, the liquid fuel produced would require improvement to address its technical challenges such as viscosity, acidity, and stability (Adeniyi, Azimov & Burluka, 2018).

Microalgae pyrolysis can be categorised into four different classes, depending on the heating rate, heating route, and the presence of catalysts. The categories are fast, slow, catalytic, and microwave pyrolysis. Generally, fixed-bed and fluidised-bed reactors are employed, where fixed-bed reactors are widely used in slow, catalytic, and microwave pyrolysis, and frequently fluidised-bed reactors are employed for fast pyrolysis.

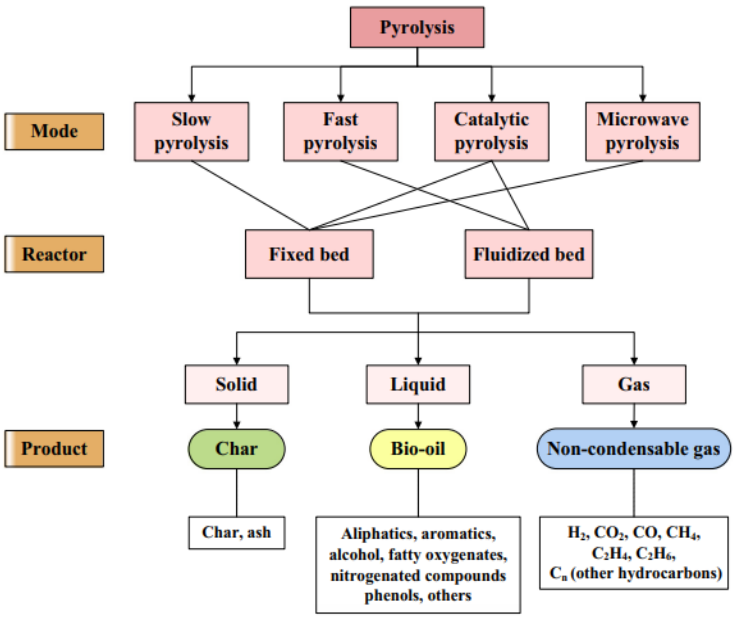

Figure 2-9: A schematic diagram of microalgae pyrolysis (Chen *et al*., 2015).

2.10.1.2 (a) Slow pyrolysis

Slow pyrolysis is a slow thermal decomposition of microalgae, where the heating rate is low, between 5-10 C/min, and the residence time is 10-the 30s. Low residence time implies that the process requires high energy input. The main product for this method is biochar, and the bio-oil produced has a high viscosity because the process is generally operated in a discontinuous fashion. Typically, the bio-oil yield produced from microalgae is 23 to 43 wt% with a pH value between 9 and 10 and HHV between 24 and 34 MJ/kg. In a study of the slow pyrolysis of microalgae, (Demirbaş, 2006) noted that the bio-oil yield increased with temperature until about 773,15 K but would decrease as the temperature continued to rise.

2.10.1.2 (b) Fast pyrolysis

In contrast to slow pyrolysis, fast pyrolysis occurs at a high heating rate (10-600 C/s), and brief residence time of hot vapour (1-3s), and with finely ground feed. The main product for this method is bio-oil. Fast pyrolysis is the most commonly used method for producing bio-oil with a yield ranging between 18-72 wt% and HVV between 24-41 MJ/kg (Chen *et al*., 2015).

2.10.1.2 (c) Catalytic pyrolysis

Catalytic pyrolysis is the pyrolysis of microalgae in the presence of a catalyst. The most frequently utilised catalysts for the pyrolysis of microalgae include Na_2CO_3 and ZSM-5-based zeolites such as Fe-ZSM-5 Cu-ZSM-5, H-ZSM-5, Ni-ZSM-5. The method is usually operated at temperature ranges 573,15-873,15 K and catalyst-to-biomass mass ratios between 0.2-5. The method has a bio-oil yield approximately in the fields of 19-40 wt% and 20-33 MJ/kg in HHV.

Although bio-oil derived from microalgae is high in oxygen content, it requires improvement to enhance stability, increase energy density, and prevent polymerisation and condensation reactions. Catalytic pyrolysis was suggested by (Suali & Sarbatly, 2012) as an appropriate process to enhance the bio-oils produced from microalgae, thus achieving higher bio-oil yields with less oxygen content. In a catalytic pyrolysis study of *Nannochloropsis sp*. residue, (Pan *et al*., 2010) found that bio-oil had a lower oxygen content (19.5 wt%) than the direct pyrolysis (30.1 wt%). In another study, (Babich *et al*., 2011) found that the gas yield for the pyrolysis of *Chlorella* in the presence of Na_2CO_3 as a catalyst is higher than non-catalytic pyrolysis of the same temperature. However, the liquid yield decreased.

2.10.1.2 (d) Microwave pyrolysis

Microwave pyrolysis refers to the pyrolysis of microalgae with microwave-assisted heating. Though microwave-assisted heating is commonly used in the industry, only a few studies reported on microalgae pyrolysis with microwave-assisted heating. Typically, the yield of bio-oils produced from microwave pyrolysis is between 18-59 wt%, and the HHV is between 30-42 MJ/kg. The advantage of this method is its homogenous heating of feedstock, brisk heating, agitation via fluidisation is unnecessary, and rapid response for immediate start-up and shut down. To enhance the yield and quality, microwave absorbers such as char, metallic oxides, activated carbon, sulphuric acid, SiC, and ionic liquids are blended with microalgae (Salema & Ani, 2012).

2.10.1.2 (e) Studies in literature

(Milano *et al*., 2016) studied the potential of the different processes to produce biofuel on a large scale. The study commended the various methods and noted that the production of liquid fuels has the potential to produce high-quality fuel oils at higher yields. In another study, (Hong *et al*., 2017) concluded that a greater bio-oil yield is possible when protein-rich algae are considered. This is due to its low polycyclic aromatic hydrocarbons (PAHs) content. The study also recommended that algae with high carbohydrates are better suited for syngas production. (Yang *et al*., 2016) also noted that most algae high in protein content have the potential of producing liquid fuels that are low in pressure, with low heating values, and low thermal stability. Figure 2-10 shows a list of microalgae pyrolysis studies under different operating conditions and modes.

Feedstock	Pyrolysis mode	Reactor	Operating condition				Bio-oil yield (wt%)
			Temp. (°C)	Heating rate (°C min^{-1})	Sweep gas flow rate (mL min^{-1})	Duration (min)	
Chaetocerous muelleri	Slow	Fixed bed	500	10	100	20	33
Chlorella like	Slow	Fixed bed	500	10	100	20	41
Chlorella vulgaris	Slow	Fixed bed	500	10	100	20	41
Dunaliella tertiolecta	Slow	Fixed bed	500	10	100	20	24
Tetraselmis chui	Slow	Fixed bed	500	10	100	20	43
Nannochloropsis sp.(res)	Slow	Fixed bed	300–500	10	30	120	21–31
Synechococcus	Slow	Fixed bed	500	10	100	20	38
Spirulina platensis	Slow	Fixed bed	350–500	3.5–7	250	60	23–29
C. protothecoides	Fast	Fluidized bed	500	36,000	6667		58
C. protothecoides	Fast	Fluidized bed	500	36,000	6667		18
C. vulgaris	Fast		400–700				58–72
C. vulgaris (res)	Fast	Fluidized bed	500				53
M. aeruginosa	Fast	Fluidized bed	500	36,000	6667		24
Scenedesmus sp.	Fast	Fluidized bed	440		33,000		22
Scenedesmus sp.	Fast	Fluidized bed	480				55
Chlorella	Catalytic (Na_2CO_3)	Fixed bed	300–450	100–150		30	35–55
Chlorella	Catalytic (ZSM-5) [a]		500		250		29–36
Nannochloropsis sp.(res)	Catalytic (HZSM-5)	Fixed bed	400	10	30	120	21–25
Chlorella sp.	Microwave [b]	Fixed bed	433–644		500	20	18–27
Chlorella sp.	Microwave [c]	Fixed bed	650–800		300	20	21–36
Chlorella vulgaris	Microwave	Fixed bed	450–550			30	41–57
Nannochloropsis	Microwave	Fixed bed	450–550			30	41–59

Figure 2-10: A summary of microalgae pyrolysis studies (Chen *et al*., 2015)

2.10.1.3 Liquefaction

Liquefaction is another thermochemical method of converting liquid fuels from wet microalgal biomass (Raheem *et al*., 2015). The method is also known as thermochemical or hydrothermal liquefaction (HTL). During liquefaction, hot compressed or sub-critical water is employed (Chen *et al*., 2015) to overcome the high moisture content of wet microalgal biomass. The process is generally operated with the aid of a catalyst at temperatures between 473,15-773,15 K and at high pressures between 5-20 bar to keep the water in the liquid phase (Raheem *et al*., 2015). The mass fraction of the microalgal in the slurry is between 5-50 % (Chen *et al*., 2015). The process can produce up to 73% of bio-oil, an ash content of up to 0.5%, and a gaseous mixture content of up to 20% (Raheem *et al*., 2015).

The process involves the decomposition of wet microalgae biomass (proteins, lipids, and carbohydrates) in hot compressed water into small molecules. The small molecules produced undergo depolymerisation or hydrolysis and then repolymerisation, thus producing oil products. In the early stage of the process, hydrolysis is the dominant mechanism. After that, the highly reactive molecules repolarise. Liquefaction is classified into two streams, direct and indirect liquefaction. The direct method refers to the fast pyrolysis of microalgae to bio-oil, condensable organic vapour, and liquid tar.

On the other hand, the indirect method employs a catalyst to convert organic vapour and liquid tar into liquid products (Raheem *et al*., 2015). The advantage of liquefaction is that it eliminates the cost or energy-intensive drying process of wet microalgae biomass (Raheem *et al*., 2015). However, the disadvantage of the method is that it is expensive due to the slightly complex reactors and fuel requirements (Raheem *et al*., 2015). Figure 2-11 shows a schematic representation of microalgal liquefaction.

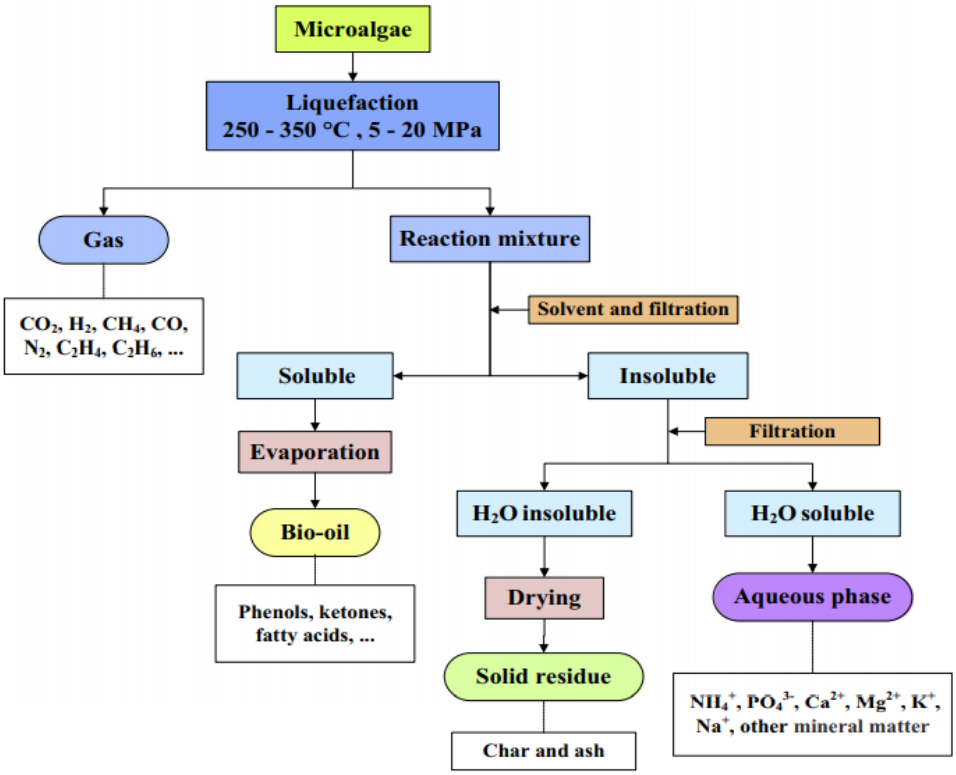

Figure 2-11: A schematic diagram of microalgae liquefaction (Chen *et al*., 2015).

2.10.1.3 (a) Studies in literature

In (Dote *et al*., 1994) study of the thermochemical liquefaction of *Botryococcus braunii*, a bio-oil yield of 64% at 573,15 K was achieved, with a 45.8 MJ/kg higher heating value (HHV). In another study of *D. tertiolecta*, a 42 % bio-oil yield on a dry basis, with an HHV of 34.9 MJ/kg, was noted. (Matsui *et al*., 1997) studied oil production from the protein-rich *Spirulina sp*. in the absence of a catalyst. A bio-oil yield of 54% was noted. (Yang *et al*., 2004) suggested that the optimum conditions for a liquefaction reaction are 613,15 K, a 30 min holding time, and 5% catalyst loading. Generally, the bio-oil content is between 30-65 wt%, and the calorific value is 30-50 MJ/kg.

(Biller, 2013) performed a GC/MS analysis of a fraction of bio-crude oil that was produced through HTL under various conditions. The study investigated microalgae species such as *Porphyridium*, *Chlorella*, *Nannochloropsis*, and *Spirulina*, processing under sodium carbonate, water, or formic acid. As shown in Figure 2-12, the predominant GM-MS identified compounds included phenols, phytol, indole, pyrrols, piperdine, hexadecamide, heptadecane, pentadecane, octanoic acid, and hexadecenoic acid.

Bio-crude condition	Albumin			Soya Protein			Asparagine			Glucose			Starch			Sunflower oil			Chlorella			Nannochloropsis			Porphyridium			Spirulina		
GC-MS Identified Compound	*H2O*	*Na2CO3*	*HCOOH*	*H2O*	*Na2CO3*	*HCOOH*	*H2O*	*Na2CO3*	*HCOOH*	*H2O*	*Na2CO3*	*HCOOH*	*H2O*	*Na2CO3*	*HCOOH*	*H2O*	*Na2CO3*	*HCOOH*	*H2O*	*Na2CO3*	*HCOOH*	*H2O*	*Na2CO3*	*HCOOH*	*H2O*	*Na2CO3*	*HCOOH*	*H2O*	*Na2CO3*	*HCOOH*
Phenols	x	x	x	x	x	x		x			x			x	x				x	x	x	x		x	x	x	x	x	x	x
Phytol								x												x			x		x	x			x	
Indole	x	x	x	x	x	x		x											x		x	x	x	x	x		x	x	x	x
Pyrrols	x		x	x		x	x		x										x							x		x	x	x
Piperdine	x			x		x													x	x							x	x	x	
Hexadecamide																			x		x						x	x		x
Cyclohexylamine							x		x																					
Hexadecane																x						x								
Heptadecane																x				x	x	x	x			x		x	x	x
Pentadecene																			x											
Octanoic acid																			x		x									
Cyclohexanone											x		x	x																
Cyclopentanone										x	x	x		x	x															
Benzene										x		x	x		x															
Indenone										x		x	x		x															
Ethanone										x		x	x		x															
Tetradecanoic Acid																x		x								x				
Oleic Acid																x		x												
Hexadecanoic Acid																x		x			x	x		x						x

Figure 2-12: Predominant GC-MS identified compounds in bio-crude oil (Biller, 2013)

A comparative techno-economic study was conducted by (Gu *et al*., 2020) for the production of algal biofuels through HTL. The investigation compared the one-stage HTL (conventional) and two-stage HTL (sequential). The study found that the minimum fuel selling price for the two-stage sequential process was lower by $0.49/L. Furthermore, the two-stage process's capital and operating costs were reduced, with the total installed costs for the hydrothermal processing facilities lower by $23 million. Additionally, the two-stage had a higher energy returned on energy invested and required less energy.

(Obeid *et al*., 2020) studied the reaction kinetics of compounds found in renewable crude oil from hydrothermal liquefaction. The investigation concluded that HTL of lipids produces fatty acids. Carbohydrates produce renewable crude that includes phenols, aromatics, furans, ketones, and aldehydes. Proteins produce renewable crude that includes amines, aromatics, amides, short hydrocarbon chains, and carboxylic acids. Lignins produce renewable crude, which is predominantly phenolic compounds. Examples of the compounds are summarised in Table 2-1.

Table 2-1: Example of compounds found in renewable crude oil (Obeid *et al*., 2020).

Lipids	Benzene, oleic acid, guaiacol, glutaric acid, 6-octadecanoic acid, dodecanoic acid, palmitoleic acid, ethyl oleate, octanoic acid.
Proteins	Heptane, pyrrolidine, benzoic acid, uric acid, propofol, urea.
Carbohydrates	Phenol, acetic acid, furan 2-5-dimethyl, cyclohexanone, benzyl alcohol.
Lignin	Formic acid, phenol, naphthalene.

(Chen & Quinn, 2021) conducted a techno-economic and life cycle analysis on the production of algal biofuels using HTL as a suitable technology. The investigation showed that conversion costs could be reduced by 19% when the temperature independently decreased from 623,15 K to 533,15 K while sustaining the yield. It also highlighted that fuel conversion costs could be varied by $0.07/L of gasoline-equivalent when different thermodynamic property models are used, having used PSRK and NRTL.

2.10.1.3 (b) Key parameters affecting conversion

Temperature

The liquefaction performance is critically influenced by temperature. The temperature is normally kept between 573,15-648,15 K, in which carbohydrates and proteins in microalgae can be converted. At lower temperatures, 523,15 K, the conversion of lipids is expected (Chen *et al*., 2015).

Holding time

Holding time is the duration of the temperature sustained for the liquefaction process. Generally, the holding time is kept within 60 min but can sometimes exceed up to 120 min. Therefore, the bio-oil yield increases with increasing holding time until 60 min. Beyond that, the yield decreases. Typically, a higher bio-oil yield can be obtained if a higher temperature and shorter holding time are considered (Chen *et al*., 2015).

Feedstock load

Liquefaction performance can also be affected by the mass fraction of microalgae in a slurry. However, the influence on the process is only significant at low mass fractions (Chen *et al*., 2015).

Catalysts

Both homogenous (alkali salts) and heterogeneous catalysts (alkali metals) can be employed for the liquefaction process. However, the most commonly used alkali salt for microalgae

liquefaction is sodium carbonate (Na_2CO_3), as studies such as (Yang *et al*., 2004) have observed that it enhances the bio-oil yield.

Studies have also shown that adding alkali metals in liquefaction can increase the bio-oil yield and the HHV while decreasing the O content. For example, a study by (Biller, Riley & Ross, 2011) and another by (Duan & Savage, 2010) both noted that the presence of catalysts such as $Co/Mo/Al_2O_3$, $CoMo/c\text{-}Al_2O_3$, $Ni/SiO_2\text{-}Al_2O_3$, Pt/Al_2O_3, Pt/C caused an increased in bio-oil yield.

2.10.1.4 Combustion

Direct combustion is a thermochemical method of burning algae biomass in a furnace, steam turbine, or boiler at around 1273,15 K (Raheem *et al*., 2015), (Adeniyi, Azimov & Burluka, 2018). In this process, photosynthetically stored chemical energy in the microalgae is converted in the presence of air to hot gases. Typically, the hot gasses produced are used in the production of electricity. Though the combustion process can accept different types of biomass, the moisture content of the biomass has to be less than 50% to reduce air pollution (Adeniyi, Azimov & Burluka, 2018). Therefore, this process requires some level of preparation before burning the biomass. The pre-treatment commonly employed includes cutting and crushing into small combustible particles and dehydration. This step makes the cost of energy production via direct combustion slightly higher (Raheem *et al*., 2015). Figure 2-13 shows the combustion of algae for power generation.

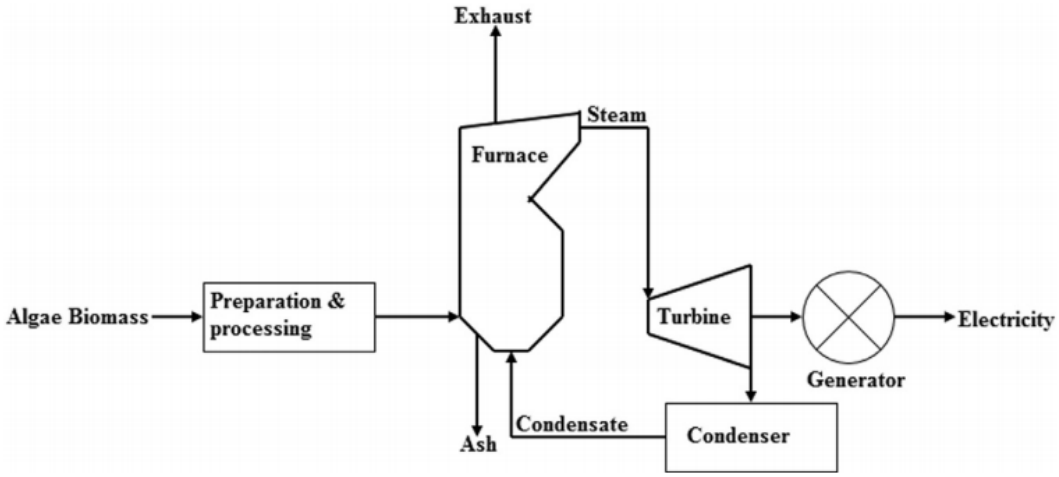

Figure 2-13: The combustion of algae biomass for power generation (Adeniyi, Azimov & Burluka, 2018).

2.10.2 Biochemical conversion technologies

There are several different conversion technologies in the biochemical conversion process of microalgal biomass. These include, fermentation, anaerobic digestion, and photobiological techniques (Raheem *et al*., 2015). In these technologies, algal biomass is converted into biofuels mostly through microorganisms and enzymatic processes (Baskar *et al*., 2019). However, the problem with this conversion process is that it is environmental benign, has low conversion rates

by microbes and/or enzymes, requires long reaction time, and has high production costs (Baskar *et al*., 2019), (Raheem *et al*., 2015).

2.10.2.1 Fermentation process

The fermentation process is a biochemical process that converts algae biomass into bioethanol. This metabolic reaction involves enzyme activities to convert cellulose sugar or starch stored in the biomass into alcohol. Yeast is utilised to convert the sugar compositions in the biomass such as mannitol, alginate, and laminarin into ethanol. The process is also known to produce acetone and butanol through acidogenesis and solventogenesis (Adeniyi, Azimov & Burluka, 2018).

The productivity of algal bioethanol is five times higher than the production of bioethanol from corn and two times higher from sugarcane. *Chlorella vulgaris* is a good source of bioethanol from microalgae because of its high carbohydrate content, with a conversion efficiency of up to 65%. For an efficient fermentation of microalgae, the pre-treatment processes such as liquefaction, milling, and saccharification or alginate extraction are necessary (Adeniyi, Azimov & Burluka, 2018). The general expression of the conversion of biomass to bioethanol is expressed as follows (Tran *et al*., 2019):

$$(C_6H_{10}O_5)_n + nH_2O \rightarrow nC_6H_{12}O_6 \rightarrow 2nC_2H_5OH + 2nCO_2 \quad (2.1)$$

There are four configurations of fermentation that have been studied: separate hydrolysis and fermentation (SHF), simultaneous saccharification and co-fermentation (SSCF), and simultaneous saccharification and fermentation (SSF), and consolidated bioprocessing (CBP).

2.10.2.1 (a) Separate Hydrolysis and Fermentation (SHF)

The configuration allows for enzymatic hydrolysis to occur separately from fermentation. The advantage of this configuration is that it allows each process to operate at its optimal condition. However, the enzymes used by the hydrolysate are inhibited, and the hydrolysis rate decreases, ultimately affecting the ethanol yield (Özçimen & İnan, 2015), (Aui, Wang & Mba-Wright, 2021). Furthermore, the use of different reactors makes this costly (Özçimen & İnan, 2015). Both enzymatic hydrolysis and fermentation occur at their optimal temperatures of 323,15 K for hydrolysis and 301,15-305,15 K for fermentation (Bušić *et al*., 2018).

2.10.2.1 (b) Simultaneous Saccharification and Fermentation (SSF)

In this configuration, pre-treatment and enzymatic hydrolysis co-occur with fermentation in the same reactor, making it a cost-effective option. Adding dilute acid or hot water at a high temperature significantly improves the efficiency of the configuration. Inhibition of enzyme activity is considerably low. Therefore, low amounts of enzymes are required. In addition, a high

yield of ethanol can be attained for a shorter bioprocessing time (Bušić *et al*., 2018). The disadvantage of this configuration is that the different temperatures between saccharification and fermentation result in various effects on the growth of microorganisms (Özçimen & İnan, 2015). As a result, both processes cannot operate at their optimum conditions (Aui, Wang & Mba-Wright, 2021). The optimal temperature for this configuration is approximately 311,15 K, which is representative of the optimal temperature for hydrolysis, 318,15-323,15 K, and fermentation 303,15 K (Bušić *et al*., 2018).

2.10.2.1 (c) Simultaneous Saccharification and Co-fermentation (SSCF)

Conversion of carbohydrates through fermentation using saccharomyces cerevisiae is difficult under moderate conditions. This results in impure biomass and decreases product yield. The utilisation of recombinant yeasts overcomes this challenge by converting residue carbohydrates such as pentose and hexose to ethanol. In this configuration, recombinant yeasts and cellulase enzyme complex are fed into the same reactor (Özçimen & İnan, 2015). As a result, the fermentation of pentose and hexose co-occurs, possibly reducing contamination (Bušić *et al*., 2018). However, although this configuration allows for a more straightforward and effective process which could reduce capital cost, it can result in a lower biofuel yield because the processes are co-occurring (Aui, Wang & Mba-Wright, 2021).

2.10.2.1 (d) Separate Hydrolysis and Co-fermentation (SHCF)

This configuration is essentially a combination of SSCF and SHF. Fermentation and hydrolysis occur in different reactors, allowing each step to appear at its optimal conditions. Compared with the SHF configuration, SHCF can produce ethanol with high productivity (Özçimen & İnan, 2015). Although the product yield is higher than SHF, there is limited literature on SHCF operations. Furthermore, the approach requires a high enzyme load and can experience an increased contamination risk (Danquah, Liu & Harun, 2011).

2.10.2.1 (e) Consolidated bioprocessing (CBP)

In this configuration, genetic engineering combines saccharification, hydrolysis and fermentation into one operating unit. This approach requires only one microorganism but involves four biological reactions; enzyme production, carbohydrate hydrolysis, fermentation of hexoses, and fermentation of pentoses (Bušić *et al*., 2018). The optimal temperature is 338,15 K and pH is from 6.5-7.4 (Danquah, Liu & Harun, 2011). It is a less energy-intensive and economical option due to more straightforward feedstock processing (Aui, Wang & Mba-Wright, 2021). In addition, it has a higher conversion efficiency than SHF processes (Levin *et al*., 2015). The challenge with this approach is the lack of suitable organisms that singularly integrate all the features during the process and the difficulty in process control (Danquah, Liu & Harun, 2011).

2.10.2.1 (f) Studies in literature

In a study (Chen *et al*., 2018) noted that bioethanol yield depends on the energy requirements of the utilised pre-treatment method. The same study also indicated that hydrothermal pre-treatment of microalgae could improve the yield significantly. Due to the absence of lignin in brown algae, the hot water wash strategy was recommended by (Fasahati, Woo & Liu, 2015) as a more economical alternative but can also improve yields. To reduce pre-treatment costs (Jambo *et al*., 2016) suggested using enzymatic hydrolysis in the production of bioethanol. Around the time of the study industry, economic and technical evaluations were still required to determine the best fermentation methods for algae bioethanol.

(Chen *et al*., 2018) suggested that more research is required on structural, metabolic, and genetic engineering. This will be crucial for comprehensively assessing the environmental risk associated with the industrial bioethanol processes. For industrial processes, genetically modified microorganisms are utilised in place of the traditional fermentation process. Though brown algae are widely considered one of the most suitable biomasses for bioethanol production, to produce bioethanol, the fermentation of the microorganisms involved must be efficient. (Lee & Lee, 2016) noted that higher bioethanol yields from brown algae are noticeable when there is an increase in the carbon source during the fermentation.

(Ashokkumar *et al*., 2017) suggested that the anaerobic fermentation process is a suitable pathway for bioethanol production after lipid extraction of biodiesel. The study showed that fermentation could be used to obtain bioethanol from residue biomass with the conversion of hydrolysate. The study further showed that a theoretical yield of 83.4 % brown algae could produce bioethanol and biodiesel. However, the commercialisation of bioethanol still depends on the development of economical processing and cultivation methods.

(Kavitha *et al*., 2021) studied the CBP configuration using *Nannochloropsis gaditana* as the microalgal biomass to convert to bioethanol under optimal conditions. Maximum bioethanol of 12.90 ± 0.987 g/L was obtained using pre-treated *N.gaditana* biomass. Optimised parameters were found to be temperature 306,15 K, a pH of 5, and agitation of 120 rpm at 24 hours.

2.10.2.1 (g) Key parameters affecting conversion

The key parameters affecting the conversion of microalgae include the pH level, temperature, osmotic tolerance, alcohol tolerance, growth rate, resistance to inhibitors, genetic stability (Balat, Balat & Öz, 2008), fermentation time, inoculum size, sugar concentration and agitation time (El-Mekkawi *et al*., 2019).

In an analysis of critical parameters that affect bioethanol production, (Fakruddin *et al*., 2012) suggested that temperature, pH, and sugar concentration affect ethanol production and

intrinsic factors such as culture medium, immobilisation, dissolved O_2, and other micronutrients. The study concluded that the optimum temperature for a maximum ethanol yield is 303,15 K, and the pH ranges between 5,0 and 6,0. At low temperatures, between 298,15-303,15 K, the ethanol yield gradually increases, but higher temperatures decrease the ethanol yield.

Furthermore, reducing sugar concentrations between 5-8% will result in a higher product yield. Immobilised cells produced a maximum yield of 94,8 g/L or increased production up to 13% when the sugar concentration was reduced by 5,50% at 48h. Finally, the influence of boron, chromium, copper, and magnesium on the production of ethanol was investigated. Only chromium showed slight effects on the product yield, whereas copper drastically decreased the ethanol yield (Fakruddin *et al*., 2012).

2.10.2.1 (h) Microbiology of conversion

The conversion of microalgae to bioethanol takes place in two stages. The first stage involves the extraction of starch from microalgae cells with aid from a suitable enzyme or mechanical machine. The second stage consists of adding *Saccharomycess cerevisiae* into the microalgae raw material for fermentation to take place, thus forming ethanol and carbon dioxide. This stage occurs when the microalgae cells begin to degenerate. The final step involves draining and pumping ethanol into a holding tank for purification. The reaction equations representing the mentioned stages are (Wang, 2013):

Stage 1: $C_{12}H_{22}O_{11}(sucrose) \rightarrow C_6H_{12}O_6(glucose) + C_6H_{12}O_6(fructose)$ (2.2)

Stage 2: $C_6H_{12}O_6 + yeast\ (catalyst) \rightarrow 2C_2H_5OH(ethanol) + 2CO_2 \uparrow$ (2.3)

2.10.2.2 Anaerobic digestion

Anaerobic digestion is a biochemical process that converts organic compounds to biogas through the activity of microorganisms under anaerobic conditions. Dry biogas is widely accepted as a mixture of methane (between 50-70% by volume), carbon dioxide with traces of ammonia, hydrogen sulphide and volatile organic compounds. This conversion method is recognised as a robust technology and well established in treating organic waste streams. It is widely used because of its environmental benefits, high energy output to input ratio, and simplicity compared to other biodiesel or bioethanol producing processes (Adeniyi, Azimov & Burluka, 2018). The economic and environmental benefits of the process are that effluents and emissions can be captured and reused (Wu *et al*., 2019).

Anaerobic digestion is a suitable technology for organic feedstock with high moisture content, such as wet algae biomass, which can be directly applied with little dewatering (Baskar *et al*., 2019). In addition, due to the negligible lignin content in algal biomass, harsh pre-treatment is unnecessary (Wu *et al*., 2019).

The anaerobic digestion process involves three biochemical steps which happen in nature, namely, hydrolysis, acidogenesis and acetogenesis, and methanogenesis. During hydrolysis, macromolecules such as proteins, polysaccharides, and lipids break down into simpler compounds such as sugars, amino acids, glycerol, and fatty acids (Adeniyi, Azimov & Burluka, 2018), (Wu *et al*., 2019). Thereafter, the hydrolysed molecules are converted to primarily acetate, volatile fatty acids, carbon dioxide, and hydrogen. This step is referred to as the acidogenesis and acetogenesis stage. Finally, in the methanogenesis stage, the acetate, carbon dioxide, and hydrogen is converted to methane (Wu *et al*., 2019). Figure 2-14 shows the basic steps of anaerobic digestion.

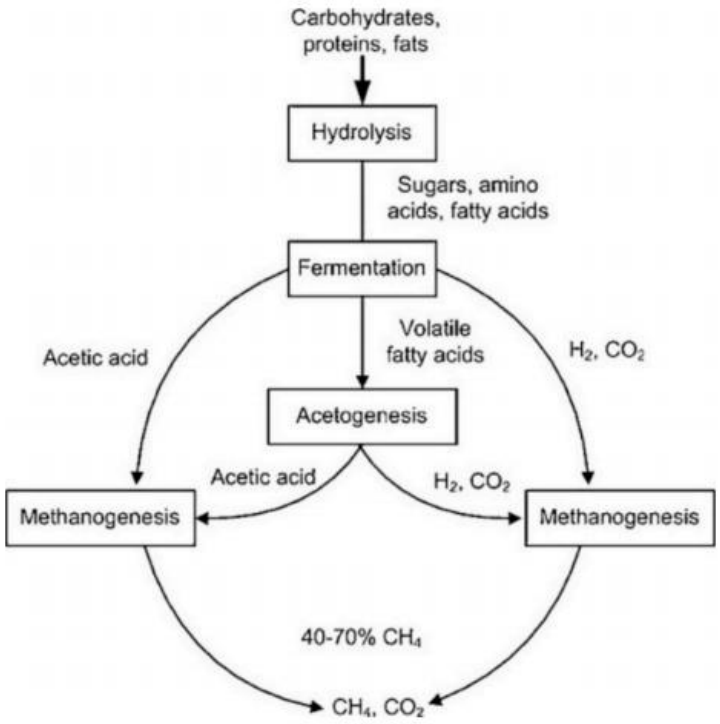

Figure 2-14: Basic steps of anaerobic digestion (Zabed *et al*., 2020).

2.10.2.2 (a) Studies in literature

Many studies of techno-economic assessments have been conducted for the production's algal biodiesel. However, there remains a need for techno-economic assessments on algal biogas, especially on full-scale production. Though the process has the potential, its development is hindered by the questions related to the net energy output and economic feasibility when microalgae are considered as the feedstock. (Wu *et al*., 2019) suggested that biogas yield could be low due to the composition and structure of the microalgae cell wall, which would require high energy inputs to disrupt the cell walls during pre-treatment. The review further suggested that the algae cultivation could be high, and productivity could be low.

(Rodriguez *et al*., 2015) proposed that thermal pre-treatment should be employed to achieve a high methane yield during anaerobic digestion. However, the study pointed out that further research in algae anaerobic digestion is necessary as the pre-treatment methods for this method require high energy. (Marsolek *et al*., 2014) also identified thermal pre-treatment as a suitable method to achieve the highest methane yield. The study noted that the excess heat from other algae conversion processes could require energy during pre-treatment.

2.10.2.2 (b) Key parameters affecting conversion

The conversion of microalgae to biogas through the anaerobic digestion process depends on several factors, such as temperature, pH, carbon-nitrogen ratio, lipids content, the recalcitrance of cell wall, (Baskar *et al*., 2019), hydraulic retention time (HRT), organic loading rate (OLR), reactor configurations, pre-treatment methods, and biodegradability of algal biomass (Wu *et al*., 2019). In addition, many other factors can affect the yield and productivity of the process. A few of these will be briefly discussed.

Temperature

There are three temperature regimes that anaerobic digestion microorganisms can grow in: psychrophilic (278,15-293,15 K); mesophilic (298,15-318,15 K); and thermophilic (318,15-338,15 K). An increase in temperature could benefit the process by improving enzymatic activity, but temperatures beyond the tolerable range cause inhibition by inactivating microbes (Wu *et al*., 2019).

pH

The pH affects the biogas composition, enzyme activity, and the growth of microbes. This means that the pH needs to be maintained at appropriate levels to obtain the best conversion of biomass to biogas. The optimum pH levels vary with each step of the process but generally, for a single-stage anaerobic digester, the pH is maintained between 7 and 8 (Wu *et al*., 2019).

Salinity and sulphide

Studies show that biomass grown in saline environments offers a more sustainable alternative when compared to other biomass. Still, processing microalgae that are high in salinity could be problematic because high salinity hinders anaerobic digestion (Wu *et al*., 2019).

Sulphide is an essential micronutrient for anaerobic microorganisms, but high concentrations, about 200 mg/L, could be toxic (Wu *et al*., 2019).

Lipids content and C/N ratio

Lipids have a high theoretical methanol potential but also have the potential to inhibit the anaerobic digestion process. Generally, when lipids concentrations exceed 30%, inhibition is highly likely to occur (Wu *et al*., 2019).

Generally, the C/N ratio for microalgal anaerobic digestion is kept below ten, while the optimum C/N ratio for anaerobic digestion is between 15 and 30. To achieve a higher biogas yield and productivity from microalgae, the C/N ratio would have to be increased (Wu *et al*., 2019).

2.10.2.2 (c) Microbiology of conversion

The central components of anaerobic digestion are microorganisms. Each step in the conversion process has its own microflora. The hydrolysis and acidogenesis stage occur through more than 50 kinds of bacterial species including the genera *Cellulomonas*, *Bacteroides*, *Clostridium*, *Microbispora* etc. The acetogenesis step occurs through acetogenic bacteria like *Acetobacterium* and *Sporomusa*, and non-acetogenic bacteria like *Clostridium*, *Eubacterium*, and *Ruminococcus*. The methanogenesis step occurs through 65 archaeal species such as *Methanosaeta*, *Methanobacterium*, *Manospirillum*, and methylotrophic (Zabed *et al*., 2020).

Anaerobic digestion of microalgal biomass is expressed as follows (Zabed *et al*., 2020):

$$C_6H_{10}O_5\ (Carbohydrates) + H_2O \rightarrow 3CH_4 + 3CO_2 \quad (2.4)$$

$$C_{16}H_{24}O_5N_4\ (Proteins) + 14.5H_2O \rightarrow 8.25CH_4 + 3.75CO_2 + 4NH_3 \quad (2.5)$$

$$C_{50}H_{90}O_6\ (Lipids) + 24.5H_2O \rightarrow 34.75CH_4 + 12.25CO_2 \quad (2.6)$$

2.10.3 Chemical Conversion Technologies

2.10.3.1 Transesterification process

2.10.3.1 (a) Lipid extraction techniques

Before transesterification, the microalgae lipids require extraction. Lipid extraction is a crucial step that affects the quantity and quality of biodiesel and the cost efficiency of the production. Therefore, selecting a suitable technique that is selective, cost-effective, solvent-free, and efficient is critical (Moradi-kheibari *et al*., 2019). The main extraction techniques include the use of chemical solvents, physiochemical extraction, biochemical extraction, supercritical carbon dioxide extraction, and direct (in situ) transesterification.

Chemical solvent extraction is the most common lipid extraction method in microalgae processes. Typically, chemical solvents such as methanol, ethanol, and n-hexane are used as they are easily accessible. Chemical solvents have a high selectivity and solubility towards lipids, making inter-lipid extraction easy (Mujeeb, Vedamurthy & Shivasharana, 2016). The

disadvantage of using this method is that it is less effective when the biomass is wet (Veillette *et al*., 2012) and uneconomical when drying is employed before lipid extraction due to the energy requirements of the drying process. Furthermore, chemical solvents are toxic to humans and the surrounding environment. The effectiveness of lipid extraction is highly dependent on microalgae strains and the thickness of the cell walls. Therefore, cell disruption techniques can be used before enhancing the efficiency of this method of extraction (Mujeeb, Vedamurthy & Shivasharana, 2016).

Supercritical carbon dioxide extraction uses carbon dioxide as a solvent to extract from microalgae while maintaining the integrity of extracts. This occurs under controlled temperatures and pressures to create a phase change in CO_2. This method is safe and non-toxic. It is easy to recover, allows for the penetration of tiny pores, and can be used at low critical temperatures (Mujeeb, Vedamurthy & Shivasharana, 2016). The disadvantage of this method is that it requires expensive equipment that uses significant amounts of energy to reach high pressures (Veillette *et al*., 2012).

Physicochemical extraction includes techniques such as autoclaving, homogenisation, microwave, freeze-drying, osmotic shock, bead-beating, sonication and grinding. These techniques can be utilised in microalgae cell disruption. Of these methods, bead-beating and microwave have the most potential to increase lipid yield (Veillette *et al*., 2012). Physicochemical techniques are widely used for the recovery of lipids. However, they are time-consuming and have the potential to cause degradation or undesirable chemical changes to the products not unless careful control is employed (Kapoore *et al*., 2018).

Direct in situ transesterification is another option that has been investigated. The method involves blending microalgae with a catalyst and alcohol without prior extraction. The use of a heterogeneous catalyst and a less polar solvent, coupled with microwave heating, could be more effective. The disadvantage of this option is that it requires dry microalgal biomass, thereby increasing the harvesting costs (Veillette *et al*., 2012).

2.10.3.1 (b) Transesterification

Algae biomass can also be converted into biodiesel through a chemical conversion known as transesterification or alcoholysis. During this process, triglyceride (lipid) reacts with alcohol in the presence of a suitable catalyst such as acidic, alkaline, or enzyme-based to produce fatty acid methyl esters (FAME) with glycerol. The process has been widely used to reduce the viscosity of the algal oil, thereby increasing the fluidity (Baskar *et al*., 2019) such that it can be blended with petroleum diesel (Adeniyi, Azimov & Burluka, 2018).

The conversion of raw algae lipid to FAME of lower molecular weight depends on the type of catalyst, the type of alcohol, molar ratio etc. Ethanol and methanol are the most commonly used alcohols for this process as they are both economical and readily available (Baskar *et al*., 2019). However, an alkaline catalyst can be used to achieve a high yield of up to 90% FAME conversion from microalgae such as *oedigonium* and *spirogyrus* (Adeniyi, Azimov & Burluka, 2018).

The process can be described by the chemical equation in Figure 2-15 below.

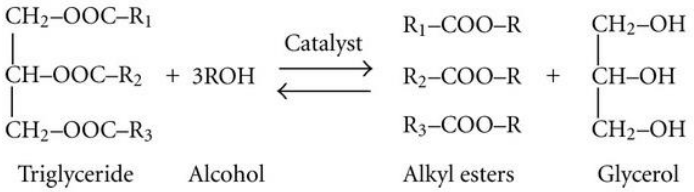

Figure 2-15: A chemical equation for algal transesterification (Koohikamali, Tan & Ling, 2012).

There are two types of transesterification processes in biodiesel production: direct, also known as in-situ, and conventional (Baskar *et al*., 2019). Direct transesterification is a single-stage non-catalytic method that involves simultaneously extracting lipid content, as shown in Figure 2-16. Then, the algae biomass, which is wet and unwashed, is fed into the reaction system. The advantage of this process is that pre-treatments such as degumming and extraction are eliminated, it yields more diesel if the wet biomass is extracted, and considerable amounts of solvent are used for treating the biomass (Adeniyi, Azimov & Burluka, 2018).

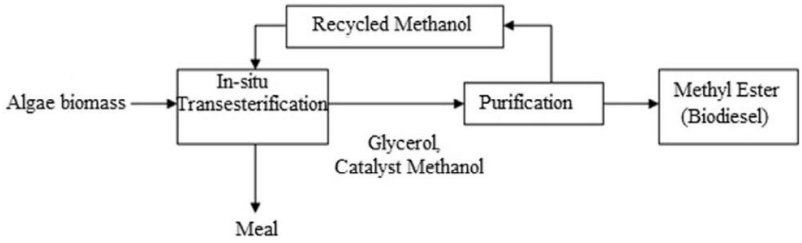

Figure 2-16: Flow diagram of direct transesterification of algae biomass (Adeniyi, Azimov & Burluka, 2018).

Conventional transesterification is a two-stage catalytic method that involves the extraction of lipids before transesterification through a mechanical process. This method requires pre-treatment operations such as degumming and extraction, making its production costs high. In addition, this method is energy-intensive and relatively time-consuming, mandating the separation of oil, catalyst, alcohol and impurities from the biodiesel (Baskar *et al*., 2019) (Adeniyi, Azimov & Burluka, 2018). A process flow diagram of the process is illustrated in Figure 2-17.

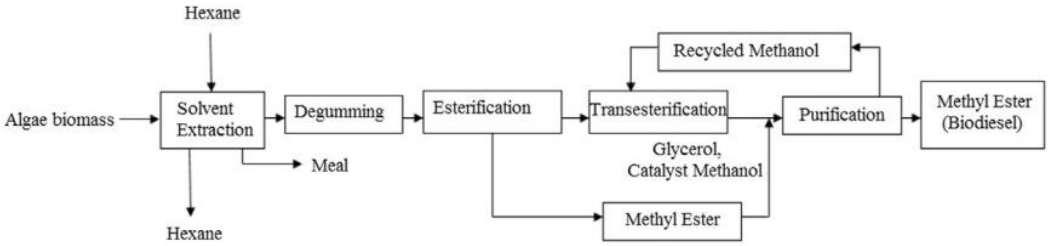

Figure 2-17: Flow diagram of conventional transesterification of algae biomass (Adeniyi, Azimov & Burluka, 2018).

Figure 2-18 shows a list of different studies on transesterification compiled by (Özçimen, Gülyurt & İnan, 2013) under different conditions.

Algae strain	Method	Alcohol	Alcohol / oil molar ratio	Temp.	Time	Results
Heterotrophic C. Protothecoides (microalga)	Acidic trasesterification	Methanol	56:1	30 °C	4 h	80% (FAME Yield
Chlorella vulgaris ESP-31 (microalga)	Enzymatic transesterification (Lipase)	Methanol	98.81	25-40 °C	48 h	94.78% (FAME Yield)
Chlorella vulgaris (microalga)	in situ alkaline transesterification	Methanol	600:1	60 °C	75 min	71% (FAME Yield)
Nannochloropsis oculata (microalga)	heterogeneous transesterification	Methanol	30:1	50 °C	4 h	97.5% (FAME Yield)
Chlorella (microalga)	In-situ acidic transesterification	Methanol	315:1	23 and 30 °C	15 min-2 h	70-92% (FAME Yield)
Chlorella sp. (microalga)	Alkali Transesterification	Methanol	-	100 °C	25 h	90 (Fluorometric Reading)
Schizochytrium limacinum (microalga)	Acidic Transesterification	Methanol	-	90 °C	40 min.	82.6% (biodiesel Yield)
Chlorella emersonii	Alkali trasesterification	Methanol	5:1	60 °C	2 h	93% conversion
Fucus spiralis (macroalga)	Alkali Transesterification	Methanol	6:1	60 °C	4 h	1.6-11.5% (Process Yield)
Commercially refined macroalga (Kelp)	McGyan process	Methanol	32:1	360 °C	30 s	94.7% (FAME Yield)

Figure 2-18: Different studies on transesterification (Özçimen, Gülyurt & İnan, 2013).

2.10.3.1 (c) Studies in literature

(Jazzar *et al*., 2015) critically studied the direct transesterification process using wet unwashed *Chlorella sp* to make transesterification economically feasible and cost-effective. Based on the study, high lipid conversions to biodiesel are attainable by the direct supercritical methanol transesterification method. In a review study on in situ technology for simultaneous extraction and transesterification during biodiesel production (Skorupskaite, Makareviciene & Gumbyte, 2016) proposed the use of fast-growing algae strains to obtain high oil content for a cost-effective direct transesterification process.

(Salam, Velasquez-Orta & Harvey, 2016) suggested that the required energy for the pre-treatment of the wet algae could be provided by using microalgal residue for biogas production, thereby reducing the production cost. However, this would only be possible if critical process variables such as moisture content, reaction time, stirring rate, temperature, alcohol to oil ratio, type of catalyst and microalgae cell wall are considered.

To alleviate the high pre-treatment costs of drying the wet algae, (Martinez-Guerra & Gude, 2018) suggested conjoining the ultrasound irradiation and microwave techniques, thereby eliminating the drying process, which is energy-intensive. The application of this method would yield 90% FAME with less than one ratio of energy input to output.

(Tejada Carbajal *et al*., 2020) conducted a techno-economic analysis using *Scenedesmus dimorphus* microalgae biomass in five biorefinery scenarios for the production of biodiesel and glycerol valorisation. Simulations were performed for a reactive distillation column and a continuously stirred tank reactor for the transesterification stage. The scenario modelled with a reactive distillation column achieved the highest reaction rates and presented the best economic performance.

(Tsavatopoulou, Aravantinou & Manariotis, 2021) investigated the conversion of *Chlorococcum sp.* and *Scenedesmus sp.* biomass by direct and conventional transesterification. Direct transesterification separately employed H_2SO_4 and NaOH as catalysts, while the traditional process subsequently used the essential and the acidic catalyst. When *Chlorococcum sp.* was analysed, similar results were obtained between the direct and conventional methods. However, the traditional transesterification showed better results when *Scenedesmus sp.* was analysed. The conclusion was that the type of algal species and growth conditions would strongly influence the kind of methyl esters produced.

2.10.3.1 (d) Key parameters affecting conversion

The yield of transesterification can be influenced by the ratio of alcohol to oil, the time of catalyst and concentration, the temperature, reaction time and agitation rate (Adeniyi, Azimov & Burluka, 2018).

Reaction temperature

The reaction temperature is an essential parameter in converting microalgae to transesterification. Typically, the temperatures for transesterification should be less than the boiling point of alcohol to impede the evaporation of alcohol. The temperature range is between 323,15 K and 333,15 K, depending on the fats or oils employed. Reaction temperatures beyond the optimal level decrease biodiesel yield as higher temperatures accelerate the hydrolysis of esters or saponification of triglycerides (Mathiyazhagan & Ganapathi, 2011).

Reaction time

Reaction time is another critical parameter that affects transesterification. An increase in reaction time beyond the optimal time does not increase the product yield; instead, it reduces biodiesel due to the reversible reaction (Mathiyazhagan & Ganapathi, 2011).

Catalyst time and concentration

The concentration of the employed catalyst also affected biodiesel's formation and the time of mixing the catalyst. To avoid inhibiting the production of biodiesel, the catalyst should be mixed with methanol before adding the oil or fats, as the contrary will produce amounts of water due to the hydrolysis reaction. On the other hand, sufficient amounts of the catalyst are required for a complete conversion. Furthermore, an increased concentration of the catalyst and oil leads to an increase in biodiesel (Mathiyazhagan & Ganapathi, 2011).

Molar ratio of alcohol

The ratio of alcohol to oil plays a crucial role in the formation of biodiesel. Typically, excess amounts of alcohol to a particular concentration increases the yield of biodiesel within a short time. On the other hand, a further increase in concentration leads to a rise in the cost of alcohol recovery. Additionally, the ratio of alcohol to oil varies with the catalyst employed. For example, when using an alkali catalyst, the ratio is 6:1 (Mathiyazhagan & Ganapathi, 2011).

2.11 Challenges of Biofuel Production from Algal Biomass

Although microalgae are a promising candidate for an alternative fuel source and are an excellent choice for cleansing the environment, their use for the production of bioenergy and

products faces limitations and challenges that cannot be overlooked. Addressing these issues requires improving technologies from the lab to the commercial scale. (Veeramuthu & Ngamcharussrivichai, 2021) noted the critical problems to improve as; the algal biomass productivity, dewatering and biomass productivity, pre-treatment and extraction, and the production of biofuels. Though strides have been made in the advancement of technology for large-scale processes, microalgal biofuel production is still costly. This is partly attributed to the cultivation system design requiring temperature and growth-limiting conditions such as CO_2, optimisation, and water and nutrient sources. Another challenge lies in biomass dewatering because it is an energy-intensive process that requires high volumes of water and is very costly (Medipally *et al*., 2015).

In large-scale algal cultivation, both of the most common options for biomass production, the close PBR and open raceway ponds, have their issues. Closed PBR systems are more expensive and face significant operating challenges such as fouling and overheating due to gas exchange limitations. On the other hand, raceway ponds face contamination issues (Veeramuthu & Ngamcharussrivichai, 2021).

Extraction is also a significant challenge in biofuel production. This is also a cost issue as extraction mainly involves expensive solvents, which increases the production cost considerably. Much research is still underway for advanced technologies that eliminate drying and solvent extraction, thus reducing biomass pre-treatment costs.

2.12 Technoeconomic assessment

(Beal *et al*., 2015), performed a comprehensive techno-economic and life cycle assessment of algal biofuel production in a 100-ha facility. The biomass production was greater than 23 g/m^2-day. The study considered processes such as thermal conversion, fermentation, catalytic hydrothermal gasification, centrifugation and solvent extraction, wet extraction, hydrothermal liquefaction, and combined heat and power. The study pointed out that the barriers to large-scale production include enormous capital costs, geographic sensitivity, and carbon acquisition. However, integrated pathways presented in the survey remain the solution to global fuel and protein demands.

(Thomassen *et al*., 2016), performed techno-economic assessments of four scenarios: basic, intermediate, advanced, and alternative. The primary and intermediate scenarios employed commercial technology and open systems, and the advanced and alternative scenarios used improved technologies like photobioreactors. The assessment was for producing 170 tonnes of microalgae per annum in Belgium. The study noted that scenarios utilising open ponds and specialised membranes for medium recycling were the most profitable, and the investment costs of photobioreactors were four times higher than that of open systems.

(Dutta, Neto & Coelho, 2016) conducted a comparative techno-economic and life cycle assessment of microalgal biofuels in Portugal and the USA through the National Renewable Energy Laboratory (NREL). The NREL biofuel process involved transesterification, solvent extraction, and product purification. The Portugal case involved processes like distillation, fermentation, and hydrodeoxygenation. The cost for the Portugal process was calculated to be $1279/tonnes, and that of the NREL process was $ 430/tonnes. The significant difference was accounted to the bioethanol and biogas produced in the NREL process, which reduces the energy in the process. Basically, the valorisation of co-products in the NREL process may help increase the fuel selling price by adding revenue.

(Xin *et al.*, 2016), investigated the economic feasibility of wastewater-based algal biofuel production. The techno-economic evaluation used a photobioreactor for the production of biofuels. The total cost of production was found to be $ 0.33/kg biomass. The investigation noted that wastewater-based microalgae production could reduce operating costs. The estimated break-even selling price of biofuel is $0.59/L which is an acceptable estimate.

(Juneja & Murthy, 2017) designed a bio-oil producing plant with a processing capacity of 2.5 Mgal/hr, including hydrothermal liquefaction and hydrotreating. The primary feedstock for the process was algae cultured from wastewater. The investment cost to produce renewable biodiesel from algae was $104.96 MM, and the operating costs were found to be $17.88 MM. The investment was set up for 28.111 tons of wastewater algae per annum and 10 million litres of biodiesel. The biodiesel unit cost was $1.75/biodiesel ($6.69/gal), which falls in the lower price range reported in the literature for producing biofuels from microalgae, $0.92/ gal to $42.6/gal (Juneja & Murthy, 2017). The cost difference between hydrotreated biodiesel and crude bio-oil was $0.84. The study proved that biodiesel production from microalgae is competitive with other alternatives to diesel production.

(Rajesh Banu *et al.*, 2020) evaluated the economic feasibility of three microalgal-based biorefinery routes. The first route involved the production of biodiesel, animal feed, lipid, and pigments. The second route was to produce biogas and pigments and two-stage fermentation. The third route was to produce bio-hydrogen and pigments. The study found that the integrated biorefinery, which includes the production of biofuels with value-added products, has higher economic feasibility in terms of profit by reducing capital and operating costs.

2.13 Life Cycle Assessment

The Life Cycle Assessment (LCA) is a popular analysis tool that will be used to assess the environmental impact of the processes, services, and products of the algal biofuel processes investigated. The analysis considers all elements of the processes from the feedstock,

manufacturing, disposal, and production (Murthy, 2011). This assessment is crucial for analysing the feasibility of the processes for commercial use (Rajesh Banu *et al*., 2020).

(Pacheco *et al*., 2015) investigated the production of biohydrogen and pigments using *Spirogyra sp.* microalga biomass. The cradle-to-gate approach was used, and 1 kg of dry microalgae was considered the functional unit. The investigation found that energy consumption and CO_2 emissions are heavily impacted by harvesting, which uses centrifugation and heating of the fermentation unit. Additionally, it was noted that pigment extraction energy demands about 62% of the overall energy. However, though pigment production is less in quantity, the economic share is significant. In a comparative study previously touched on in the section above by (Dutta, Neto & Coelho, 2016), where two conversion pathways of microalgae-based biofuel processes were investigated, a life cycle assessment was conducted on SimaPro software. The conventional path, studied in Portugal, was found to have a higher greenhouse gas emission, 94% and an 84% fossil consumption due to its lipid extraction process. The integrated approach, studied in the USA, showed that the approach had a lower greenhouse emission, with the algae biomass process contributing 50% to total emissions.

(Gnansounou & Kenthorai Raman, 2016) performed an LCA on the production of diesel and its co-products using *Chlorellavulgaris* as the microalgal species. The well-to-wheel approach was used, and 1 kg of biodiesel was considered the functional unit. The investigation findings were that algal biofuel processes have less land usage, less than 95% of the land, and less CO_2 emission. Furthermore, algal biofuel systems have lower consumption of fossil oil which subsequently decreases the impacts.

In a LCA study where (Monari, Righi & Olsen, 2016) investigated the production of diesel from microalgae, *Nannochloropsis sp.*, cultivated in photobioreactors, it was noted that the algal biodiesel pathway has a higher energy demand and greenhouse emission. Additionally, the study identified that further improvement would have to be implemented to produce biofuels on an industrial scale. The approach used was the well-to-tank and the functional unit regarded was 1 MJ of biodiesel.

(Smetana *et al*., 2017) assessed the use of *Chlorella vulgaris* and *Arthrospira platensis*, and cynobacteria cultivation in autotrophic and heterotrophic conditions. The cradle-to-gate approach was used, and various functional units were considered, such as 1 kg of algal biomass, 1 kg of oil, and 1 kg of bulk proteins. The assessment noted that autotrophic and heterotrophic cultivation methods have higher environmental impacts, contrary to conventional methods.

(Dasan *et al*., 2019) performed a life cycle evaluation on microalgae biofuels production, focusing on the effects of cultivation on the carbon emissions, costs, and energy. The process used *Chlorella vulgaris* as the primary microalgal species, and its by-products were biodiesel and

bioethanol. The cradle-to-gate approach was used and 100, 000 kg of dry algae biomass for 340 days per annum was the functional unit. The study found that the process had a negative CO_2 balance and was not economically feasible. Furthermore, dewatering and lipid extraction respectively contributed 21 to 30 % and 39 to 57% of the total energy.

(Chen & Quinn, 2021) assessed the production of biofuels from microalgae through hydrothermal liquefaction. The well to wheel approach was used and the functional unit regarded was 1 MJ fuel. The baseline global warming potential was found to be +23 g CO_2 eq/MJ, significantly lower than conventional diesel, and the net energy ratio was 0,30. The study validated algae hydrothermal liquefaction as a greenhouse gas and energy-friendly alternative. As with most algal biofuel processes, algae cultivation requires more energy. The study suggested that other environmental impacts should be respected before considering hydrothermal liquefaction.

CHAPTER 3: MATERIALS AND METHODS

3.1 Introduction

This chapter outlines the methodology followed for this techno-economic assessment of algal biofuels processes. It provides in detail the selected algal biomass for this study and the criteria used for its selection. The software required for process modelling, mass and energy balances, economic analysis, equipment sizing, heat integration, and life cycle assessment were all described.

Techno-economic assessments are typically used in the chemical, energy, bioprocess, petroleum, and similar industries to analyse new technologies or optimise existing ones. The method analyses the economic performance of an industrial product, process, and service on a technical and economic basis using software modelling to estimate the operating cost, capital cost, and revenue (Burk, 2018). Ultimately the results are summarised and presented in visualisation tools such as sensitivity analysis graphs and tornado diagrams.

Techno-economic assessments follow a techno-economic model, which is an integrated process and cost model that incorporates elements of process synthesis, process modelling, equipment costing, capital and operating cost estimation. It can be performed using spreadsheet software or process simulators and has an expected accuracy of -30 % to + 50% (Bates *et al*., 2005).

Life cycle assessments are used to evaluate the environmental impact of a process, commercial product, and service. The assessment evaluates the environmental effects from the raw material extraction stage (cradle) to the final disposal or recycling stage (grave) (Ilgin & Gupta, 2010), (Curran, 2006). The analysis extensively considers all the energy and materials required for the process, product, or service and evaluates the corresponding emissions to the environment. The variants to the LCA are: the cradle-to-grave, cradle-to-gate, cradle-to-cradle or closed-loop production, gate-to-gate, well-to-wheel, economic input-output life cycle assessment, ecologically-based LCA, exergy-based LCA. Although its accuracy has been questioned in the past, it still plays a massive role in pollution studies, environmental impact assessments, and integrated waste management studies (Burnley, Wagland & Longhurst, 2019).

3.2 Feedstock selection

Many types of algal biomass exist and have been studied for the production of biofuels. On earth, more than 25 000 microspecies are available, but not all are suitable for use. Only a few can be considered in the biorefinery industry based on the quality and quantity of lipid accumulation. Both microalgae and macroalgae have been extensively studied for the production of biofuels. Additionally, much research on low and high lipid yielding macro and microalgae has been done.

For this study, microalgae with high lipid-yielding strains were selected as they have higher biofuels' productivity and simple cellular structures (Veeramuthu & Ngamcharussrivichai, 2021), higher growth rates, and higher energy productivity (Gao *et al*., 2020).

Many studies have been done on selecting suitable microalgal biomass to produce biofuels, but there is still no consensus on the best feedstock. However, aquatic unicellular green algae are generally used to produce biodiesel. This is because green algae have high growth rates, high lipid contents, and high population densities. In addition, green algae can potentially double its biomass under 24 hours if kept in good conditions (Demirbas & Fatih Demirbas, 2011). For this project, *Botryococcus sp* was selected as suitable microalgal biomass due to its accumulated high-level lipid content. *Botryococcus braunii* is a green unicellular microalga common in freshwater, reservoirs, brackish lakes, and ponds. *B.braunii* have 29-75 % oil productivity on a dry weight basis (Nagaraja *et al*., 2014).

According to (Dilia & Leila, 2018) the composition of B.braunii are as follows, lipids amount to 61%, carbohydrates 18,9%, proteins, 17,8%, carotenoids 1,2%, and chlorophyll-a amount to 0.4%. In the same study, the lipid composition of *B.braunii* was investigated. The results showed that the lipid content of the *B.braunii* contains oleic acid between 15,65-35,85%, linoleic acid between 3,05-23,15%, palmitic acid between 4,03-22,13 %, and stearic acid between 0,48-15,41%. Protein content in *B.braunii* consists of cysteine and arginine, with are essential amino acids that account for approximately 44,7% of the total amino acid profile (Dolganyuk *et al*., 2020). In another study (Tibbetts, Milley & Lall, 2014) added leucine, lysine, glutamic acid, and aspartic acid as protein compositions of *B.braunii*. The carbohydrate content in the biomass was found by (Gouveia *et al*., 2017) to contain galactose and glucose as the main sugars. Additionally, small amounts of fucose, arabinose and rhamnose were also detected (Gouveia *et al*., 2019). The elemental analysis of raw *B.braunii* is 75,7 ± 0,3 % C, 10 ± 1 % H, 1,81 ± 0,01 % N, 0,4 ± 0,1 % S, and 11 ± 1 % O. The HHV value is 40 ± 0.4 MJ/kg (Piloni *et al*., 2021). The feed components and mass fractions to be considered in this study are found in Table 3-1.

Table 3-1: Feed components and mass fractions.

Component	**Mass fractions**
Water	0.790307
Sucrose	0.005119
Algae lipids	0.010237
Triacylglycerides	0.01556
Algal cell moisture	0.007621
Glucan	0.068552
Algae proteins	0.05569
Ash	0.007166

Other cell components	0.039748

3.3 Process Simulation Methodology

All three algal conversion methods studied were simulated on Aspen Plus ®V12, an essential software in the designing of a new process and optimization of an existing process to improve its efficiency. The software allows the user to build and simulate a process model without performing complex calculations.

3.3.1 Property Method

The accuracy of simulation results is heavily dependent on the appropriate physical property method chosen. This physical property method is a collection of methods and models that Aspen Plus ®V12 uses to compute thermodynamic and transport properties. These thermodynamic properties include entropy, volume, enthalpy, Gibbs free energy and fugacity coefficient (K-values), while the transport properties include surface tension, viscosity, diffusion coefficient and thermal conductivity. Most of the property methods are built-in on Aspen Plus and are sufficient for most applications. Many of these methods have extensive built-in binary parameters, making them essentially predictive (Aspen Technology, 2000). The different methods to choose from have unique approaches to represent K-values.

The thermodynamic model used to simulate distillation columns was UNIQUAC to address the presence of polar compounds in the some of the processes (Gutiérrez Ortiz, 2020). However, the application of the UNIQUAC model is limited to low pressure conditions. Therefore, for equipment operating at high pressures and temperature predictive SRK (PSRK) was used as the base property method, which is the same model used by (Jones *et al*., 2014), (Chen & Quinn, 2021) for algal systems. Lastly, for separation of salts and neutralization of catalysts, the Electrolyte NRTL model, suitable for systems containing polar carbohydrates, was used (Varanda, Pinto & Martins, 2011).

3.3.2 Process Simulation Steps

The following procedures were followed to simulate the processes studied. The first step involves the construction of block and process flow diagrams based on the rigorous literature review in the precursory chapter. The second step was to identify the thermodynamic models and subsequently construct a process model on Aspen Plus for each process. During the second step, working conditions for each unit operation modelled and thermodynamic conditions were identified and inputted. All the process simulations modelled were perfectly adequate for determining the process properties of the processes investigated, which is essentially objective 3.

3.4 Mass and Energy Balances

Mass balances are essential in determining the amounts of raw material and the products that a process will produce. They are also essential in studying the plant operations and troubleshooting and can be used to locate sources of material loss or to check performance against design (Sinnott, 2005). Therefore, mass balance calculations are crucial in process design. Energy balance calculations are also imperative in process design because energy requirements of processes are determined, for example, the heating, the power and cooling required. Aspen Plus calculates the enthalpies of every stream through the enthalpies of formations for each component, which are available on the software.

3.4.1 Process Properties

The calculation of process properties is essential for comparative technoeconomic studies. The following details the equations used to perform calculations for scaling up, mass ratio, energy ratio, and process efficiencies. The Aspen Plus worksheet was extracted into Microsoft Excel where the calculations were performed.

Mass ratio

Mass ratios for each process were calculated using the equation 3.1.

$$\eta_m = \frac{mass\ of\ biofuel}{mass\ of\ biomass} \tag{3.1}$$

Energy ratio

Energy ratios based on biomass in the feed were calculated for each process using the equation 3.2.

$$\eta_e = \frac{|mass\ of\ biofuel\ x\ HHV\ of\ biofuel|}{|mass\ of\ biomass\ x\ HHV\ of\ biomass|} \tag{3.2}$$

Energy efficiency

Energy efficiency for each process was calculated using the equations below. To determine the amount of biomass energy converted into fuel energy the liquid fuel energy efficiency, $\eta_{liquid\ fuel}$ was calculated. Unlike the liquid fuel efficiency, the overall energy efficiency, $\eta_{overall}$ of the process will also include the electricity power produced, $E_{elec.power}$.

$$\eta_{liquid\ fuel} = \frac{|mass\ of\ biofuel\ x\ HHV\ of\ biofuel|}{|mass\ of\ biomass\ x\ HHV\ of\ biomass| - \frac{Power\ produced}{Eff.for\ biomass\ to\ elec}} \tag{3.3}$$

$$\eta_{overall} = \frac{|mass\ of\ biofuel\ x\ HHV\ of\ biofuel| + E_{elec.power}}{|mass\ of\ biomass\ x\ HHV\ of\ biomass|} \tag{3.4}$$

3.5 Heat Integration

Heat integration is a critical option for increasing energy efficiency in high-intensive plants such as chemical process plants and oil refineries. Various approaches can be used through heat integration to identify energy efficiency options. Three systems exist, approaches based on thermodynamics, physical insights, and strategies based on mathematical programming. A widely used method for heat integration in the industry is Pinch Analysis which combines these approaches.

This analysis is a systematic approach that aids in identifying possible heat integration problems. It is based on thermodynamics and physical insights. Pinch analysis identifies the amount of internal heat exchanging that can be done and the amount of external heating and cooling that is needed (Turton, 2013). "Pinch" refers to the point in a system of multiple heat or mass exchange networks where the driving force for mass or energy is at a minimum. Designing these networks involves identifying the pinch point, thereby using that information to design the whole network. This process is referred to as pinch technology (Turton, 2013).

Energy management of the simulated processes was achieved on Aspen Plus using the Aspen Energy Analyzer (AEA) tool. The AEA is a tool that is used to minimise process energy by performing optimal heat exchanger network design and retrofit. As a result, the tool cuts down avoidable energy use and heat exchanger network emissions that are energy-related for a more cost-effective and sustainable process design. In addition, by utilising the AEA, a reduction in operating, capital and design costs is expected (AspenTech, 2021). The following steps were used to conduct heat integration for each process using the Aspen Energy Analyzer (AEA). This is an iterative method.

- A base case was constructed; this is a simulation without heat integration.
- A pinch analysis was performed on the base case by determining the duties of the streams needing heating and cooling and the maximum heat-recovery possible.
- Heat integration was performed that is clear from inspection by adding heat exchangers one at a time into the base case. Typically, heat exchangers are added till all reasonable heat integration is reached.
- The remaining duties were inputted into Aspen Energy Analyzer.

3.6 Economic Feasibility

3.6.1 Equipment Sizing and Cost Estimation

Once the mass and energy balances calculations for all the investigated processes are performed, sizing and costing of equipment must be performed to fulfil objective 4 of this study, which is determining the economic feasibility of the studied process. The mass and energy balances in

Aspen Plus and literature sources were used to perform the sizing and cost of equipment on Aspen Icarus, also known as Aspen Capital Cost Estimator (ACCE). The ACCE accurately predicts the size and price of standard equipment such as compressors, flash drums, distillation columns, and separators. To accurately perform sizing and costing of equipment on the software, the simulated processes in Aspen Plus were imported into the ACCE, and additional specific information such as the material of construction and process unit orientation were entered.

3.6.1.1 Equipment Cost Updates

Since literature sources were used for the sizing and costing of equipment, equation 3.6 was used to update the equipment costs. The base size and base cost were considered to be values from literature, and the scaling factor (n) was also derived from literature sources. As the cost estimation of equipment was performed by using literature sources with different years, equation 3.6 was used to update the costs to the year of the investigation. The Chemical Engineering Plant Cost Index (CEPCI) was essential for these calculations (Chen & Quinn, 2021).

$$New\ cost = Base\ cost\ x\ \left(\frac{New\ size}{Base\ size}\right)^{n} \tag{3.5}$$

$$New\ cost\ at\ 2021 = Base\ cost\ x\ \left(\frac{CEPCI\ in\ 2021}{CEPCI\ at\ base\ year}\right) \tag{3.6}$$

3.6.1.2 Installation costs

The ACCE is also valuable for estimating installation costs. Equation 3.7 was used to determine the installation costs for the investigated processes. The installation factor for the equipment cost on the ACCE was either determined using the ACCE. For that equipment not available on the software, the values were derived from literature.

$$Installation\ cost = \ Purchased\ equipment\ cost\ x\ installation\ factor \tag{3.7}$$

3.6.2 Economic Analysis Methodology

An economic analysis is a critical tool for comparing the investigated processes. This stage is used to determine the potential of each of the processes in the marketplace. The economic analysis for each of the processes studied will be based on the total mass and energy balances performed on Aspen Plus in the earlier stages of the project. All calculations for this analysis were performed in Microsoft Excel.

3.6.2.1 Capital Investment

Capital investment refers to the amount of money used to enhance a production process's objectives. First, a preliminary estimate of the plant costs of each process will be performed. Then, according to (Sinnott, 2005), an accuracy of ±30% can be expected. The calculation method used to determine the fixed capital investment (FCI) and the total capital investment (TCI) was obtained from the works of (Davis *et al*., 2014), (Jones *et al*., 2014). As purchased and installed

costs are determined in the equipment sizing and cost estimation stage, additional costs (direct and indirect) are to be determined. The TCI would then be the sum of the FCI, land cost, and working capital.

3.6.2.2 Variable operating cost

Variable operating cost (VOC) is the expenses that change with the production rate. Examples of such costs include raw material, electricity, waste disposal, and recurring costs. The latest available information costs and the processes' mass and energy balances were used to determine the variable operating costs. In addition, literature was used to source the base raw material costs and other main variable operational costs for the different processes.

3.6.2.3 Fixed operating cost

Fixed operating costs (FOC) refer to the expenses that do not change with the plant operation rate. These costs are incurred regardless of plant productivity. Examples of the expenses include various overhead items and labour costs. The method used to perform these calculations was based on reports by (Davis *et al*., 2014), (Jones *et al*., 2014).

3.6.2.4 Discounted cash flow analysis

Discounted cash flow analysis is a model used to estimate the current value of the investment based on projected cash flows. Once the TCI, VOC, and FOC were determined, a cash flow analysis was performed based on literature.

3.6.2.5 Economic sensitivity analysis

Sensitivity analysis helps determine the effects of changing economic parameters (Odoki, Stannard & Kerali, 2006). This is a vital step in a techno-economic study as much uncertainty is involved in the evaluation. Sensitivity analysis parameters considered include the cost of raw materials, internal rate of return, the selling price of products, etc.

3.7 Life Cycle Analysis Methodology

To assess the environmental impact of the algal biofuel processes, the LCA method was selected. The technique involves four critical stages that are standardised by the international standards ISO 14040 and 14044:

1. Goal and scope definition
2. Life Cycle Inventory (LCI)
3. Life Cycle Impact Assessment (LCIA)
4. Interpretation

The fourth stage occurs throughout the other steps, as shown in Figure 3-1. The software used for the LCA was openLCA, an open-source software.

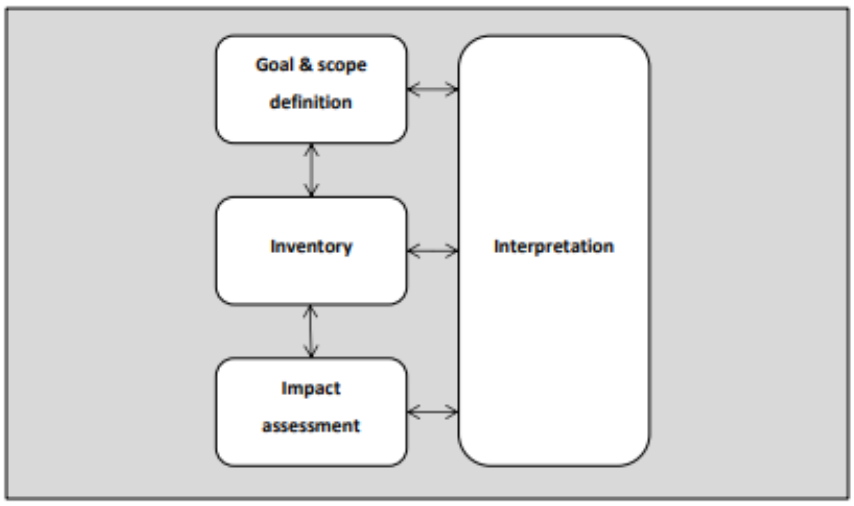

Figure 3-1: Interaction of four phases of a LCA.

3.7.1 Goal and scope definition

The intended application of the product, system boundary and functional unit is fundamental modelling elements of the LCA described in Phase 1 (Sharifzadeh *et al*., 2019).

Description of LCA scenarios

This study focuses on four biofuels; therefore, four LCA scenarios were considered. The environmental impact of the conversion of microalgae to:

1. Biodiesel
2. Biomethane
3. Biohydrogen
4. Bioethanol

System boundary

System boundaries for each scenario were established employing the cradle-to-gate approach. The cradle in all methods was the microalgae harvesting, and the gate was the biorefinery, not product application.

Functional unit

The functional unit for all scenarios was decided. The functional unit of 1kg bioproduct produced was used to compare all scenarios and fossil fuel production.

Allocation procedure

Most of the processes investigated in this study produce more than one output product. Therefore, it is essential to allocate the environmental impacts of the processes across the desired products and the co-products. Environmental impact can be allocated by physical relation (mass or energy),

economic value, and volume. The most used are physical relation and economic value. Allocation by mass was selected for all four scenarios investigated.

3.7.2 Life cycle inventory analysis

For each unit operation, inventory data related to all inputs and outputs across the system boundary were sourced and entered into openLCA to compare the environmental impact of each scenario in the third stage.

3.7.3 Life cycle impact assessment

LCIA is a stage for evaluating the potential impacts of the investigated processes. This is accomplished by converting the LCI results into specific impact indicators. The evaluation involves selecting impact categories for analysis, assigning the LCI results to different types (classification), and lastly, calculating the potential impact indicators (characterisation) (Mu, Xin & Zhou, 2019).

In this third stage, all four scenarios were compared using the CML-IA baseline methodology for characterisation. Impact categories evaluated were global warming, eutrophication, acidification, toxicity, and abiotic depletion.

CHAPTER 4: PROCESS DESIGN BASIS

4.1 Introduction

This chapter describes the technology selection for the investigated processes (section 4.2). This includes process descriptions, including relevant BFDs for the investigated processes (section 4.4).

4.2 Process and equipment selection

4.2.1 Cultivation selection

Open raceway ponds were selected as a suitable technology for biomass production because they are cheaper to build and operate. They are also easily scaled up to several metres, making them a convenient alternative for commercial-scale biomass production. Furthermore, many commercial microalgal biomass processes, about 95%, use open raceway ponds. This is also the case for high-value-added bioproducts which are significantly profitable (Veeramuthu & Ngamcharussrivichai, 2021).

4.2.2 Harvesting selection

Sedimentation was selected as a suitable technology for harvesting microalgae because it is easy to operate, economical, and has potential for water recycling. Additionally, chemical flocculants will be used to improve the efficiency of harvesting. However, this still makes the harvesting technology economical as flocculation is low in costs, has low cell damage (Rawat *et al*., 2013), is easy to control, has a lower operating time, and requires less energy (Peralta-Ruiz, Obregon & González-Delgado, 2018).

4.2.3 Extraction selection

Chemical solvent extraction was selected as a suitable method because it is a standard method. Furthermore, lipid extraction using chemical solvents is easy because chemical solvents are easily accessible and have high selectivity and solubility towards lipids (Mujeeb, Vedamurthy & Shivasharana, 2016), thus producing high oil yields. In addition, the method is quick, repeatable and has reproducible results (Jahirul *et al*., 2013).

4.2.4 Thermochemical Conversion Technology Selection

HTL was selected as a suitable conversion method because (Yang *et al*., 2017); it produces higher bio-oil yields, lower char yields, lower energy consumption ratio, and bio-oil with higher energy density. Bio-oil may contain up to 75% of the energy of the original biomass (Jena & Das, 2011)). In addition, the method yields bio-oil with superior fuel properties such as thermal and storage stabilities, converts high moisture algae (> 80% moisture) and eliminates the energy consumption of water evaporation and dewatering of the whole algae cell. Thus the biomass is not limited to

high-lipid strains (Jones & Snowden-swan, 2021), has a versatile chemistry, improved selectivity, and scalable (Martinez-Fernandez & Chen, 2017), has significant carbon recovery yields.

The main components of biocrude oil from the HTL reactor are classified into the following functional groups; aliphatic, aromatic, alcohols, phenols, and furans. The components in the aliphatic functional group include octadecanoic acid ($C_{18}H_{36}O_2$). The component in phenols is bisphenol ($C_{15}H_{16}O_2$) and dibenzofuran ($C_{12}H_8O$) in furans. In a study on the HTL of *Botryococcus braunii*, green colonial microalgae (Ren *et al*., 2018) found that oleic acid ($C_{18}H_{34}O_2$), n-Hexadecanoic acid ($C_{16}H_{32}O_2$) were the few aliphatic acids present in significant amounts in the evaluated biocrude oil. The alcohol compound found was 1-Hexadecanol ($C_{16}H_{34}O$), and the aromatic compound was 1,3 Dimethylbenzene (C_8H_{10}).

Chemical conversion

Alkali transesterification was found as a suitable technology for biodiesel production because it is simple to extract esters, is the most adopting method, and is cheaper than enzymatically catalysed transesterification (Math & Chandrashekhara, 2016). In addition, it has a fast reaction time under atmospheric pressure and moderate temperature conditions (323,15-343,15 K) and produces a higher biodiesel yield. Furthermore, alkali transesterification is 4000 times faster than acid-catalysed transesterification (Okoronkwo, Galadima & Leke, 2012).

The solids produced in HTL will be used to produce activated char, which is a valuable by-product in varying ways. The activation of char requires the KOH as a chemical activator. During the process, gaseous components such as water vapour, carbon monoxide, and hydrogen are removed to produce highly porous activated char (Masoumi & Dalai, 2021). For simplicity of the project, the section was not simulated.

4.2.5 Biochemical Conversion Technology selection

Anaerobic digestion and fermentation were selected as suitable technology for bioethanol and biogas production. Anaerobic digestion is a robust and well-established technology. Additionally, it is simple to use, cost-effective has a high energy output to input, and is an environmentally beneficial technology. On the other hand, consolidated bioprocessing (CBP) was selected as a suitable technology for the fermentation of sugars because it is a cost-effective technology that is less energy-intensive, offers more straightforward microalgal processing, and has higher conversion efficiencies (Levin *et al*., 2015). For simplicity of the study, the consolidated bioprocessing will be modelled using a typical fermentation reactor setup which was used in the study by (Jones *et al*., 2014).

4.3 Process synthesis

4.3.1 Process descriptions

Process descriptions accompanied with block flow diagrams for the thermochemical and biochemical conversion are given in this section. The diagrams show detailed structures of the processes while also displaying an overview of the utilities. Both process modelling scenarios examined assume that feedstock with 20% solids is delivered after upstream dewatering.

4.3.1.1 Thermochemical conversion

The thermochemical conversion consists of the following sections:

- Feed preparation: The whole w*et al*gal biomass with 20 wt% solids is pumped and heated.
- HTL processing section: The algal biomass is depolymerised through thermal cracking, dehydration, and decarboxylation. Water under supercritical or subcritical conditions acts as a catalyst in this process.
- Hydrotreating processing section: Hydrogen is used as a reactant at high reaction temperatures and pressures with a high activity catalyst to remove contaminants in the biocrude oils. Here, hydrogen removes the high oxygen content and other heteroatoms in biocrude oils.
- Hydrocracking processing section: The process uses hydrogen as a reactant at high pressures and in the presence of an increased activity catalyst to remove contaminants. Here, the heavy oils and residues are converted into lighter fractions.

The block flow diagram for the process is shown in Figure 4-1.

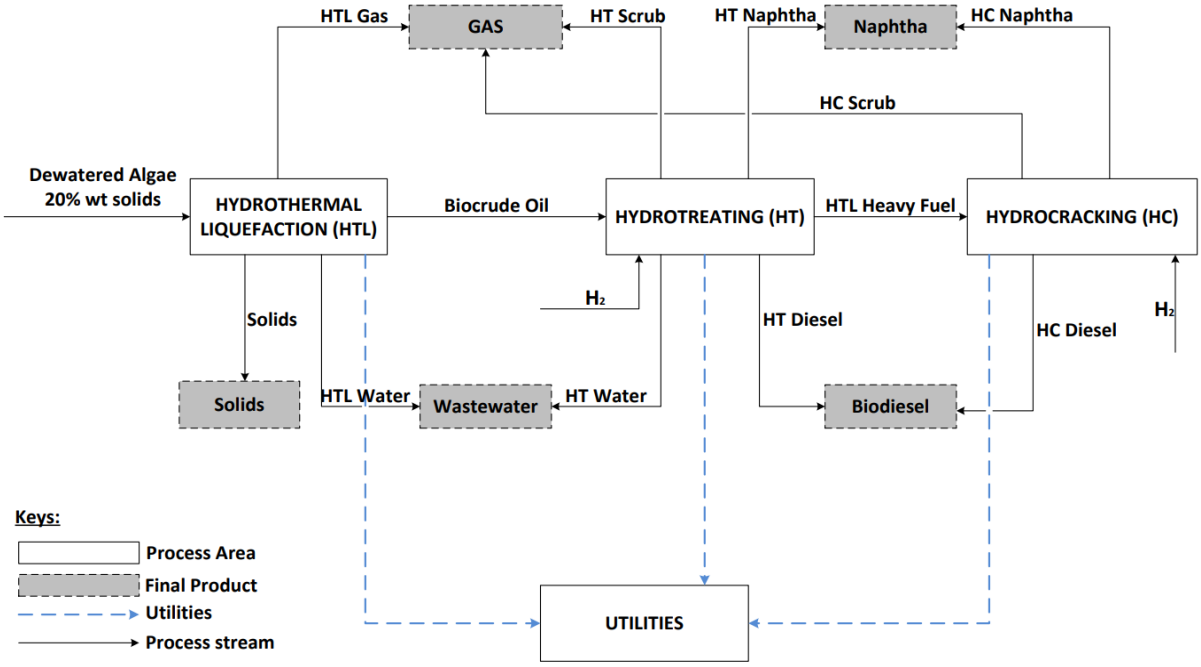

Figure 4-1: A simplified block flow diagram of the thermochemical conversion method.

The biochemical conversion consists of the following sections:

- Feed preparation: The whole wet algal biomass with 20 wt% solids is pumped along with dilute sulphuric acid, which is heated.
- Pre-treatment and conditioning: The biomass and dilute sulphuric acid are fed into the pre-treatment reactor, where compounds are broken down into monomeric sugar constituents. The hydrolysate slurry is flashed, vaporising a fraction of the water. The hydrolysate is fed to the conditioning reactor. Conditioning requires the addition of dilute ammonia (ammonia gas with dilution water) to raise the pH of the hydrolysate to 5.
- Fermentation: The hydrolysate from pre-treatment is fermented using *Saccharomyces cerevisiae* (yeast) to ethanol.
- Purification: The fermentation broth is fed to the beer distillation column, rectification distillation column, and the vapour-phase molecular sieve adsorption. This step results in a pure bioethanol product.
- Anaerobic digestion: Waste streams are fed anaerobic digesters to recover valuable nutrients. A gas turbine is used to generate power.

The block flow diagram for the process is shown in Figure 4-2.

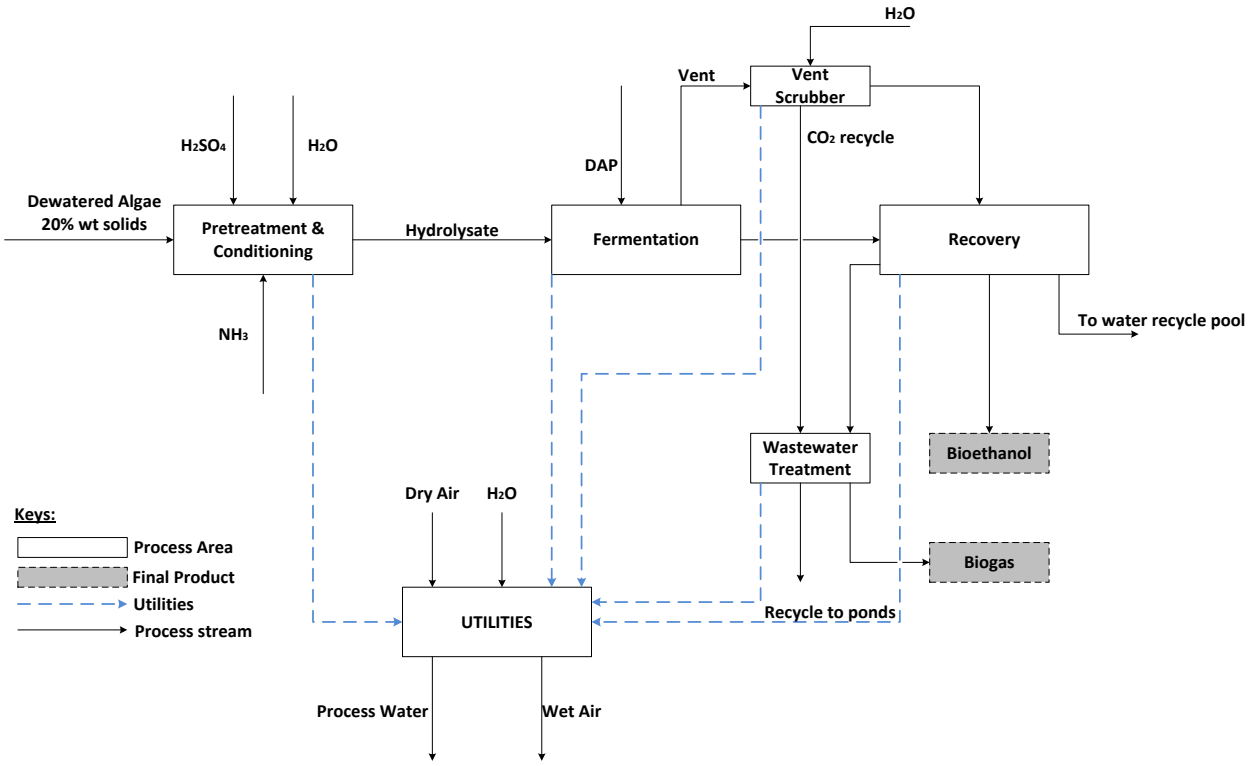

Figure 4-2: A simplified block flow diagram for the biochemical conversion method.

CHAPTER 5: RESULTS AND DISCUSSION

5.1 Introduction

This chapter overviews essential process design aspects for the investigated processes. This includes the PFDs used for the investigation, process simulation, results from mass and energy balance calculations obtained from Ms Excel through Aspen Plus simulations (section 4.2), preliminary equipment sizing and cost estimations from Aspen Capital Cost Estimator (section 4.3), heat integration from Aspen Energy Analyzer (section 4.4), process economic analysis from Ms Excel (section 4.5), and life cycle analysis from OpenLCA (section 4.6).

5.2 Process Flow Diagram

5.2.1 Thermochemical conversion

The thermochemical conversion was synthesised into three primary processing sections. These include the HTL processing, the HT processing, and the HC processing.

The thermochemical conversion PFD consists of the following sections:

- Feed preparation: The whole w*et al*gal biomass with 20 wt% solids enters at 298 K and 1.01 bar. The feed is pumped to 220 bar and further heated to 625 K.
- HTL processing section: The algal biomass is treated through the HTL reactor (R-301) operating at 625 K and 220 bar. The treated biomass is further flashed (SEP-01) to separate the gaseous phase from the aqueous phase. The aqueous stream is then separated (SEP-02) to remove the solids, and the stream is further separated in (SEP-03). The resulting aqueous stream is further split (M-01), where 90% of the aqueous stream is recycled to the (SEP-02), while 10 % of the aqueous stream is used in pre-treatment (HX-01).
- Hydrotreating processing section: The HTL oil is fed into the hydrotreating reactor (R-310Y) operating at 448 K and 105 bar. Hydrogen is also fed into the reactor to remove high oxygen contents found in bio-oils. The resultant stream is cooled and separated (SEP-04), where the gaseous stream is recycled to the feed preparation section. The aqueous stream is further separated to remove scrubs and water. The aqueous stream is then sent through a series of distillation columns, D-01, 02, 03. The resulting light streams for these are scrubs, naphtha, and diesel.
- Hydrocracking processing section: The heavy oil stream from the HT section is heated before being fed into the HC reactor (R-350Y), operating at 668 K and 70 bar. The resulting stream is then separated (SEP-06) to remove the gaseous phase. The heavy stream is then fed into a distillation column (D-04), where naphtha is the resultant light

stream and diesel is the heavy stream. The figure below shows the PFD for this process. A stream table for the simulation can be found in Appendix B.1.

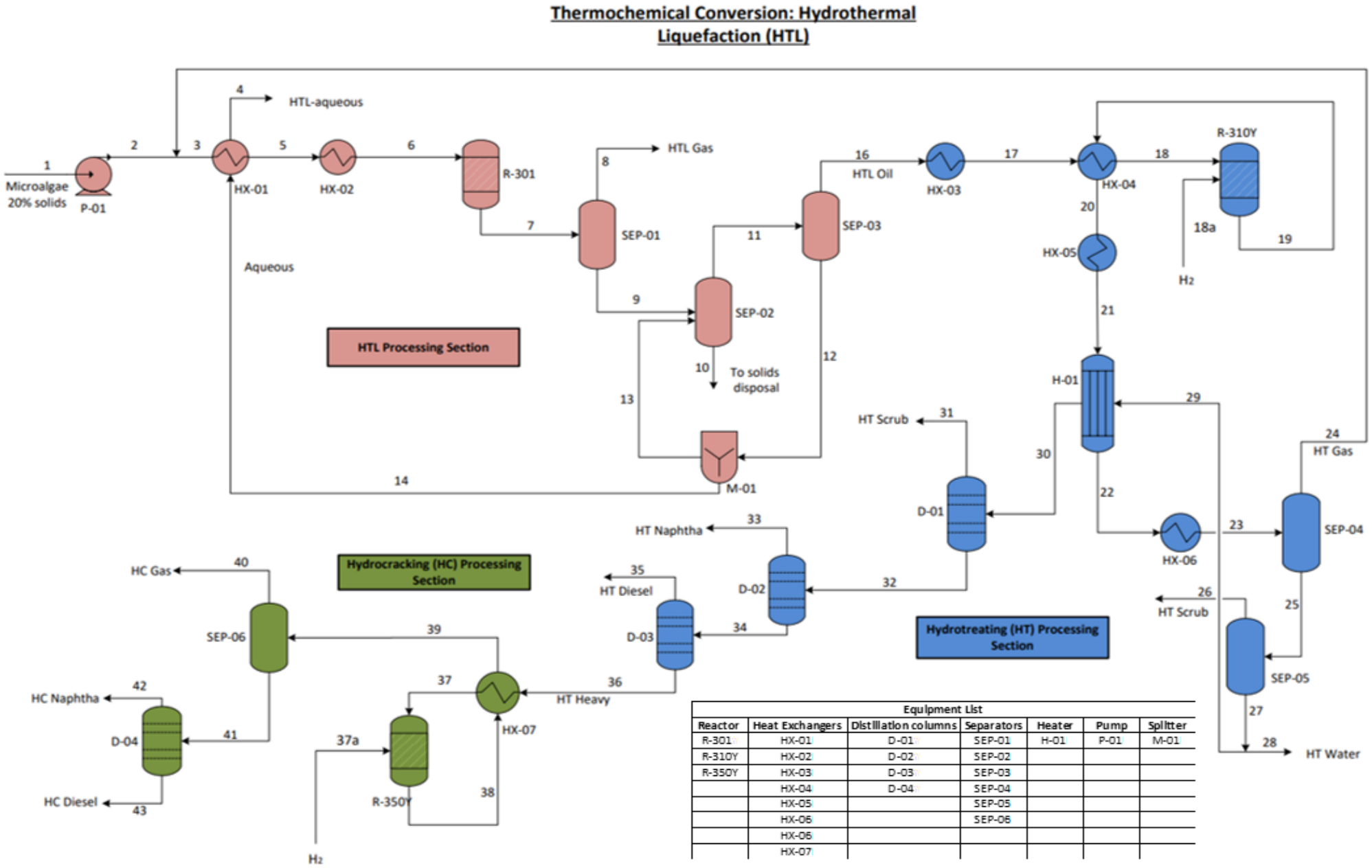

Figure 5-1: PFD of the thermochemical conversion.

5.2.2 Biochemical conversion

The biochemical conversion PFD consists of the following sections:

- Feed preparation: The whole wet algal biomass with 20 wt% solids was fed at 298 K and 1,01 bar. Steam fed at 444 K, and the wet algal biomass was fed into a heater to increase the feed temperature. After that, the heated wet algal biomass was mixed with dilute sulphuric acid (10 wt% H_2O), and more steam was added to further increase the temperature of the feed before entering the pre-treatment reactor.
- Pre-treatment and conditioning: The biomass and dilute sulphuric acid were fed into the pre-treatment reactor operating at 425 K and 4,96 bar. The resulting hydrolysate slurry was cooled and flashed, keeping 20 wt% solids in the hydrolysate and vaporising a fraction of the water. The hydrolysate was fed into the conditioning reactor operating at 373,15 K and 1,01 bar. Dilute ammonia was also fed for conditioning or neutralisation.
- Fermentation: The conditioned hydrolysate was cooled before entering fermentation. The operating conditions for the seed train and fermentation reactors were 310,15 K and 1,01 bar. Diammonium Phosphate (DAP) was fed into both reactors. The fermentation vent was sent to the vent scrubber to recover the additional ethanol.
- Purification: The fermentation broth was collected in the beer well and then sent to the beer distillation column. The stillage was sent to anaerobic digestion, and the gaseous stream was sent to the vent scrubber. The ethanol stream was fed into the rectification distillation column, where the heavy stream was sent to the water pool, and the light stream was sent for molecular sieve adsorption for further purification. This configuration results in a 99,7 wt%.
- Anaerobic digestion: Spillage from the beer column and other waste streams were fed into an anaerobic digestor. The figure below shows the PFD for this process. A stream table for the simulation can be found in Appendix B.2.

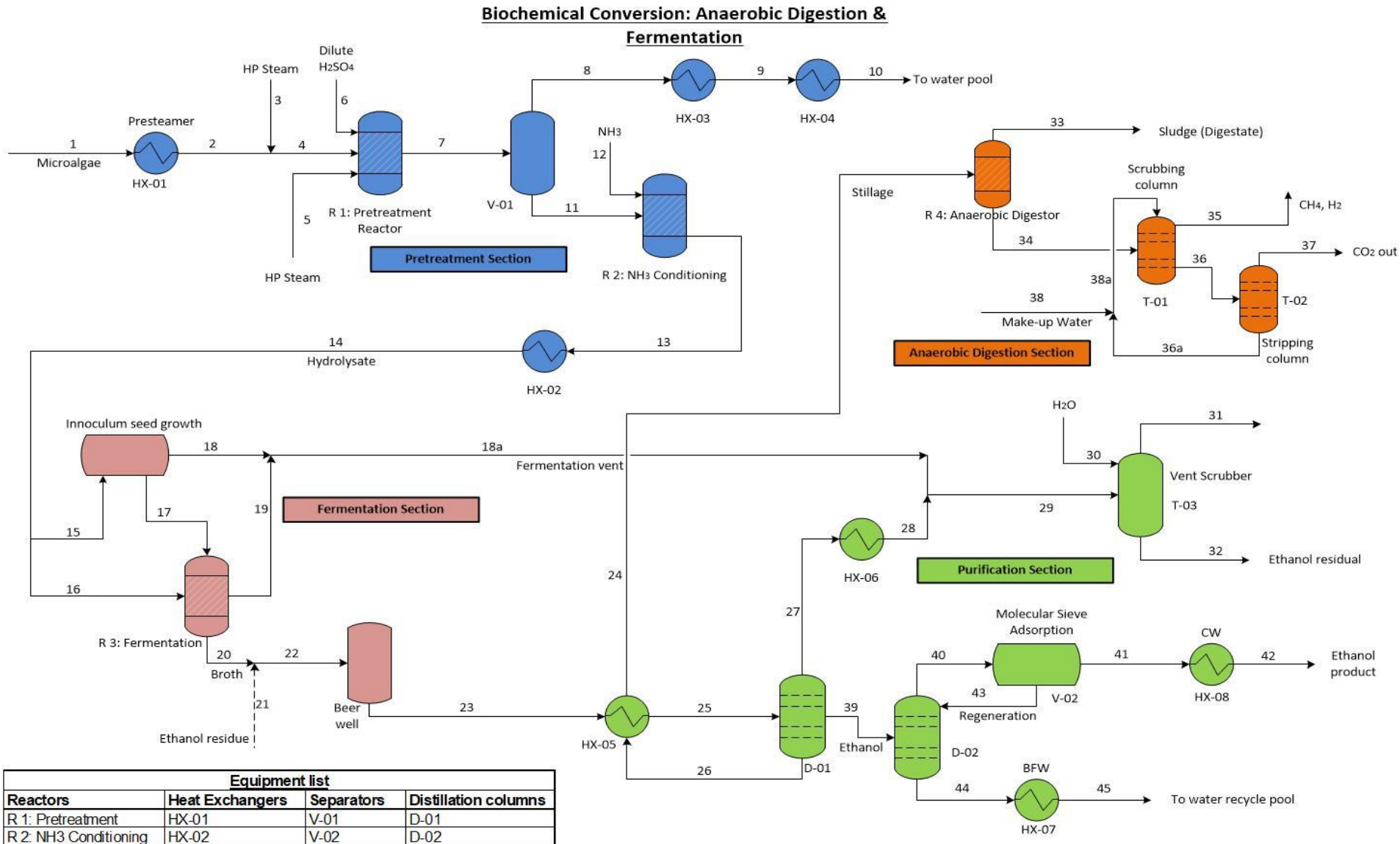

Equipment list			
Reactors	**Heat Exchangers**	**Separators**	**Distillation columns**
R 1: Pretreatment	HX-01	V-01	D-01
R 2: NH3 Conditioning	HX-02	V-02	D-02
R 3: Fermentation	HX-03	T-01	
Innoculum seed growth	HX-04	T-02	
R 4: Anaerobic Digestor	HX-05	T-03	
	HX-06		
	HX-07		
	HX-08		

Figure 5-2: PFD of the biochemical conversion method.

5.3 Process Simulation

5.3.1 Thermochemical conversion simulation

The process starts when algal biomass is fed at 298,15 K and 1,01 bar with a 20 wt% solids content. The whole wet algae slurry is heated and fed to the HTL reactor R-301 at 623,15 K and 210,11 bar. The HTL reactor was simulated as an RYield model. Yields for individual compenents were retained proportional within their product phase. The mass fraction of a component in the product was defined, regardless of the yield of the product. This assumption excluded ash, water, and dissolved salts. The reactor was modelled as an isothermal, and the heat of the reaction was assumed to be negligible. The yield specifications of the model were sourced from (Jones *et al*., 2014), (Chen & Quinn, 2021) and can be found in Appendix A. The products were then separated in V-301, a two-phase separator. The gaseous phase was released while the aqueous stream was further separated in F-301 to extract the solids content from the HTL aqueous stream. The HTL biocrude oil was cooled before being fed together with hydrogen into a hydrotreating reactor R-310Y operating at 673,15 K and 104,46 bar. The hydrogen used was assumed to be 4,3% of the biocrude flow rate (Chen & Quinn, 2021). The assumption was informed by experimental studies that found the range of 3,9-5,2% for hydrogen. The yield specifications for the model can be found in Appendix A.

The biocrude oil was then separated to remove scrubs and ammonia. The biocrude stream is then fed into the purification section, where a series of distillation columns were modelled as Radfrac. The product streams from purification included scrubs from T-301, naphtha from T-320, biodiesel and heavy oil from T-330. The heavy oil stream was further fed into the hydrocracking section. In this section, the heavy oil is heated and fed together with a hydrogen stream into the hydrocracking reactor R-350Y operating at 673,15 K and 70,32 bar. The yield specifications for this model can be found in Appendix A. The flow rate of the H_2 stream was assumed to be 2% of the heavy oil flow rate based on experimental studies on hydrocracking (Chen & Quinn, 2021). Furthermore, it was assumed that the H_2 used for the upgrading was purchased from an off-site facility close by.

The resulting stream is cooled and flashed to remove gases in V-375, operating at 333,15 K and 69,36 bar. Next, the stream was flashed again in V-351, operating at 333,37 K and 20,68 bar. The aqueous stream was then fed into a distillation column T-350, where more naphtha and biodiesel were produced. The hydrotreating and hydrocracking were modelled directly from (Jones *et al*., 2014). Regardless of the simulated conditions, the naphtha and biodiesel produced were assumed to have a constant specific energy. A summary of all the distillation columns used in this process can be found in Appendix A.

5.3.2 Biochemical conversion simulation

The process starts when algal biomass with a 20 wt% solids content is fed into A100. The biomass is heated by passing the feed stream through a pre-steamer and adding high-pressure steam. The heated stream is then fed into the pre-treatment reactor R-101 with dilute sulphuric acid. The operating conditions for the reactor are 425 K with a zero vapour fraction. The reactor is modelled as an RStoic, and the model's specifications are summarised in Table 5-1. The reactions and assumed conversions were sourced from (Davis *et al*., 2014).

Table 5-1: Specifications of the R-101 model.

Rxn No.	**Conversion**	**Reactant**	**Reaction**
1	90%	Glucan	Glucan + H_2O → Glucose
2	0,3%	Glucan	Glucan → HMF + 2 H_2O
3	100%	Sucrose	Sucrose →2 H_2O + HMF + Glucose

The product stream is cooled and flashed at 403,15 K and 2,66 bar. The vapour stream is cooled and sent to the water pool, while the hydrolysate is fed with diluted ammonia to the conditioning reactor R-102. The operating conditions of the reactor are 373,15 K and 1,01 bar. The specifications of the model are summarised in Table 5-2. The reactions and assumed conversions were sourced from (Davis *et al*., 2014).

Table 5-2: Specifications of the R-102 model.

Rxn No.	**Conversion**	**Reactant**	**Reaction**
1	100%	Acetic Acid	Acetic Acid + NH_3 → Ammonium Acetate
2	100%	H_2SO_4	H_2SO_4 + 2 NH_3 → NH_4SO_4
3	1%	Arabinose	Arabinose → Tar
4	0%	Glucose	Glucose → 1,2 Tar
5	1%	Galactose	Galactose → 1,2 Tar
6	1%	Mannose	Mannose → 1,2 Tar
7	0%	Sucrose	Sucrose + H_2O → 2,4 Tar

The resultant stream is then cooled and sent into the fermentation area. Fermentation requires DAP for the reaction to occur successfully. The DAP used for fermentation is assumed to be purchased from an off-site facility. The hydrolysate stream is split, where 10% of the stream is directed to the inoculum seed growth reactor R-201, operating at 305,15 K and 1,01 bar. The specifications of the reactor are summarised in Table 5-3. The reactions and assumed conversions were sourced from (Davis *et al*., 2014). *S. cerevisiae* is modelled as Zymo, *Zymomonas mobilis*.

Table 5-3: Specifications of the R-201 model.

Rxn No.	Conversion	Reactant	Reaction
1	55%	Glucose	Glucose → 2 Ethanol + 2 CO_2
2	40%	Glucose	Glucose + 0,3704 Protein + 0,018 DAP → 6 Zymo + 2,4 H_2O

The rest of the hydrolysate is fed into the fermentation reactor R-202 operating at 310,15 K and 1,01 bar. The specifications of the reactor are summarised in Table 5-4. The reactions and assumed conversions were sourced from (Davis *et al*., 2014).

Table 5-4: Specifications of the R-202 model.

Rxn No.	Conversion	Reactant	Reaction
1	95%	Glucose	Glucose → 2 Ethanol + 2 CO_2
2	2%	Glucose	Glucose + 0,3704 Protein + 0,018 DAP → 6 Zymo + 2,4 H_2O

The resulting broth from R-202 was flashed in V-202. The flash operated at 1,01 bar and zero duty. The resulting broth from R-201 was flashed in V-201 and heated before being fed into R-202. The vent from the flash drum was sent to the vent scrubber. The hydrolysate was heated and then sent into purification. The first distillation column, T-301, produces ethanol and a gaseous stream. The gaseous stream is mixed with the fermentation vent and fed to a vent scrubber T-303. With the addition of water, the scrubber separates the ethanol residue and CO_2, which is recycled into the ponds. The ethanol stream from T-301 was further purified in T-302, where the resulting water stream was sent to the water recycle pool and the ethanol stream was passed through molecular sieve adsorption and the cooled. The specifications of the distillation columns can be found in Appendix A. The number of stages used for all purification models was sourced from (Davis *et al*., 2014).

The stillages produced in the T-301 and the wastewater stream produced from vent scrubbing were fed into two anaerobic digesters, R-501 and R-502, operating at 308,15 K and 2,03 bar. The gaseous stream was then fed into a scrubbing column where biogas was produced. Finally, the aqueous stream was stripped to produce CO_2 and water. Both R-501 and R-502 reactors were modelled as RYield. The specifications for these models are summarised in Appendix A. The assumed yields used were sourced from (Humbird *et al*., 2011).

5.4 Mass and Energy Balances

This section reports the results of the mass and energy balance calculations completed on MS Excel. The calculations were based on stream results extracted from the process simulations modelled on Aspen Plus for each method investigated. This section is essential in determining

each method's mass, energy efficiencies, and other significant parameters. In addition, these process parameters indicate the potential of each process.

5.4.1 Thermochemical conversion

Overall mass balance calculations for the thermochemical method are summarised in Table 5-5. The error percentage of the calculations was 6,05e-05 % which is a reasonably low error figure. A full PFD and streams table is found in Appendix A.

Table 5-5: Overall mass balances for the thermochemical method.

Stream Name	**Mass In (kg/hr)**	**Stream Name**	**Mass Out (kg/hr)**
FEED	75428,19	**BIODIESL**	4939,12
H2O	335,83	**NAPHTHA**	973,99
		A100SOL	2312,32
		A100H2O	65266,16
		A100GAS	2272,40
Total (kg/hr)	**75764,02**		**75763,98**

Overall energy balance calculations are summarised in Table 5-6. The error percentage of the calculations was 9,62% which is an acceptable error percentage.

Table 5-6: Overall energy balances for the thermochemical method.

Stream Name	**Enthalpy In (MW)**	**Stream Name**	**Enthalpy Out (MW)**
FEED	-283,82	**BIODIESL**	-1,73
H2O	0,05	**NAPHTHA**	-0,44
		A100SOL	-0,63
		A100H2O	-273,45
		A100GAS	-4,08
Total (MW)	**-283,82**		**-280,30**
Equipment Energy Summary			
Energy required (MW)	42,23		
Energy released (MW)	-13,04		

The process mass intensity (PMI) is a mass-based metric defined as the ratio of the total mass of feedstock to the mass of processed material (Monteith *et al.*, 2020). The metric is essential in evaluating improvements towards a sustainable process. The PMI for the thermochemical was found to be 12,76. This means that for every kg of biofuels produced, 12,76 kgs of microalgae are employed. A lower value of PMI means a more efficient process. The mass ratio of the process was calculated to be 0,39.

Energy is associated with high costs; hence it is vital to know the energy intensity of a process. High energy intensity means a high cost of converting energy into the final product. The energy intensity of the process is -172,79 MJ per kg of biofuels processed. This energy intensity indicates that the plant is associated with high costs. The energy ratio of the process was found to be 0,39, and the energy efficiency of 47,45%. Therefore, the conversion of the process is 100%.

5.4.2 Biochemical conversion

Overall mass balance calculations for the biochemical method are summarised in Table 5-7. The error percentage of the calculations was 0,0003 % which is a reasonably low error figure. A PFD with a complete streams table is found in Appendix A.

Table 5-7: Overall mass balances for the biochemical method.

Stream Name	**Mass In (kg/hr)**	**Stream Name**	**Mass Out (kg/hr)**
DA	1,00	**S51**	5133,58
DAP	10500,00	**S54**	26672,78
DAP2	12500,00	**S73**	9668,50
H2O	7751,00	**S75**	140757,53
NH3	1100,00	**S121**	2014613,62
S1	75428,19	**WA**	101,73
S3	20000,00		
S5	1420,00		
S8	35000,00		
S34	15500,00		
S110	2017740,81		
Total (kg/hr)	**2196941,00**		**2196947,74**

Overall energy balance calculations are summarised in Table 5-8. The error percentage, which reflects the energy into the process and out of the process, was 11,72% which is an acceptable error percentage.

Table 5-8: Overall energy balances for the biochemical method.

Stream Name	**Enthalpy In (MW)**	**Stream Name**	**Enthalpy Out (MW)**
DA	0	**S51**	-8,57
DAP	-26,27	**S54**	-61,79
DAP2	-31,27	**S73**	-20,86
H2O	-34,09	**S75**	-615,41
NH3	-0,83	**S121**	-8870,83
S1	-290,61	**WA**	-0,44
S3	-73,04		

S5	-3,41		
S8	-127,83		
S34	-68,30		
S110	-8884,13		
Total (kW)	**-9539,78**		**-9577,90**
Equipment energy summary			
Energy required (MW)	-596,12		
Energy released (MW)	558,07		

The PMI for this process was 5,10. This means that for every kg of biofuels produced, 5,10 kgs of microalgae are used. A lower value of PMI means a more efficient process. The mass ratio was calculated to be 0,98. The conversion of the biomass was assumed to be 100%. The energy intensity of the process is -70,68 MJ per kg of microalgae processed. The energy ratio was found to be 0,7286, and the energy efficiency was 73,11%.

5.5 Equipment Sizing

This section of the report examines the sizing of the process equipment for both the thermochemical and biochemical conversion methods. The choice of material of construction that will be used for both plants is also discussed. The information from this section is necessary for the cost evaluation of the entire process. Additionally, it should be noted that while optimum values for equipment sizes may be calculated in this section, most of the equipment that will be obtained from equipment manufacturers will have specifications that comply with standards set nationally or by trade associations (Sinnott, 2005). Therefore, the equipment obtained from the manufacturer will not have the optimum specifications calculated below but will instead be as close as possible. Using standardised equipment sizes includes reduced costs, easy interchangeability, and incorporation into the process (Sinnott, 2005).

5.5.1 Choice of Material of Construction

The choice of construction material is vital to the successful operation of any plant, as the choice of construction material affects the longevity, maintenance, and replacement requirements, including the plant's safety. If the incorrect material is chosen, this can lead to equipment corrosion and malfunctioning, or even explosion in severe cases. Therefore, when selecting the type of construction material, three primary considerations need to be accounted for: safety, cost and material characteristics. It should also be noted that while minimising the costs of the plant is essential, the prevention of the contamination of the process stream is the most crucial consideration. Therefore, significant factors of concern include temperature and pressure limitations and the material's corrosion resistance (Sinnott, 2005).

5.5.2 Thermochemical conversion

5.5.2.1 Heat Exchangers

Table 5-9 below summarises all the information about the heat exchangers present in the process. The calculations used for this section can be found in Appendix B. Shell and tube heat exchangers with a counter-current arrangement are used. These types of heat exchangers offer many advantages, e.g. large surface areas are still achieved in small volumes, easy cleaning procedures are allowed, and a wide range of construction materials are used (Sinnott, 2005). Heat exchangers were selected as fix tubes due to their cost-effectiveness and being the easiest to manufacture. Reboilers were chosen as kettle reboilers because they are easy to maintain and can withstand high vapourisation of up to 80%. Condensers were selected to be Utube because of its simple structure, good tightness, low cost, convenient maintenance and cleaning.

Table 5-9: Sizing of heat exchangers used in the thermochemical method.

HX Name	**Type**	**Q (MW)**	**Area (m^2)**	**Material of Construction**
A100.HTL.E-304	Fixed tube	7,01	414,32	CS shell/CS Tube
A100.HT.H-311 cold	Fixed tube	0,56	2,87	CS shell/CS Tube
Reboiler@A100.HT.T-320	Kettle	0,44	27,38	CS Shell/ SS Tube
Reboiler@A100.HT.T-330	Kettle	0,46	61,55	CS Shell/ SS Tube
A100.HC.Q-R350_Exchanger	Fixed tube	0,03	1,26	CS shell/CS Tube
A100.HC.H-351 cold	Fixed tube	0,06	3,38	CS shell/CS Tube
A100.HT.HX-318A cold	Fixed tube	0,19	5,19	CS shell/CS Tube
A100.HTL.E-301 cold	Fixed tube	23,25	447,87	CS shell/CS Tube
Condenser@A100.HC.T-350	U Tube	0,05	0,65	CS Shell/ SS Tube
Condenser@A100.HT.T-320	U Tube	0,19	3,18	CS Shell/ SS Tube
Condenser@A100.HT.T-310	U Tube	4,20E-03	1,75	CS Shell/ SS Tube
Condenser@A100.HT.T-330	U Tube	0,49	2,70	CS Shell/ SS Tube
A100.HC.HX-381	Fixed tube	0,10	0,50	CS shell/CS Tube
A100.HT.HTLCOOL	Fixed tube	0,81	17,72	CS shell/CS Tube
Reboiler@A100.HT.T-310	Kettle	0,35	6,84	CS Shell/ SS Tube
Reboiler@A100.HC.T-350	Kettle	0,09	4,34	CS Shell/ SS Tube
A300.CWTOWER.CWHX	Fixed tube	5,82	35,43	CS shell/CS Tube
A100.HT.E-310	Fixed tube	0,17	9,85	CS shell/CS Tube
A300.AIRCOOL.COOLFAN	Fixed tube	0,57	34,03	CS shell/CS Tube
A100.HT.HX-320	Fixed tube	1,92	8,22	CS shell/CS Tube
A100.HC.H-352	Fixed tube	0,02	1,01	CS shell/CS Tube
A100.HTL.E-306	Fixed tube	2,86	51,70	CS shell/CS Tube
A100.HC.HX-380	Fixed tube	0,04	0,12	CS shell/CS Tube
A100.HC.H-381	Fixed tube	0,04	0,87	CS shell/CS Tube
A100.HTL.E-305	Fixed tube	0,58	4,45	CS shell/CS Tube
A100.HT.H-316	Fixed tube	0,53	12,40	CS shell/CS Tube
A100.HTL.R301Q-2_Exchanger	Fixed tube	1,59	94,87	CS shell/CS Tube

A100.HT.V-315	Fixed tube	0,16	10,14	CS shell/CS Tube
A100.HC.V-351	Fixed tube	4,36E-04	0,04	CS shell/CS Tube

5.5.2.2 Reactor

There are three types of reactors used in the process, namely: R-350Y, R-310Y and R-301 are approximately sized. Table 5-10 summarises the design information for the reactors.

Table 5-10: Sizing of reactors.

Reactor name	**Volume (m^3)**	**Material of Construction**
A100.HC.R-350Y	9,96	Stainless steel
A100.HT.R-310Y	98,85	Stainless steel
A100.HTL.R-301	110,55	Stainless steel

5.5.2.3 Flash drum

The flash drum was decided to have a vertical orientation as they are better suited for high-pressure applications. In addition, a decision to not include a demister, which aids in trapping liquid droplets in the rising vapour, in the flash drum was made for computational ease (Wankat, 2012). The data calculated regarding the design specifications of the flash drum are tabulated below in Table 5-11. Refer to Appendix C for the complete calculation and assumptions of the design specifications for the flash drum.

Table 5-11: Sizing of flash drums.

Flash Drums	**Volume (m^3)**	**Length (m)**	**Material of Construction**
A100.HC.V351	54,23	8,27	Carbon Steel
A100.HC.V-375	207,45	12,93	Carbon Steel
A100.HT.V-311	16230,01	55,30	Carbon Steel
A100.HT.V-315	1138,85	22,81	Carbon Steel

5.5.2.4 Distillation columns

There are 5 distillation columns used in the process. Table 5-12 summarises the important design values with regards to both distillation columns.

Table 5-12: Sizing of distillation columns.

Vessel Name	**Volume (m^3)**	**Pressure (bar)**	**Temperature (K)**	**Material of Construction**
A100.HC.T-350	1,10	1,38	477,42	Carbon Steel
A100.HT.T-310	0,49	3,31	465,33	Carbon Steel
A100.HT.T-320	1,96	1,72	545,52	Carbon Steel
A100.HT.T-330	3,06	1,29	630,37	Carbon Steel

A300.CWTOWER.COOLTOW	152,14	1,01	307,16	Carbon Steel

Table 5-13 summarises the design information with regards to the trays used in both distillation columns.

Table 5-13: Sizing of distillation column trays.

Tray name	**Area (m^2)**	**No. of trays**	**Material**	**Type of tray**
A100.HC.T-350	0,16	5	Carbon Steel	Sieve
A100.HT.T-310	0,07	5	Carbon Steel	Sieve
A100.HT.T-320	0,29	5	Carbon Steel	Sieve
A100.HT.T-330	0,46	5	Carbon Steel	Sieve
A300.CWTOWER.COOLTOW	27,73	3	Carbon Steel	Sieve

5.5.2.5 Condenser

The process has 5 condensers which have a horizontal orientation. Table 5-14 summarises the design information for the condensers used.

Table 5-14: Sizing of condensers.

Tank name	**Volume (m^3)**	**Material of Construction**	**Orientation**
A100.HC.T-350	2,07	Stainless Steel	Horizontal drum
A100.HT.T-310	2,07	Stainless Steel	Horizontal drum
A100.HT.T-320	2,07	Stainless Steel	Horizontal drum
A100.HT.T-330	2,07	Stainless Steel	Horizontal drum

5.5.2.6 Separators

Table 5-15 summarises the design information for the five separators used in the process.

Table 5-15: Sizing of separators.

Tank name	**Length (m)**	**Diameter (m)**	**Volume (m^3)**	**Material of Construction**
A100.HT.NH3SEP	3,66	1,07	3,76	Stainless Steel
A100.HT.V-300	3,66	0,91	2,76	Stainless Steel
A100.HTL.C-301	6,71	2,29	31,63	Stainless Steel
A100.HTL.F-301	7,01	2,29	33,07	Stainless Steel
A100.HTL.V-301	7,01	2,29	33,07	Stainless Steel

5.5.2.7 Compressors

The selection and sizing of compressors rely on the flow rate of the stream that needs compression, the corrosiveness of the gas and abrasive solids (if present), temperature difference and power consumption (Perry *et al*., 1997). The construction material for the compressor is carbon steel due to the stream's low operation temperature and pressure. Centrifugal compressors are used because the power required correlates to the range where centrifugal compressors are applicable, and they are assumed to be operating at 72% efficiency (Perry *et al*., 1997).

Table 5-16: Sizing of compressors.

Compressor Name	**Type**	**Duty (MW)**	**Material of Construction**
A100.HC.C-350	Centrifugal	6,89	Carbon Steel
A100.HC.C-351	Centrifugal	0,52	Carbon Steel
A100.HT.C-310	Centrifugal	317,27	Carbon Steel
A100.HT.C-311	Centrifugal	92,71	Carbon Steel
A300.AIRCOOL.ACFAN	Centrifugal	19,68	Carbon Steel

5.5.2.8 Pumps

There are two main classifications of pumps, namely dynamic and centrifugal (Sinnott, 2005). To choose between dynamic and centrifugal pumps, consideration of factors such as flow rates, fluid head required and whether the fluid is corrosive or not must be made. Centrifugal pumps seemed fit for all five pumps present in the plant. This is based on the fact that they can meet the discharge pressure and volume capacity (Sinnott, 2005). However, for a centrifugal pump, the change in size and operating conditions also affects the pump's efficiency (Sinnott, 2005). This, and the design specifications of pumps can be seen in Table 5-17.

Table 5-17: Sizing of pumps.

Pump Name	**Duty (MW)**	**Pressure (bar)**	**Materials of Construction**
A100.HC.P-350	2,95	70,05	Carbon steel
A100.HT.P-310	27,93	103,42	Carbon steel
A100.HTL.HTLPUMP	790,83	217,86	Carbon steel
A300.CWTOWER.COOLPUMP	79,60	4,15	Carbon steel
A300.CWTOWER.WARMPUMP	14,02	0,72	Carbon steel

5.5.2.9 Storage

It has been decided to use multiple storage tanks instead of one for all the species that need to be stored. This is because having one large storage tank is unreasonable, and if the tank needs to be

replaced or undergo maintenance, the entire plant needs to be shut down, or the product will be lost. Therefore, one of the ten storage tanks will act as a standby tank. This tank is only used in the case of an emergency or when maintenance is necessary for one of the other storage tanks. Industrial storage tanks for fuels are up to 110 m^3 (GSCTanks, 2018).

The material of construction for all storage tanks will be stainless steel because it prevents the possible contamination of the species during storage (Sinnott, 2005). Table 5-18 summarises the design specifications of the storage tanks for biomass, biodiesel, and naphtha.

Table 5-18: Sizing of storage.

Tank name	**Volume (m^3)**	**Material of Construction**	**No of tanks**	**Days of storage**
100FEED	110	Stainless Steel	164,79	7
Biodiesel	110	Stainless Steel	30,76	7
Naphtha	110	Stainless Steel	36,01	7

5.5.2.10 Valves

Apart from the process control valves, three valves (HTVALVE, HTL.VALVE306 and HTL.VALVE310) are used for pressure reduction. In addition, a globe valve made of stainless steel will be used for all three valves. This selection was based on the valve's properties, including its use for the reduction of pressure through flow regulation. Table 5-19 shows the sizing information for the valves.

Table 5-19: Sizing of valves.

Unit	**ΔP (bar)**	**Inlet pressure (bar)**	**ΔT (K)**	**Material of Construction**	**Type**
A100.HT.HTVALVE	54,47	104,46	7,56	Stainless steel	Globe valve
A100.HTL.VALVE306	62,32	200,40	2,05	Stainless steel	Globe valve
A100.HTL.VALVE310	172,55	194,25	2,97	Stainless steel	Globe valve

5.5.3 Biochemical conversion

5.5.3.1 Heat Exchangers

Table 5-20 below summarises all the information about the heat exchangers present in the process. Shell and tube heat exchangers with a counter-current arrangement are used. In addition, heat exchangers were selected to be fixed tubes, reboilers were chosen to be kettle reboilers, and condensers were selected to be Utube.

Table 5-20: Sizing of heater exchangers for the biochemical method.

HX Name	**Type**	**Q (MW)**	**Area (m^2)**	**Material of Construction**
H-101	Fixed tube	-7,68	199,60	CS shell/CS Tube
HX-201	Fixed tube	-9,98	9330,78	CS shell/CS Tube
HX-101	Fixed tube	-0,38	33,48	CS shell/CS Tube
HX-302	Fixed tube	0,39	261,28	CS shell/CS Tube
H-201	Fixed tube	0,08	1,26	CS shell/CS Tube
HX-301	Fixed tube	10,34	304,76	CS shell/CS Tube
HX-303	Fixed tube	-83,88	75251,93	CS shell/CS Tube
HX-305	Fixed tube	-0,12	42,90	CS shell/CS Tube
HX-306	Fixed tube	-2,47	2267,39	CS shell/CS Tube
HX-304	Fixed tube	-2,88	285,88	CS shell/CS Tube
HX-307	Fixed tube	-2,36	151,17	CS shell/CS Tube
HX-01	Fixed tube	-19,01	17663,24	CS shell/CS Tube
HX-501	Fixed tube	-0,04	198,68	CS shell/CS Tube
HX-01	Fixed tube	20,46	178,74	CS shell/CS Tube
HX-401	Fixed tube	-23,54	29112,49	CS shell/CS Tube
T-302-cond	U Tube	-395,26	97588,50	CS Shell/ SS Tube
T-302-reboiler	Kettle	486,50	41418,85	CS Shell/ SS Tube
T-301-cond	U Tube	-27,55	8113,25	CS Shell/ SS Tube
T-301-reboiler	Kettle	32,96	1158,88	CS Shell/ SS Tube

5.5.3.2 Reactors

There are six types of reactors used in the process, that are approximately sized. Table 5-21 summarises the design information for the reactors.

Table 5-21: Sizing of reactors.

Reactor name	**Volume (m^3)**
R-202	74,36
R-201	13,45
R-501	2197,35
R-502	118,59
R-101	5908,53
R-102	342,63

5.5.3.3 Turbines

Table 5-18 summarises the process conditions concerning these units. Furthermore, the type of turbine along with the material of construction is specified. Sizing this equipment is not required because costing is based on each respective equipment's duty (work). The material of construction for turbines is chosen as stainless steel, and this is because turbines typically operate at high pressures and temperatures. Steam is used for power generation; hence steam turbines are used. A turbine efficiency of 72% is applied for preliminary sizing purposes. Table 5-22 below represents the design specifications obtained from Aspen Plus.

Table 5-22: Sizing of the turbine.

Turbine Name	**Type**	**Duty (MW)**	**Material of Construction**
K-501	Axial	1,18E-02	Stainless steel

5.5.3.4 Distillation

There are 3 distillation columns used in the process. Table 5-23 summarises the important design values with regards to both distillation columns.

Table 5-23: Sizing of distillation columns.

Vessel Name	**Volume (m^3)**	**Length (m)**	**Height (m)**	**Material of Construction**
T-302	5844,12	41,45	12,50	Carbon Steel
T-301	391,43	29,87	3,81	Carbon Steel
T-303	9,82	7,32	1,22	Carbon Steel

Table 5-24 summarises the design information with regards to the trays used in both distillation columns.

Table 5-24: Sizing of distillation column trays.

Tray name	**Area (m^2)**	**No. of trays**	**Material**	**Type of tray**
T-302	122,59	62	Carbon Steel	Sieve
T-301	11,4	43	Carbon Steel	Sieve
T-303	1,17	6	Carbon Steel	Sieve

5.5.3.5 Pumps

The process comprises of nine pumps, and an additional two that are reflux pumps. All pumps were chosen to be centrifugal pumps. Table 5-25 summarises the sizing information of pumps.

Table 5-25: Sizing of pumps.

Pump Name	Duty (MW)	Pressure (bar)
P-101	0,02	7,09
P-201	0	1,01
P-402	0,28	5,17
P-401	0,05	5,78
P-302	0,02	6,33
T-302-reflux pump	-395,26	1,62
P-103	-4,40E-03	1,01
P-102	1,29E-04	4,96
T-301-reflux pump	-27,55	2,07
P-301	0,04	6,09
P-202	4,36E-03	4,66

5.5.3.6 Storage tank

Table 5-26 below summaries the design specifications of the storage tanks for the biomass, DAP, ammonia, dry air, bioethanol, and biogas.

Table 5-26: Sizing of storage tanks.

Tank name	Volume (m^3)	Material of Construction	No. of tanks @110 m^3
Feed	18126,85	Stainless Steel	165
DAP	4401,44	Stainless Steel	40
NH_3	300172,86	Stainless Steel	2729
Dry Air	164,31	Stainless Steel	2
Bioethanol	1265,50	Stainless Steel	12
Biogas	1691654,44	Stainless Steel	15379

5.5.3.7 Condenser

Table 5-27 summarises the design information for the two compressors used in the process.

Table 5-27: Sizing of condensers.

Tank name	Volume (m^3)	Material of Construction	Orientation
T-302-cond acc	79,69	Stainless Steel	Horizontal
T-301-cond acc	11,10	Stainless Steel	Horizontal

5.5.3.8 Flash drum

The flash drum was decided to have a vertical orientation instead of a horizontal one. A decision not to include a demister for simplicity. The data calculated regarding the design specifications of the flash drum are tabulated below in Table 5-28.

Table 5-28: Sizing of flash drums.

Tank name	**Volume (m^3)**	**Length (m)**	**Material of Construction**
V-202	269035,46	140,99	Stainless Steel
V-301	4,33	3,56	Stainless Steel
V-101	366910,19	156,35	Stainless Steel
V-201	6520,15	40,80	Stainless Steel
V-401	68,25	8,93	Stainless Steel
V-501	1734252,12	262,40	Stainless Steel

5.5.3.9 Separators

The process used five separators; the design information is summarised in Table 5-29 below.

Table 5-29: Sizing of separators.

Tank name	**Volume** m^3	**L (m)**	**D (m)**	**Material of Construction**
C-302	3,27	3,66	1,07	Stainless Steel
C-502	18,79	3,66	0,91	Stainless Steel
C-01	6,08	6,71	2,29	Stainless Steel
C-301	60,05	7,01	2,29	Stainless Steel
C-501	22,34	7,01	2,29	Stainless Steel

5.6 Heat Integration

5.6.1 Heating and Cooling Requirements

Before the heat integration, the heating and cooling utility requirements were considered. Table 5-30 shows that the biochemical conversion is a more energy-intensive method. The cost of utilities based on the ACCE, the biochemical conversion is 51,52% costlier than the thermochemical conversion.

Table 5-30: Comparison of the heating and cooling requirements.

	Units	**Thermochemical**	**Biochemical**
Heating Utilities	MW	16,52	556,80
Cooling Utilities	MW	7,81	596,20

Cost of Utilities (ACCE)	R/yr	22 374 903,60	46 148 793,30
Power	MW	2,54	0,73
Heat	MW	19,68	-68,10

5.6.2 Thermochemical conversion

The energy analysis for this method was investigated using the activated energy analysis tool. The cold utilities used for the process were air and cooling water. The hot utilities used were low and high-pressure steam and a fired heater. Aspen Plus showed saving potentials in the following heat exchangers: coolers; A100.HC.HX-381, A100.HT.HTLCOOL, A100.HT.E-310, A100.HT.HX-320, heaters; A300.CWTOWER.CWHX, A300.AIRCOOL.COOLFAN, A100.HC.H-352.

The available energy savings for the utilities was 15 620 MW which was 64,2% of the actual utility energy. The available savings for carbon emissions was 1 836 kg/hr, which was 47,27% of the actual carbon emissions of the method. The results shown by the energy analyser are the maximum possible savings potential as informed by thermodynamics. The design changes found by the energy analysis included three scenarios; modifying exchangers, adding exchangers, and relocating exchangers.

Scenario 1

The first scenario involves modifying heat exchangers. Modifying heat exchangers included adding area to heat exchangers that require more area. Aspen calculates the required area. A100.HC.H-351 (process exchanger), A100.HC.HX-380 (cooler) required additional area for possible saving, 7,42 and 0,13 respectively. In this scenario, there is no significant energy saving and zero greenhouse gas reduction.

Scenario 2

The second scenario involves adding a process exchanger E-100 with an area of 13,6 m2. This scenario adds to scenario 1, which adds 7,552 m2. In total, the new area is 21,15 m2. Under this scenario, five solutions are presented. Table A-17 in Appendix D shows a summary of the solutions. The first option gives the highest energy saving with 23,56%, which is the closest to the target energy reduction of 64,2%. Furthermore, this option has a 17,3% greenhouse gas reduction, for which the target reduction was 47,3%. Therefore, this option was the most suitable design as it presents the highest energy and carbon emissions reduction at a low cost. The HEN for this is illustrated in Figure A-9.

Scenario 3

This scenario involves relocating the process exchanger A100.HC.H-351. Under this scenario, four solutions were available. Refer to Table A-18 in Appendix D for a summary of the solutions. This new area added for this option is 5,806 m2 with additional capital of $ 1005. Option 1 has the highest energy saving at 22,98%, which also has an economical extra capital cost of $ 4050. The greenhouse gas reduction for this option was 16,9%.

5.6.3 Biochemical conversion

Energy analysis was also employed for this conversion. The cold utilities employed were air, cooling water, and refrigerant 1. The hot utilities employed were low and medium-pressure steam. The available energy savings was 59 950 MW which is 9,92% of the actual energy of the process. The available carbon emissions savings was 13 536 kg/hr, which is 10,27% of the actual carbon emissions of the process. Ideas for potential change were identified for the following coolers: A200.S77_Exchanger, A200.S78_Exchanger, A100.S79_Exchanger, A500.HX-501, A200.HX-201, A400.HX-401, A300.HX-306, A300.HX-307, A300.HX-304. No design alternatives were identified for this process. Using retrofit mode, other scenarios were created. However, all designs were more expensive than the base case. The reason for no design alternatives to improve the current heat exchanger network is due to the low available energy savings for the process. The HEN for this is illustrated in Figure A-10 in Appendix D.

5.7 Process Economics

The ultimate purpose of this study beyond the conceptual designs, process models, equipment sizing, and heat integration is to determine the economics of the processes investigated. Therefore, an economic analysis is essential in determining the economic feasibility of the proposed methods. This section summarises the various calculations that were computed for the analysis. These include the capital investment costs, manufacturing costs, and profitability analysis using the discounted cash flow method to establish the internal rate of return (IRR) and the net present value (NPV).

5.7.1 Thermochemical Conversion

5.7.1.1 Total Capital Investment Estimation

The total capital cost investment of a process is defined as the total of both the fixed capital investment (capital required for the complete construction of a new plant) and the working capital (fully recoverable capital needed to operate a plant until there is an income) (Sinnott, 2005). The fixed capital investment (FCI) and working capital will be evaluated in detail in this section. Some of the components of the FCI that will be considered include the estimation of purchased equipment costs, piping, equipment installation, buildings, insulation etc.

5.7.1.1 (a) Purchased Equipment Costs Estimation

Base Purchase Cost

The purchased equipment cost was determined using the equation below (Turton *et al*., 2009). All purchased cost data used for calculations can be found in Appendix E.1.

$$log_{10}C_p^o = K_1 + K_2 log_{10}(A) + K_3[log_{10}(A)]^2 \quad (5.1)$$

Bare Module Cost

The bare module cost for all equipment was determined using the following equation (Turton *et al*., 2009):

$$C_{BM} = C_P^o F_{BM} \quad (5.2)$$

Bare module cost factors employed in calculations can be found in Appendix E.1.

The bare module cost equation is expanded for different equipment due to different expressions of the bare module cost factor. For example, for heat exchangers (shell & tube), compressors, pumps (centrifugal) and process vessels, the bare module cost equation becomes (Turton *et al*., 2009)*:*

$$C_{BM} = C_P^o F_{BM} = C_P^o (B_1 + B_2 F_M F_P) \quad (5.3)$$

For the furnaces, the bare module cost equation becomes (Turton *et al*., 2009)*:*

$$C_{BM} = C_P^o F_{BM} F_T F_P \quad (5.4)$$

For the distillation column, the bare module cost equation becomes (Turton *et al*., 2009)*:*

$$C_{BM} = C_P^o F_{BM} N F_q \quad (5.5)$$

For the cooling tower, the bare module cost equation becomes (Turton *et al*., 2009)*:*

$$C_{BM} = C_P^o F_P F_M \quad (5.6)$$

The cost estimation for the cooling towers, furnaces, and compressors was determined using a slightly different equation given below. This equation is used when there is not enough data to be accessed for specific equipment (Sinnott & Towler, 2013).

$$C_e = a + bS^n \quad (5.7)$$

The purchase equipment cost was determined using the U.S Gulf Coast Chemical Engineering Index of 478,6 for 2016. This cost index was specifically used when the above equation was applied.

Pressure and Material Factors

To determine the pressure factor for most of the equipment in the process, Equation 5.8 was used. The pressure constants used for these calculations can be found in Appendix E.1.3. (Turton *et al*., 2009).

$$log_{10}F_p = C_1 + C_2 log_{10}P + C_3(log_{10}P)^2 \quad (5.8)$$

To determine the pressure factor for tanks, vessels and towers the following equation was used:

$$F_{p,vessel} = \frac{\frac{(P+1)D}{2SE-1.2P}+CA}{t_w} \quad (5.9)$$

For vessels with a thickness greater than 0,0063 m, the pressure factor was assumed to be 1 (Turton *et al*., 2009).

Exchange Rate

All costing data used in this section is by (Turton *et al*., 2009) and reported in US dollars. To report the costs in South African Rands, an exchange rate of R 14,79 per US dollar was used (ExchangeRates, 2022) . For accuracy, the exchange rate considered was an average for the past 12 months.

Effect of Capacity

All equipment in the plant has its capacity or duty requirement, which was determined during equipment sizing. This sizing information was then used in costing calculations to determine purchased equipment cost estimations. The expression shown by Equation 5.10 below was then employed to justify the capacity effects on equipment cost.

In cases where the equipment requirements were above or below the range (purchased cost data is available at specific ranges), the sixth-tenths rule was applied. The sixth-tenths rule is employed to scale up or down to find a new size or capacity. The cost exponent for various equipment ranges from 0,3-0,9, but for most equipment, the cost exponent, n, used is 0,6 (Turton *et al*., 2009).

$$\frac{C_a}{C_b} = \left(\frac{A_a}{A_b}\right)^n \quad (5.10)$$

Effect of Time

The critical data used in this cost estimation was reported in 2001 and 2006. Since the estimation heavily depended on records, the following expression was used to convert the costs for the present time (Turton *et al*., 2009). This expression is essential for accuracy as it considers the changing economic conditions or inflation.

$$C_2 = C_1\left(\frac{I_2}{I_1}\right) \quad (5.11)$$

Table 5-31: CEPCIs considered for costing calculations.

Year	CEPCI	Source
2001	397.00	(Turton *et al*., 2009)
2020	596,2	(Maxwell, 2022)
2022	726,5	(Maxwell, 2022)

A synopsis of both the purchased equipment costs and the bare module for all equipment is found in Table 5-32.

Table 5-32: Summary of equipment costs.

Equipment Name	Number of Equipment	Purchase costs (R)	Bare Module (R)
Heat Exchangers	33	6 790 070,60	59 175 257,53
Pumps	5	2 178 405,211	32 456 033,08
Flash drum	4	108 907 874,3	219 228 533,5
Reactors	3	48 681,46286	356 343,4032
Compressors	5	2 416 092,818	13 947 078,98
Condenser	4	32 492 322,52	65 406 144,94
Vessels	5	1 665 967,557	15 931 039,74
Trays	23	2 151 684,894	3 937 529,158
Separators	5	31 290 781,93	62 987 477,02
Storage tanks	3	19 458 827,43	39 170 080,46
Total		**207 402 507,10**	**512 595 517,78**

Total Module Cost

It is important to know how much it would cost to make small to moderate alterations or expansions to an existing facility. This is referred to as the total module cost. To evaluate this, the following equation was used (Turton *et al*., 2009).

$$C_{TM} = 1.18 \sum_{i=1}^{n} C_{BM,i} \quad (5.12)$$

Grass Roots Cost

Grassroots costs refer to the costs for constructing a completely new plant in undeveloped land. To evaluate this the following equation was used (Turton *et al*., 2009).

$$C_{GR} = C_{TM} + 0.5 \sum_{i=1}^{n} C_{BM,i}^{o} \quad (5.13)$$

The results for these evaluations are found in Table 5-33.

Table 5-33: Summary of equipment costs.

Equipment Cost	Cost (R)
C_{BM}	512 595 517,78
C_p°	453 721 525,35

C_{BM}°	379 541 363,68
C_{TM}	604 862 710,97
C_{GR}	831 723 473,65

5.7.1.1 (b) Total Other Direct Costs

The total other direct costs are the amounts considered for instrumentation and controls, insulation, electrical installation, building's construction, yard improvement, services facilities, equipment installation, piping and finally, land (Turton *et al*., 2009). These costs are calculated as a certain percentage of the purchased equipment cost. Table 5-34 gives a synopsis of all the other direct costs. Refer to Appendix E.5 for the heuristics used to calculate the additional direct costs.

Table 5-34: Total direct costs.

	From	**To**	**Used**		**Price (R)**	
Instrumentation	5%	30%	30%	% of Purchased Equipment Cost	R	113 862 409,10
Insulation	0%	8%	8%	% of Purchased Equipment Cost	R	30 363 309,09
Electrical	10%	15%	12%	% of Purchased Equipment Cost	R	45 544 963,64
Buildings	30%	45%	45%	% of Purchased Equipment Cost	R	170 793 613,66
Yard Improvement	10%	20%	15%	% of Purchased Equipment Cost	R	56 931 204,55
Services	25%	75%	75%	% of Purchased Equipment Cost	R	284 656 022,76
Equipment installation	32%	43%	40%	% of Purchased Equipment Cost	R	151 816 545,47
Piping	36%	66%	55%	% of Purchased Equipment Cost	R	208 747 750,03
Land					R	22 772 481,82
	Total Other Direct Costs				**R**	**1 085 488 300,13**
Total Direct Costs	Bare Module + Other Direct Costs				**R**	**1 598 083 817,91**

5.7.1.1 (c) Total Indirect Costs

The indirect costs comprise engineering and supervision costs, construction costs, contractor rates, and contingency allowances. These costs are quantified as a percentage of either purchased equipment or direct costs (Turton *et al*., 2009). Table 5-35 gives a synopsis of the indirect costs. Refer to Appendix E.6 for the heuristics utilised to calculate the indirect costs.

Table 5-35: Total indirect costs.

Indirect Costs	**From**	**To**	**Used**		**Cost (R)**	
Engineering + Supervision	25%	30%	30%	% of Purchased Equipment Cost	R	113 862 409,10
Construction	8%	10%	10%	% of Total Direct Costs	R	159 808 381,79

Contractor	2%	8%	6%	% of Total Direct Costs	R	95 885 029,07
Contingency	10%	25%	25%	% of Total Direct Costs	R	399 520 954,48
Total Indirect Costs					**R**	**769 076 774,45**

5.7.1.1 (d) FCI and Working Capital

To calculate the FCI of the plant, total direct costs were added to the total indirect costs of the plant. Generally, working capital cost is between 15 to 20 % of the FCI (Turton *et al*., 2009). For this process, the working capital cost was assumed to be 20 % of the FCI. The working capital can be found in Table 5-36.

Table 5-36: Grassroots and working capital costs.

FCI	Total direct + Total indirect costs			**R**	**2 367 160 592,35**
	From	**To**	**Used**	**Price (R)**	
Working capital	15.00%	20.00%	20.00%	**R**	**473 432 118,47**
Total capital investment	FCI + Working Capital			**R**	**2 840 592 710,82**

5.7.1.2 Manufacturing costs

The manufacturing costs also referred to as the production costs, are the money necessitated for the daily operation of the process to produce the desired styrene product. The manufacturing cost is divided into three sections: direct manufacturing, fixed manufacturing, and general expenses. Direct manufacturing expenses vary with the production rate of biodiesel, while fixed manufacturing and general expenses are unaffected by the production rate of biodiesel. General expenses include activities unrelated to the manufacturing process like management and administrative costs, research costs or even product distribution and selling costs (Turton, 2013).

To calculate the total manufacturing amount, it was required to know the following:

- The FCI cost
- The cost of raw material
- The cost of waste treatment
- The cost of operating labour and the cost of utilities.

These costs were calculated using heuristics and information from (Turton, 2013). Table 5-37 gives a summary of all the costs mentioned above.

Table 5-37: Summary of all the costs affecting the manufacturing costs.

Cost affecting the Manufacturing Cost	**(R/year)**
Raw Material Cost (C_{RM})	R 6 146 093 786,72
Utilities Cost (C_{UT})	R 22 374 903,60
Waste Treatment Costs (C_{WT})	R 62 588 269,76
Operating Labour Cost (C_{OL})	R 4 348 142,40
Fixed Investment (FCI)	R 2 367 160 592,35

Refer to Appendix E.8 for the calculation of the raw material cost, the wastewater treatment cost and operating labour costs. The utilities cost and fixed capital investment were not calculated and the explanations as to why, are given below.

5.7.1.2 (a) Utilities Cost

The cost of utilities was extracted from the process model on Aspen Plus. The cost of utilities is R22 374 903,60.

5.7.1.2 (b) Total Manufacturing Costs

Once the amount of raw materials, operating labour, utilities, and waste treatment together with the FIC were determined, the total cost of manufacturing (COM) was calculated with the use of the following equation:

$$COM = 0.280FCI + 2.73C_{OL} + 1.23(C_{UT} + C_{WT} + C_{RM}) \quad (5.14)$$

However, if the value of the depreciation was unknown, the following equation could be utilised:

$$COM_d = 0.180FCI + 2.73C_{OL} + 1.23(C_{UT} + C_{WT} + C_{RM}) \quad (5.15)$$

Since the depreciation was unknown, Equation 5.15 was used to calculate the total manufacturing cost (COM_d), which was calculated to be R7 037 479 644,51.

5.7.1.2 (c) Subdivision of the Manufacturing Costs

Once the total manufacturing cost is calculated, it is possible to calculate the subdivision costs that make up the manufacturing costs, this includes: the direct manufacturing; the fixed manufacturing, and the general expenses. Each of these amounts were calculated using the following equations:

Direct Manufacturing Cost (DMC)

$$DMC = C_{RM} + C_{WT} + C_{UT} + 1.33C_{OL} + 0.03COM_d + 0.069FCI \quad (5.16)$$

Fixed Manufacturing Cost (FMC)

$$FMC = 0.708C_{OL} + 0.069FCI \quad (5.17)$$

General Expenses (GE)

$$GE = 0.177C_{OL} + 0.009FCI + 0.16COM_d \quad (5.18)$$

Table 5-38 provides a summary of the manufacturing costs.

Table 5-38: Summary of the direct and fixed manufacturing cost as well as the general expense.

Manufacturing cost divides	**(R/year)**	**Contribution of the manufacturing costs (%)**
Direct Manufacturing Cost	R5 745 705 165,57	81,64
Fixed Manufacturing Cost	R164 045 405,10	2,33
General Expenses	R1 148 070 809,66	16,31

5.7.1.2 (d) Revenue

The plant's revenue is obtained from selling the biodiesel, the naphtha, the activated carbon, AD digestate being produced and the additional electricity being generated. Table 5-39 gives a summary of total revenue, as well as the contribution of the factors mentioned earlier affecting the revenue.

Table 5-39: Summary of the costs affecting the revenue.

Revenue from Species	**(R/year)**
Biodiesel	R2 140 387 720,69
Naphtha	R2 143 004 541,56
Activated Carbon	R760 125 537,56
Electricity	R281 014 461,00
AD digestate	R2 249 952 383,81
CO_2 gas stream	R9 376 261,91
Steam	R95 120 816,33
Total Revenue	R7 678 981 722,85

Refer to Appendix E.8 for the full calculation of each revenue contributing source.

5.7.1.3 Profitability Analysis

A profitability analysis includes the provision of expenses and profitability analysis across a start-up company. Conducting a profitability analysis is extremely important for the company because it shows future investors possible returns once expenses have been deducted from the revenue. A Cash Flow Diagram (CFD) is made for the biodiesel-producing plant, factoring in taxation and depreciation. The profitability analysis was conducted using a discounted profitability criterion. This is because the non-discounted criteria do not allow for the time value of money and is usually not recommended for large projects. The main difference between the two criteria is that the discounted criteria discount each yearly cash flow back to zero (Sinnott, 2005).

5.7.1.3 (a) Plant Lifespan and Fixed Capital Outlay

There is a direct link between the profitability of a project and plant life. Process equipment usually has operating lives of much more than ten years but a class life of 9,5 years with no salvage value. Therefore, common plant lives of 10, 12 and 15 years are used with a construction period of 2 years. Consequently, it is decided that the plant studied will be operational for 15 years and have a plant construction period of 2 years.

The FCI was calculated, as stated above. The FCI was distributed over the two-year plant construction period. The FCI used in year 1 is 60% and 40% in year 2. As shown above, a working capital which is decided to be 20% of the FCI, was used.

5.7.1.3 (b) Discount Rate and Tax Rate

The discount rate is a significant value for profitability because it influences the NPV of the process. This is defined as the rate at which cash inflows are discounted or reduced. For equities, an average discount rate of 15% to 20,5% is used (Howard, 2016). A discount rate of 17.5% was decided upon.

All registered companies in South Africa must pay corporate tax to the South African Revenue Services (SARS). However, the corporate tax rate for South Africa has flat-lined at a percentage of 28% since 2014 (SARS). The corporate tax rate for South Africa has flat-lined at a percentage of 28% since 2014 (SARS, 2021). Therefore, a tax rate of 28% was used.

5.7.1.3 (c) Depreciation

The method used for depreciation in the plant is the Modified Accelerated Recovery Cost System (MARCS). The MARCS method makes use of the double-declining and straight-line depreciation methods. The cash flow seen in the early years of a plant's operation is usually higher than those seen in the later years because of the depreciation allowance (Turton *et al*., 2009). This method is commonly used because it allows the recovery of the FCI over a specified plant project life by deducting the cash value in smaller amounts (Kagan, 2021).

5.7.1.3 (d) Discounted Cash Flow Analysis

The Cumulative Cash Flow diagram in Figure 5.1 below was generated by setting up cash flow diagrams in Microsoft Excel. The NPV was found to be R 568 578 718. This was calculated with a biodiesel selling price of R60,5/kg (AFDC, 2021), naphtha selling price of R 267,3/kg (Davis *et al*., 2014), activated carbon selling price of R 39,9 /kg (León *et al*., 2020) and electricity selling price of R 2,2/kg.

A positive NPV shows positive profitability. The plant could reach a break-even point at seven years five months with a discounted payback period of 7,2 years. The Present Value Ratio (PVR) must be over the value of 1 to show profitability. The PVR obtained is 1,57.

The IRR of a plant is the rate of growth a project is anticipated to produce. The IRR is determined on the condition that the discount rate causes the NPV to be equal zero (Fernando, 2022). The IRR was found to be 27,36%. Therefore, the plant shows that it is profitable at the current discount rate, tax rate and MARCS depreciation. It should be noted that it is assumed that these settings stay constant throughout the plant's lifetime. However, it is unlikely that some of these settings will remain constant over 17 years. Therefore, a sensitivity analysis was conducted to compensate for changes over the 17 years.

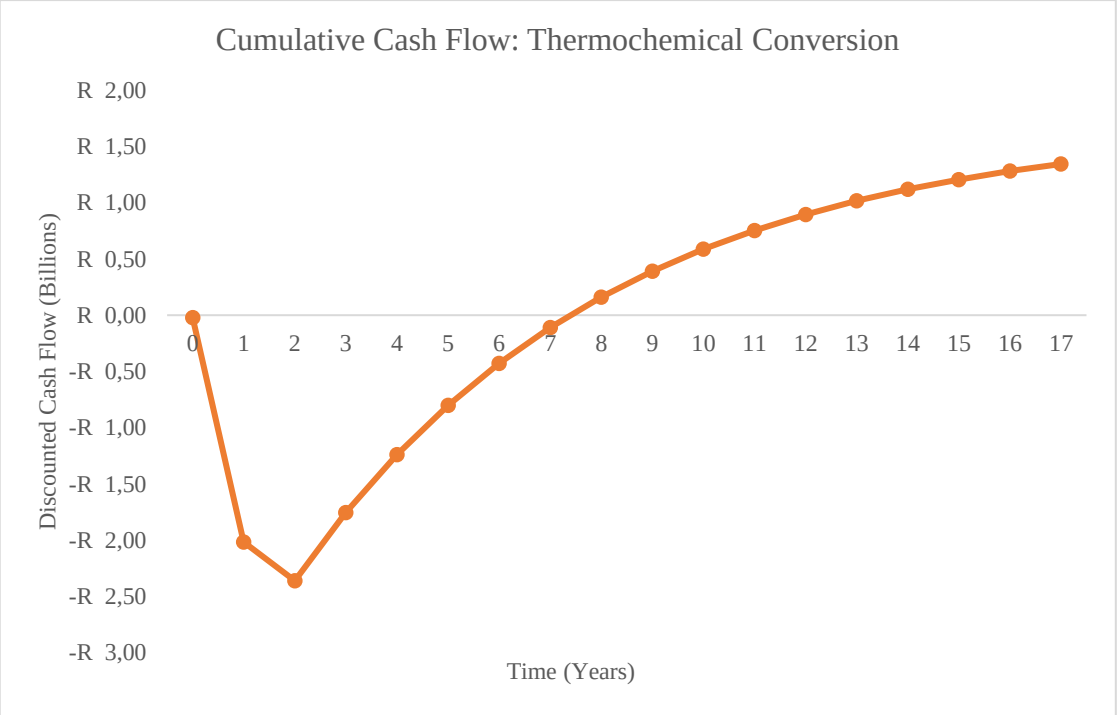

Figure 5-3: Cumulative discounted cash flow.

Refer to Appendix E.10 for the cash flow table that was used to generate this graph.

5.7.1.3 (e) Sensitivity Analysis

A sensitivity analysis was conducted to determine how a variable's outcome would differ compared to the key predictions if the variable changed (EduPristine, 2018). In this case, the outcome we are concerned about is the NPV because this value will show how possible changes in plant variables can affect profitability positively or negatively.

There are many uncertainties associated with the chemical industry. If some of these uncertainties were to occur during the 15-year operational life of the plant, it could cause lower profitability that investors must be prepared to encounter. The sensitivity analysis below looked at changes in the exchange rate, selling price, operator salaries, tax rate and discount rate. Table 5-40 below summarises the analysis.

Table 5-40: Sensitivity analysis results (All cash flow values are in billions of Rands - $x10^9$)

Variable	Default	Unit	Minimum value	NPV (min)	Default NPV	Maximum value	NPV (max)
Exchange rate	14,79	R/$	12,57	0,48	0,57	17,01	0,66
Products	7, 68	R/yr	6, 53	-2,21	0,57	8, 83	3,35
Biodiesel	52,64	R/kg	44,75	-0,21	0,57	60,54	1,34
Plant life	15,00		12,75	0,56	0,57	17,25	0,57
Operator rate	52,82	R/hour	44,90	0,57	0,57	60,74	0,57
Land	22 772 481,82	R	19 356 609,55	0,58	0,57	26 188 354,09	0,56
Tax rate	0,28	%	0,24	0,74	0,57	0,32	0,40
Discount rate	0,18	%	0,15	1,04	0,57	0,20	0,20
FCI	2, 37	R	2, 01	1,08	0,57	2, 72	0,06
Raw Material	5, 28	R/yr	4, 49	2,72	0,57	6, 07	-1,58

The results in Table 5-40 are represented in the tornado diagrams, which clearly show how changes in specific plant variables affect the IRR and the NPV. Refer to Figure 5-

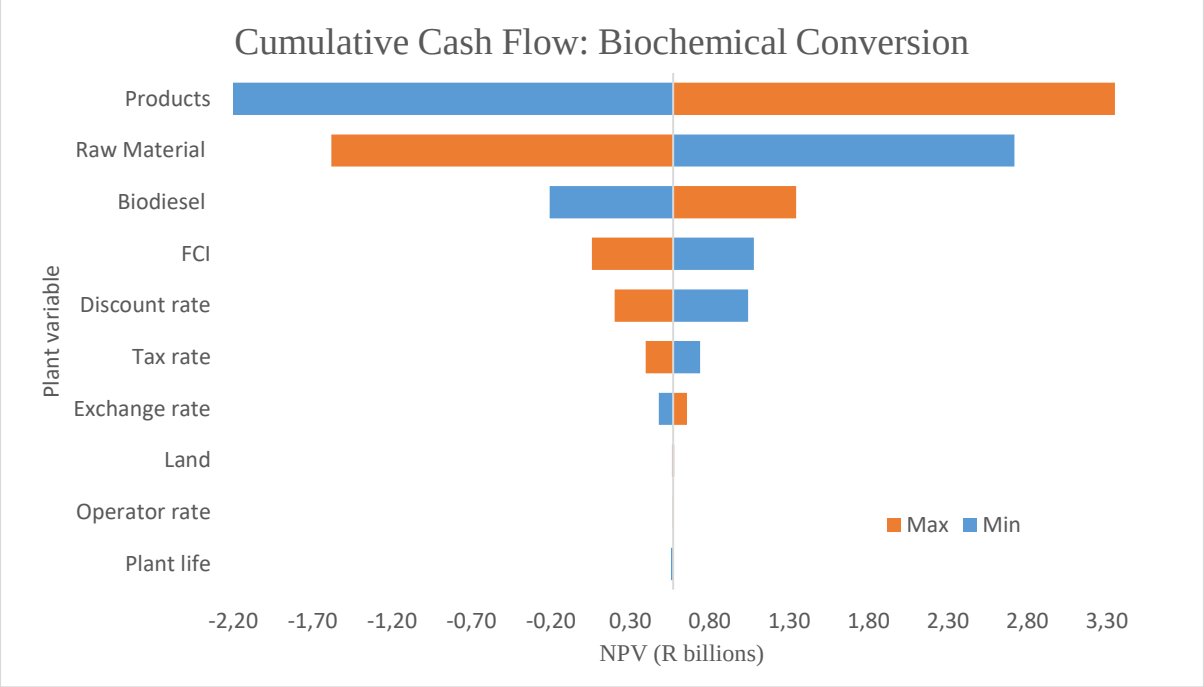

Figure 5-4: Tornado diagram showing sensitivity analysis on NPV.

Figures 5-2 show that the NPV was primarily affected by the cost of the products, FCI, raw material, exchange rate and discount rate. The rest of the plant variables, namely, cost of land, plant life and operator rate, had a minimal to no effect on the NPV value. NPV values remained the same when the respective plant variable was maximised and minimised.

The cost of products and raw materials have the most impact on the profitability of the process but in contrasting ways. When the cost of products is maximised, the NPV increased, but when the cost of raw materials was maximised the NPV decreased. The opposite effect occurred when the costs were minimised. Raw material availability and a rise in production costs for microalgae can cause an increase in the selling price of biofuels. Another factor that can cause changes in the selling price of biofuels is significant advances in technology.

Fixed capital investment is also a big profitability driving factor. All equipment for this process were costed using R14,79/$ as an exchange rate, which is relatively high. This inflated the fixed capital amount, which can be lessened through the localisation of equipment suppliers.

Other significant plant variables that showed a decrease in NPV when the parameter was maximised include the discount rate, and tax rate. Again, the opposite effect occurred when the parameters were minimised. Ultimately, investors can expect a return on their investment when the cost of products or the exchange rate is increased but can expect a loss when the FCI, discount rate, tax rate, or cost of raw material is decreased.

5.7.2 Biochemical Conversion

5.7.2.1 Total Capital Investment Estimation

5.7.2.1(a) Purchased Equipment Costs Estimation

The equipment used for the process was calculated in a similar manner as in the previous section. The purchased equipment costs were R 428 691 192,54, and the bare module costs were R738 284 146,72. Table 5-41 summarises the equipment costs for this process.

Table 5-41: Summary of equipment costs.

Equipment Cost	**Cost (R)**
C_{BM}	R 738 284 146,72
C^o_{BM}	R 535 701 646,74
C^o_P	R 428 691 192,54
C_{TM}	R 871 175 293,13
C_{GR}	R 1 139 026 116,50

Based on the Aspen Capital Cost Estimator, the capital cost of the thermochemical conversion method was R 536 221 803, and that of the biochemical method was R 459 761 940. This is contrary to the calculations performed. This is because the ACCE has a few types of equipment that had errors or did not have costs for, thus were not included in the total equipment costs.

5.7.2.1(b) Total Other Direct Costs

Table 5-42 gives a summary of all the other direct costs. The calculation is like that of the thermochemical economic analysis.

Table 5-42: Total direct costs.

	From	**To**	**Used**		**Price (R)**
Instrumentation	5%	30%	30%	% of Purchased Equipment Cost	R 128 607 357,76
Insulation	0%	8%	8%	% of Purchased Equipment Cost	R 34 295 295,40
Electrical	10%	15%	12%	% of Purchased Equipment Cost	R 51 442 943,10
Buildings	30%	45%	45%	% of Purchased Equipment Cost	R 192 911 036,64
Yard Improvement	10%	20%	15%	% of Purchased Equipment Cost	R 64 303 678,88
Services	25%	75%	75%	% of Purchased Equipment Cost	R 321 518 394,41
Equipment installation	32%	43%	40%	% of Purchased Equipment Cost	R 171 476 477,02
Piping	36%	66%	55%	% of Purchased Equipment Cost	R 235 780 155,90
Land					R 25 721 471,55
	Total Other Direct Costs				**R 1 226 056 810,67**
Total Direct Costs	Bare Module + Other Direct Costs				**R1 964 340 957,39**

5.7.2.1(c) Total Indirect Costs

Table 5-43 gives a summary of the indirect costs.

Table 5-43: Total indirect costs.

Indirect Costs	**From**	**To**	**Used**		**Cost (R)**
Engineering + Supervision	25%	30%	30%	% of Purchased Equipment Cost	R 128 607 357,76
Construction	8%	10%	10%	% of Total Direct Costs	R 196 434 095,74
Contractor	2%	8%	6%	% of Total Direct Costs	R 117 860 457,44
Contingency	10%	25%	25%	% of Total Direct Costs	R 491 085 239,35
Total Indirect Costs					**R 933 987 150,29**

5.7.2.1(d) FCI and Working Capital

For this process, the working capital was assumed to be 20 % of the FCI. The working capital can be found in Table 5-44.

Table 5-44: Grassroots and working capital costs.

FCI	Total direct + Total indirect costs			R 2 898 328 107,68
	From	**To**	**Used**	**Price (R)**
Working capital	15,00%	20,00%	20,00%	R 579 665 621,54
Total capital investment	FCI + Working Capital			**R3 477 993 729,21**

5.7.2.2 Manufacturing Costs

Table 5-45 gives a summary of all the costs mentioned above.

Table 5-45: Summary of all the costs affecting the manufacturing costs.

Cost affecting the Manufacturing Cost	**(R/year)**
Raw Material Cost (C_{RM})	R3 202 267 009,96
Utilities Cost (C_{UT})	R617 908 452,00
Waste Treatment Costs (C_{WT})	R420 131 356,63
Operating Labour Cost (C_{OL})	R4 348 142,40
Fixed Investment (FCI)	R2 898 328 107,68

5.7.2.2 (a) Utilities Cost

The cost of utilities was R 617 908 452, 00 per year. The value was extracted from the simulation.

5.7.2.2 (b) Total Manufacturing Costs

The total manufacturing cost (COM_d) was calculated to be R5 749 146 874,99.

5.7.2.2 (c) Subdivision of the Manufacturing Costs

Direct Manufacturing Cost (DMC)

Table 5-46 below provides a summary of the direct manufacturing, fixed manufacturing, and the general expenses.

Table 5-46: Summary of the DMC, FMC and GE.

Manufacturing cost divides	**(R/year)**	**Contribution of the manufacturing costs (%)**
Direct Manufacturing Cost	R4 618 548 893,66	80,33
Fixed Manufacturing Cost	R200 164 796,14	3,48
General Expenses	R946 718 074,17	16,47

5.7.2.2 (d) Revenue

Table 5-47 gives a summary of total revenue, as well as the contribution of the above-mentioned factors affecting the revenue.

Table 5-47: Summary of the costs affecting the revenue.

Revenue from Species	**(R/year)**
Bioethanol	R621 493 995,31
Biogas	R599 648,02
AD DAP	R3 566 929 032,81
Electricity	R56 202 892,20
AD Digestate	R449 990 476,77
Steam	R19 024 163,27
Total Revenue	R4 714 240 208,37

5.7.2.3 Profitability Analysis

5.7.2.3 (a) Discounted Cash Flow Analysis

The Cumulative Cash Flow diagram in Figure 5-3 was generated by setting up cash flow diagrams in Microsoft Excel. The Net Present Value (NPV) was found to be R 2 107 302 592. This was calculated with a bioethanol selling price of R14,7/kg, the biogas selling price of R0,0075/kg, AD DAP selling price of R16,2/kg and electricity selling price of R2,22/kg. A positive NPV shows positive profitability.

The plant would be able to reach a break-even point at six years and ten months with a discounted payback period of 7 years. The Present Value Ratio (PVR) must be over the value of 1 to show profitability. The PVR obtained was 1,77, with a DPBP amount of R 448 452 137, 81.

The IRR was found to be 29,61%. Therefore, the plant shows that it is profitable at the current setting of the discount rate, tax rate and MARCS depreciation.

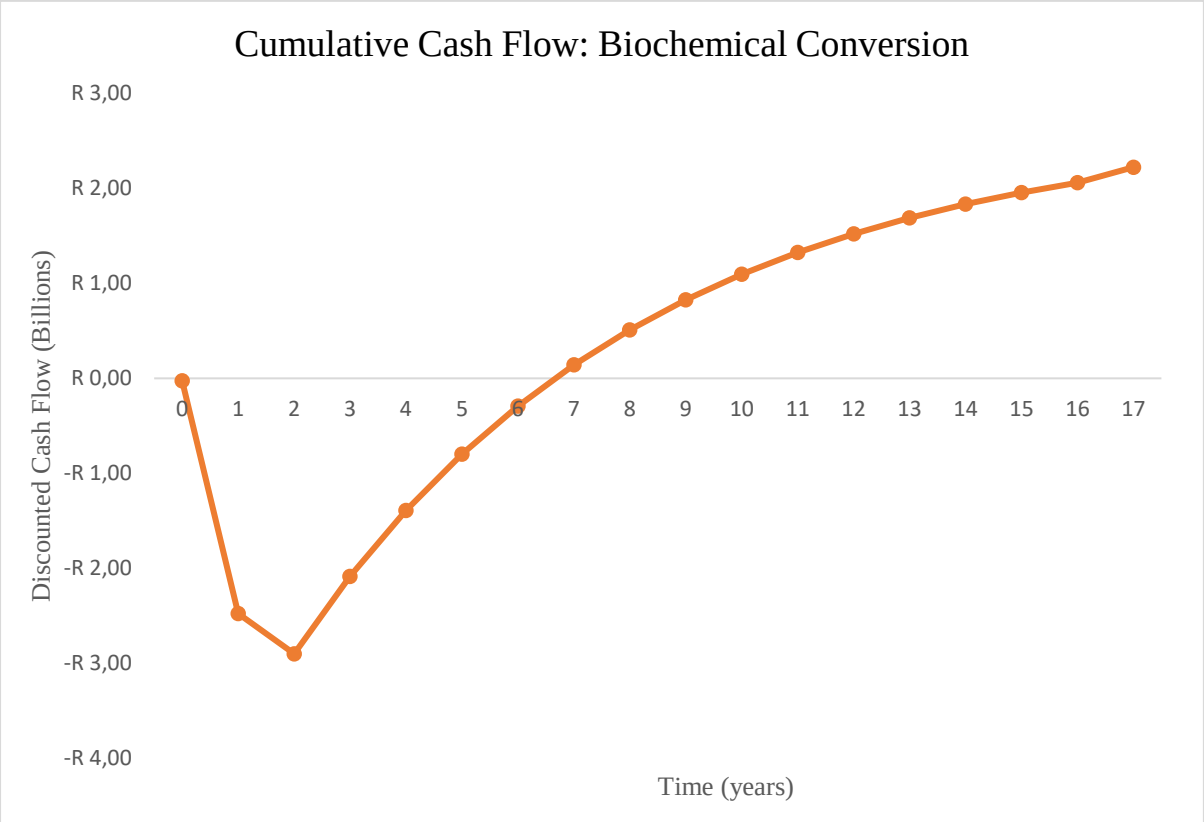

Figure 5-5: Cumulative discounted cash flow.

5.7.2.3 (b) Sensitivity Analysis

The sensitivity analysis conducted below looked at changes in the exchange rate, selling price, operator salaries, tax rate and discount rate. Table 5-48 summarizes the analysis.

Table 5-48: Sensitivity analysis results (All cash flow values are in millions of Rands- x10^9).

Variable	Default	Unit	Minimum value	NPV (min)	Default NPV	Maximum value	NPV (max)
Plant life	15,00		12,75	1,95	2,11	17,25	2,04
Operator rate	52,82	R/hour	44,90	2,11	2,11	60,74	2,11
Land	25 721 471,55	R	21 863 250,82	2,11	2,11	29 579 692,29	2,10
Biogas	0,01	R/kg	0,01	2,11	2,11	0,01	2,11
Products	4, 71	R/yr	4, 01	2,22	2,11	5, 42	1,99
Bioethanol	14,71	R/kg	12,50	1,87	2,11	16,91	2,34
Tax rate	0,28	%	0,24	2,39	2,11	0,32	1,82
Exchange rate	14,79	R/$	12,57	1,78	2,11	17,01	2,43
FCI	2, 90	R	2, 46	2,63	2,11	3, 33	1,59
Raw Material	3, 20	R/yr	2, 72	2,83	2,11	3, 68	1,38
Discount rate	0,171	%	0,15	2,96	2,11	0,20	1,44

The results in Table 5-48 are represented in the tornado diagrams, which clearly show how changes in specific plant variables affect the IRR and the NPV. Refer to Figure 5-4.

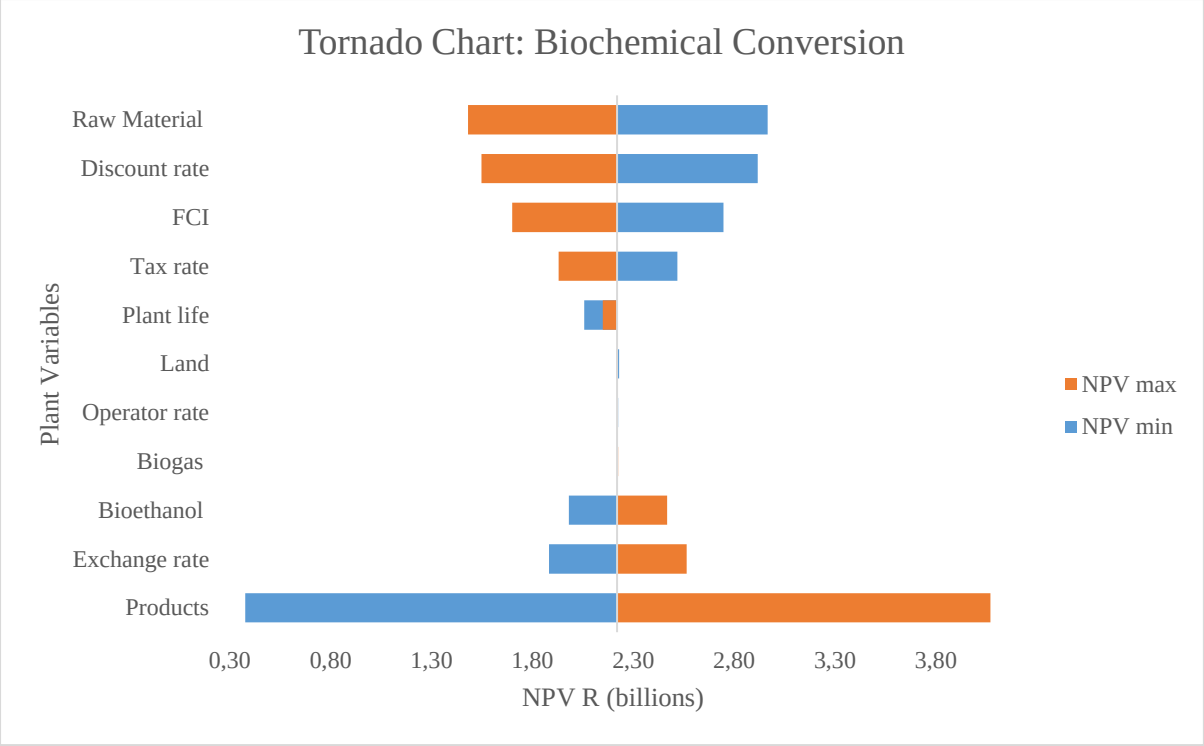

Figure 5-6: Tornado diagram showing sensitivity analysis on NPV.

From Figures 5-6, the NPV was affected mainly by the cost of the products, FCI, raw material, exchange rate and discount rate, which is like the sensitivity analysis of the thermochemical conversion. The rest of the plant variables, namely, cost of land, plant life and operator rate, had a minimal to no impact on the NPV value. When the cost of biogas and the operator rate was maximised, the NPV increased slightly, but no significant change was observed when the plant variables were minimised. When the cost of land was minimised, the NPV value increased somewhat, but when the cost was maximised, the was no change.

Investors can expect a return on their investment when the cost of products or the exchange rate is increased but can expect a loss when the FCI, discount rate, tax rate, or cost of raw material is decreased.

5.8 Life Cycle Assessment

5.8.1 Method of Analysis

The database used for this evaluation was Agribalyse v3.0.1, released in 2020, an LCI database for the agriculture and food sector. The method of analysis used to conduct the impact assessments is ReCiPe 2016 midpoint (H) method and the CML-IA baseline method. These methods are included in the latest comprehensive environmental impact assessment package, openLCA 2.1.3. These methods have been used in various bioprocessing studies (Sacramento-Rivero, Navarro-Pineda & Vilchiz-Bravo, 2016; Hiloidhari, Banerjee & Rao, 2021), including all the critical impact categories for biofuel-based LCAs, and satisfy all ISO standards. In addition, OpenLCA uses the cradle-to-gate method, where all the inputs and outputs are connected to their service provider.

5.8.1.1 Thermochemical conversion

The thermochemical conversion was evaluated using ReCiPe 2016 midpoint (H) LCIA method. The target amount was 4939,12 kg/hr of biodiesel, which was obtained from the mass balance calculations. All inflows and outflows were inputted such that the mass balances. An economic allocation method was selected. The impact results of the thermochemical conversion method are presented in Table 5-49. A model graph representing the complete supply chain of the process is found in Appendix E.

Table 5-49: Impact results of the thermochemical conversion method.

Impact category	**Reference unit**	**Result**
Fine particulate matter formation	kg PM2.5 eq	168,58
Fossil resource scarcity	kg oil eq	14118,61
Freshwater ecotoxicity	kg 1,4-DCB	1229,66
Freshwater eutrophication	kg P eq	13,27
Global warming	kg CO_2 eq	38329,11
Human carcinogenic toxicity	kg 1,4-DCB	2232,37
Human non-carcinogenic toxicity	kg 1,4-DCB	41947,46
Ionizing radiation	kBq Co-60 eq	7331,30
Land use	m^2a crop eq	508,50
Marine ecotoxicity	kg 1,4-DCB	1697,00
Marine eutrophication	kg N eq	3,29
Mineral resource scarcity	kg Cu eq	244,97
Ozone formation, Human health	kg NO_x eq	167,19
Ozone formation, Terrestrial ecosystems	kg NO_x eq	170,45
Stratospheric ozone depletion	kg CFC11 eq	0,02
Terrestrial acidification	kg SO_2 eq	494,94
Terrestrial ecotoxicity	kg 1,4-DCB	103151,7
Water consumption	m^3	559,66

5.8.1.2 Biochemical conversion

The biochemical conversion was also evaluated using ReCiPe 2016 midpoint (H) LCIA method. The target amount was 5133,58 kg/hr of bioethanol, which was obtained from the mass balance calculations. All inflows and outflows were inputted such that the mass balances. An economic-based allocation was selected. The impact results of the biochemical conversion method are presented in Table 5-50. A model graph representing the complete supply chain of the process is found in Appendix E.

Table 5-50: Impact results for the biochemical conversion method.

Impact category	**Reference unit**	**Result**
Fine particulate matter formation	kg PM2.5 eq	-17,45
Fossil resource scarcity	kg oil eq	28181,19
Freshwater ecotoxicity	kg 1,4-DCB	2270,09
Freshwater eutrophication	kg P eq	23,59
Global warming	kg CO_2 eq	68636,13
Human carcinogenic toxicity	kg 1,4-DCB	3177,75
Human non-carcinogenic toxicity	kg 1,4-DCB	81471,18
Ionizing radiation	kBq Co-60 eq	9793,09
Land use	m^2a crop eq	4173,26
Marine ecotoxicity	kg 1,4-DCB	3219,54
Marine eutrophication	kg N eq	4,61
Mineral resource scarcity	kg Cu eq	353,80
Ozone formation, Human health	kg NO_x eq	207,82
Ozone formation, Terrestrial ecosystems	kg NO_x eq	212,49
Stratospheric ozone depletion	kg CFC11 eq	0,03
Terrestrial acidification	kg SO_2 eq	-1406,27
Terrestrial ecotoxicity	kg 1,4-DCB	199547,9
Water consumption	m^3	2182,81

5.8.2 Comparison of impacts

To evaluate the impact of the investigated processes, the following LCIA impact categories were evaluated; abiotic depletion, abiotic depletion (fossil fuels), eutrophication, acidification, fresh water and marine aquatic toxicity, global warming (GWP 100a), human toxicity, photochemical oxidation, ozone layer depletion (ODP), and terrestrial ecotoxicity. The chosen LCIA categories were evaluated by varying the product by doubling the amount produced. The LCIA method used for this evaluation was the CML-IA Baseline with an economic-based allocation. The methods are compared based on 1kg of bioproduct. Table 5-51 shows the LCIA results of the project variants.

Table 5-51: LCIA results for both the biochemical and thermochemical conversion.

Indicator	**Unit**	**Biodiesel 1kg**	**%**	**Biodiesel 5000 kg**	**Bioethanol 1kg**	**%**	**Bioethanol 5000 kg**

Abiotic depletion	kg Sb eq	0,00	55	0,21	0,00	100	0,39
Abiotic depletion (fossil fuels)	MJ	112,29	57	$5{,}55 \times 10^{5}$	198,56	100	$1{,}02 \times 10^{6}$
Acidification	kg SO_2 eq	0,12	68	574,97	-0,17	-100	-883,28
Eutrophication	kg PO_4--- eq	0,01	31	70,67	-0,05	-100	-236,68
Fresh water aquatic ecotoxicity	kg 1,4-DB eq	2,90	62	$1{,}43 \times 10^{4}$	4,70	100	$2{,}41 \times 10^{4}$
Global warming (GWP100a)	kg CO_2 eq	7,53	58	$3{,}72 \times 10^{4}$	13,04	100	$6{,}69 \times 10^{4}$
Human toxicity	kg 1,4-DB eq	3,77	59	$1{,}86 \times 10^{4}$	6,44	100	$3{,}31 \times 10^{4}$
Marine aquatic ecotoxicity	kg 1,4-DB eq	$8{,}85 \times 10^{3}$	66	$4{,}37 \times 10^{7}$	$1{,}35 \times 10^{4}$	100	$6{,}92 \times 10^{7}$
Ozone layer depletion (ODP)	kg CFC-11 eq	0,00	64	0,01	0,00	100	0,01
Photochemical oxidation	kg C_2H_4 eq	0,00	69	24,56	0,01	100	37,20
Terrestrial ecotoxicity	kg 1,4-DB eq	0,02	44	104,70	0,05	100	249,72

Figure 5-7 shows the relative indicator results for the respective scenarios. The thermochemical conversion shows results for abiotic depletion (fossil fuels), human toxicity, global warming (GWP 100a), and photochemical oxidation. The biochemical conversion shows results for acidification, eutrophication, global warming (GWP 100a), human toxicity, and photochemical oxidation. In both conversion methods, the human toxicity is relatively lower.

The thermochemical conversion of algae shows a consistently lower environmental impact when compared to the biochemical conversion method. The other noticeable difference is the thermochemical method's relatively high acidification and eutrophication levels.

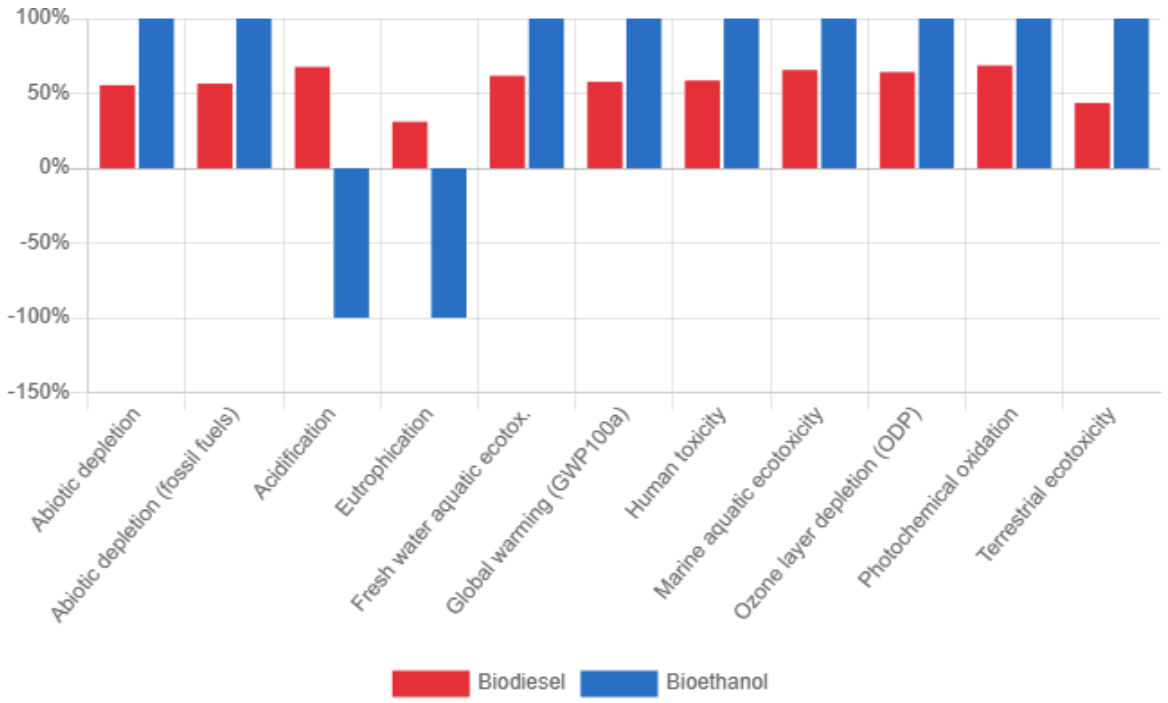

Figure 5-7: Graphical representation of LCIA results.

5.8.2.1 GWP (100-year horizon)

The GWP is the sum of greenhouse gas emissions multiplied by their corresponding GWP factors. Some notable greenhouse gases for this impact calculation include CO_2, CH_4, N_2O, and VOCs. The impact value is assessed over a period of 100 years to predict the cumulative impacts of the greenhouse gases on the global climate (Azapagic, Emsley & Hamerton, 2003). The GWP of the biochemical conversion method is 13,04 kg CO_2 eq, and for the thermochemical conversion method, its 7,53 kg CO_2 eq. Though the biochemical conversion method is double that of the thermochemical method, both approaches are higher than the 2005 RFS diesel mandate of 0,046 kg CO_2 eq per MJ.

5.8.2.2 Acidification

The acidification potential is the sum of the acidification potential of gas expressed relative to that of SO_2 multiplied by its emission in kg per functional unit. The acidification impact refers to contributions to the potential acid deposition of SO_2, HCI, NO_x, HF, and NH_3 (Azapagic, Emsley & Hamerton, 2003). The acidification for the thermochemical method was 0,12 kg SO_2 eq, double that of the biochemical process. The impact is due to the high demand for power that is needed for cultivation and harvesting. The results of this study supported the range of 0,8-2,5 kg SO_2 eq noted by (Saranya & Ramachandra, 2020).

5.8.2.3 Eutrophication

Eutrophication potential is the measure of the likelihood of causing the over-fertilisation of soil and water. The impact is calculated as the sum of the eutrophication potentials for species such as NH_4^+, NO_x, PO_4^{3-}, COD, and P, and their respective emissions (Azapagic, Emsley & Hamerton, 2003). The

eutrophication for the thermochemical method was 0,1 kg PO_4 eq, which is six times higher than the value for the biochemical method. This is significantly higher than the results (Saranya & Ramachandra, 2020) of 0,5-4,24 kg PO_4 eq.

5.8.2.4 Fossil fuel depletion

Abiotic resource depletion alludes to the exhaustion of non-renewable fuel sources such as fossil fuels. The total impact refers to the ratio of the amount of a resource employed per functional unit and its total estimated world reserves (Azapagic, Emsley & Hamerton, 2003). The fossil fuel depletion was 112,29 MJ for the thermochemical method and 198,56 MJ for the biochemical method. The fossil fuel depletion impact is primarily influenced by hydrogen because it requires natural gas in steam methane reforming. The biochemical method would therefore have a high impact value because of the complexity. Both methods correspond with the range of 106-277 MJ noted by (Saranya & Ramachandra, 2020).

5.8.2.5 Photochemical oxidation

Photochemical oxidation is expressed relative to the photochemical oxidation classification factors of ethylene. The impact is calculated as the sum of emissions from different species multiplied by their corresponding classification factors. This involves primarily VOCs, which are classified into alkanes, ketones, halogenated HCs, esters, alcohols, ethers, olefins, aromatics, acetylenes, and aldehydes (Azapagic, Emsley & Hamerton, 2003). The impact value for the thermochemical method was 0,00 kg C_2H_4 eq, and for the biochemical method, it was 0,01 kg C_2H_4 eq. In both cases, the impacts were lower than the range of 0,05-0,22 kg C_2H_4 eq noted by (Saranya & Ramachandra, 2020). In theory, photochemical oxidation can be as high as 2,69 kg C_2H_4 eq, owing to the application of hexane in the transesterification process (Hou *et al*., 2011).

5.8.2.6 Human toxicity

This human toxicity impact refers to the releases to air, water and soil, which are toxic to humans (Azapagic, Emsley & Hamerton, 2003). This impact is based on the intrinsic toxicity of a chemical compound and its potential dose (Hertwich *et al*., 2001). The human toxicity for the biochemical method was found to be 41,46% higher than the impact of the thermochemical method.

5.8.2.7 Aquatic toxicity

The aquatic toxicity potential is the sum of the toxicity classification factors of different aquatic toxic substances multiplied by their corresponding emissions to the aquatic ecosystems (Azapagic, Emsley & Hamerton, 2003). It considers all emissions during the life cycle stages of systems, services, and products. The more dominant emissions in this impact category are heavy metals and sulphuric acid, which are mostly released into the air (Borrion, Khraisheh & Benyahia, 2012). The marine aquatic toxicity of the biochemical method was found to be 34,38% higher than the impact of the thermochemical method. The freshwater aquatic toxicity for the biochemical method was 38,3% higher.

5.8.3 LCA interpretation

The results illustrated on the relative indicator chart show that the biochemical method significantly impacts most impact categories, excluding acidification and eutrophication. This means the thermochemical method is the more favourable conversion method for biofuels. However, though the thermochemical method is the eco-friendlier alternative, attention still needs to be given to the conversion method. A reduction in environmental effects below typical fuel levels through all life-cycle metrics is imperative for algal fuels.

5.9 Overall comparison

This section takes an overall comparison of the investigated processes. The approach covers the comparison by each objective of the study. Table 5-52 summarises pivotal details for each objective outlined for this research project.

Table 5-52: Overall comparison on investigated process.

	Thermochemical Conversion	Biochemical Conversion
Objective 1: Process synthesis The synthesis of both conversion methods was informed by the works of (Jones *et al*., 2014), (Chen & Quinn, 2021), (Davis *et al*., 2014) and various other literature. The thermochemical conversion focused on the three main processes mentioned below but is not limited to this. Most studies investigating this process have included anaerobic digestion, a biochemical method, and other processes. However, the cost of wastewater treatment was accounted for in the economic analysis. The thermochemical conversion investigation also considered chemical conversion methods to produce biodiesel. The biochemical conversion investigation focused on the processes mentioned and notably anaerobic digestion in this case. Fermentation and anaerobic digestion are both biochemical methods which produce biofuels.		
Feed	Wet algal biomass with 20 wt%	Wet algal biomass with 20 wt%
Process sections	1. HTL (depolymerisation) 2. Hydrotreating (removal of contaminants with H_2) 3. Hydrocracking (removal of contaminants with high activity catalyst and H_2	1. Pre-treatment with dilute H_2SO_4 2. Conditioning with dilute NH_3 3. Fermentation with *S. cerevisiae* 4. Purification (via beer distillation column, rectification column, molecular sieve adsorption unit 5. Anaerobic digestion
Objective 2: Mass and energy balances Mass and energy balance calculations were successfully completed for both investigated methods, with low errors which are a result of significant figures and unit conversions. Process properties were calculated using appropriate equations. The biochemical method had a higher mass and energy ratio, a higher energy efficiency, and a lower PMI.		
Process simulation	Reactors: R-301, R-310Y, R-350Y used RYield model.	Reactors: R-101 (pre-treatment), R-102 (conditioning), R201 (seed growth), R-202 (fermentation) used RStoic, and R-501 (anaerobic digestor), R-502 (anaerobic digestor) used RYield
	Purification; T-301, T-320, T-330, T-350 used Radfrac model.	Purification; T-301, T-302, T-303 used Radfrac

Mass ratio	0,39	0,98
Energy intensity (MJ/kg)	-172,79	-70,68
Energy ratio	0,39	0,7286
Energy efficiency %	47,45	73,11
Objective 3: Heat integration Using the AEA, the thermochemical conversion simulation was able to save 23,56 % energy and 17,3 % of carbon emissions were reduced. However, the base case simulation for the biochemical conversion had no design scenarios to improve the HEN.		
Power requirement (MW)	2,54	0,73
Heat requirement (MW)	19,68	-68,1
Available energy saving (MW)	15 620	59 950
Available carbon emissions savings (kg/hr)	1 836	13 536
Energy saving %	23,56	No design alternatives from AEA to improve HEN.
Greenhouse gases reduction	17,3	No design alternatives from AEA to improve HEN.
Objective 4: Economic Analysis The cost of equipment for the biochemical conversion was 4,83% lower, but the FCI was 18,3% higher. Therefore, the conversion also had a higher IRR and higher NPV. Generally, a project with a higher IRR and NPV is the more desirable project, which means the company can expect a higher rate of return. Though this is the case, the biochemical is not a suitable option as most of its revenue comes from by-products. Therefore, the more appropriate method would be thermochemical conversion because its revenue comes from biodiesel.		
Equipment cost (R)	453 721 525,35	428 691 192,54
FCI (R)	2 367 160 592,35	2 898 328 107,68
TCI (R)	2 840 592 710,82	3 477 993 729,21
Manufacturing (R)	7 037 479 644,51	5 749 146 874,99
Revenue (R)	7 678 981 722,85	4 714 240 208,37
NPV(R)	1 344 301 784,18	2 223 983 071,52
IRR %	27,36	29,61
Objective 5: Life Cycle Assessment The biochemical conversion proved to be a less sustainable conversion method. From the main impact categories, the biochemical conversion had a high impact on global warming (42,25% higher), a 41,46% higher impact on human toxicity, and a 38,3% higher impact on freshwater aquatic ecotoxicity.		
Global warming (kg CO_2 eq)	7,53	13,04
Human toxicity (kg 1,4-DB eq)	3,77	6,44
Fresh water aquatic ecotoxicity (kg 1,4-DB eq)	2,9	4,7

CHAPTER 6: CONCLUSIONS AND RECOMMENDATIONS

6.1 Conclusions

Comprehensive assessments of biofuel production from algae were executed in this study:

1. Process simulations and mass and energy balances by this study through literature.
2. Heat integration, equipment sizing, heat integration, and life cycle analyses were investigated on the same basis.
3. The investigated processes were compared based on process properties, economics, and life cycle assessments.

These were the following conclusions drawn from those results.

Mass and energy balance calculations were performed for the investigated process to determine the parameters. The biochemical method had a 35,1% higher energy efficiency and a 46,5% higher energy ratio. The method also had a 60,2% higher mass ratio when compared to the thermochemical conversion.

When considering the heating and cooling requirements, the biochemical conversion has a 68,1 MW heat deficiency, whereas the thermochemical conversion had 19,68 MW heat produced. The heating and cooling requirements of the thermochemical conversion proved to be significantly lower than that of the biochemical conversion.

Heat integration was successfully conducted. The thermochemical method had an energy-saving potential of 15620 MW and a greenhouse gas emission-saving potential of 1836 kg/hr. Upon performing the heat integration on AEA, 23,56% of energy was saved, and 17,3 % of carbon emissions were reduced. The biochemical conversion had an energy-saving potential of 59 950 MW and 13 536 kg/hr carbon emissions saving potential, and the base simulation had no design scenarios to improve the HEN.

Equipment sizing was successfully conducted for both investigated processes. When results were above or below the typical volume or area, appropriate calculations were used to adjust the values. Sizing of process equipment was calculated using ACCE, once the material of construction and process unit orientation were entered.

An economic analysis of both methods was performed using a 17,5% discounted cash rate and a 28% tax rate, and the processes were assumed to have a plant life of 17, including two years of construction. The thermochemical conversion had a lower IRR, 27,36 %, and a lower PVR, 1,57. The IRR for the biochemical method was 29,61%, and the PVR was 1,77. As a result, the thermochemical conversion had a lower FCI and purchased costs total but higher revenue and higher cost of raw material.

Finally, an LCA was conducted successfully using the Agribalyse database on OpenLCA. The investigation utilised the ReCiPe 2016 midpoint (H) method and the CML-IA baseline method for the impact assessment. The assessment showed that the thermochemical conversion was the eco-friendlier alternative. The biochemical process greatly impacted most categories except for acidification and eutrophication.

Overall, the thermochemical conversion of algae appeared to be the most economical and sustainable method for converting algal biomass to biofuels. Despite the biochemical conversion having a slightly higher IRR and PVR, the thermochemical conversion would be a more suitable conversion process as most of the biochemical methods revenue comes from selling its by-product.

6.2 Recommendations

- Though the investigation selected specific algae biomass that would be best suited, the research used the general composition for green algae. Further investigations on a suitable algae biomass are essential.
- This report does not consider seasonal fluctuations, which significantly impact the economics of algal biofuels production. Other studies are still required to reduce the costs of algal cultivation and harvesting.
- Further evaluations are necessary to discover alternative coproducts, thus reducing costs and the environmental impact of algal biofuel processes. However, researchers should consider such alternatives based on market volumes.
- This investigation used a significant number of yield and operating conditions assumptions. Therefore, experimental studies are required to validate the assumptions made in this design.
- This investigation did not consider the catalyst performance for upgrading HTL oil. Further examination is needed.

REFERENCES

Aspen Technology, I.. 2000. Aspen Plus ® User Guide. *Aspen Technology, Inc.*

Adeniyi, O.M., Azimov, U. & Burluka, A. 2018. Algae biofuel: Current status and future applications. *Renewable and Sustainable Energy Reviews*. 90(August 2017):316–335. DOI: 10.1016/j.rser.2018.03.067.

AFDC. 2021. *Alternative Fuels Data Center: Fuel Prices*. Available: https://afdc.energy.gov/fuels/prices.html [2022, March 17].

Akobi, C., Yeo, H., Hafez, H. & Nakhla, G. 2016. Single-stage and two-stage anaerobic digestion of extruded lignocellulosic biomass. *Applied Energy*. 184. DOI: 10.1016/j.apenergy.2016.10.039.

Anyanwu, R.C., Rodriguez, C., Durrant, A. & Olabi, A.G. 2018. Micro-Macroalgae Properties and Applications. In *Reference Module in Materials Science and Materials Engineering*. Elsevier. DOI: 10.1016/b978-0-12-803581-8.09259-6.

Ardolino, F., Cardamone, G.F., Parrillo, F. & Arena, U. 2021. Biogas-to-biomethane upgrading: A comparative review and assessment in a life cycle perspective. *Renewable and Sustainable Energy Reviews*. 139:110588. DOI: 10.1016/j.rser.2020.110588.

Arndt, C., Henley, G. & Hartley, F. 2019. Bioenergy in Southern Africa: An opportunity for regional integration? *Development Southern Africa*. 36(2):145–154. DOI: 10.1080/0376835X.2018.1447363.

Ashokkumar, V., Salim, M.R., Salam, Z., Sivakumar, P., Chong, C.T., Elumalai, S., Suresh, V. & Ani, F.N. 2017. Production of liquid biofuels (biodiesel and bioethanol) from brown marine macroalgae Padina tetrastromatica. *Energy Conversion and Management*. 135:351–361. DOI: 10.1016/J.ENCONMAN.2016.12.054.

AspenTech. 2021. *Aspen Energy Analyzer | Reduce Operations Cost | AspenTech*. Available: https://www.aspentech.com/en/products/pages/aspen-energy-analyzer [2021, September 29].

Aui, A., Wang, Y. & Mba-Wright, M. 2021. Evaluating the economic feasibility of cellulosic ethanol: A meta-analysis of techno-economic analysis studies. *Renewable and Sustainable Energy Reviews*. 145:111098. DOI: 10.1016/J.RSER.2021.111098.

Azapagic, A., Emsley, A. & Hamerton, L. 2003. Definition of Environmental Impacts. *Polymers, the Environment and Sustainable Development*. (May, 22):197–200. DOI: 10.1002/0470865172.APP2.

Babich, I. V., van der Hulst, M., Lefferts, L., Moulijn, J.A., O'Connor, P. & Seshan, K. 2011. Catalytic pyrolysis of microalgae to high-quality liquid bio-fuels. *Biomass and Bioenergy*. 35(7). DOI: 10.1016/j.biombioe.2011.04.043.

Baêta, B.E.L., Lima, D.R.S., Filho, J.G.B., Adarme, O.F.H., Gurgel, L.V.A. & Aquino, S.F. de. 2016. Evaluation of hydrogen and methane production from sugarcane bagasse hemicellulose hydrolysates by two-stage anaerobic digestion process. *Bioresource Technology*. 218. DOI: 10.1016/j.biortech.2016.06.113.

Balat, M., Balat, H. & Öz, C. 2008. Progress in bioethanol processing. *Progress in Energy and Combustion Science*. 34(5):551–573. DOI: 10.1016/J.PECS.2007.11.001.

Baskar, G., Kalavathy, G., Aiswarya, R. & Abarnaebenezer Selvakumari, I. 2019. Advances in bio-oil extraction from nonedible oil seeds and algal biomass. In *Advances in Eco-Fuels for a Sustainable Environment*. Elsevier. 187–210. DOI: 10.1016/b978-0-08-102728-8.00007-3.

Basu, P. 2018. Introduction. In *Biomass Gasification, Pyrolysis and Torrefaction: Practical Design and Theory*. Elsevier. 1–27. DOI: 10.1016/B978-0-12-812992-0.00001-7.

Bates, J., Burton, D.J., Creese, R.C., Cce, P.E., Hollmann, J.K., Cce, P.E., Mcdonald, D.F., Cce, J.P.E., et al. 2005. COST ESTIMATE CLASSIFICATION SYSTEM – AS APPLIED IN ENGINEERING , PROCUREMENT , AND CONSTRUCTION FOR THE PROCESS INDUSTRIES. *AACE International Recommended Practice*. (18).

Beal, C.M., Gerber, L.N., Sills, D.L., Huntley, M.E., Machesky, S.C., Walsh, M.J., Tester, J.W., Archibald, I., et al. 2015. DOI: 10.1016/j.algal.2015.04.017.

Biller, P. 2013. Hydrothermal Processing of Microalgae (Presentation). *Rsc*. (April). Available: http://www.rsc.org/images/w-brilman_tcm18-237400.pdf.

Biller, P., Riley, R. & Ross, A.B. 2011. Catalytic hydrothermal processing of microalgae: Decomposition and upgrading of lipids. *Bioresource Technology*. 102(7):4841–4848. DOI: 10.1016/J.BIORTECH.2010.12.113.

Blanchard, R., Richardson, D.M., O, P.J., von Maltitz, G.P. & Maltitz, V.G. 2011. Biofuels and biodiversity in South Africa. *S Afr J Sci*. 107(5). DOI: 10.4102/sajs.

Bolton, J. & Victor, J. 2018. *A Biosystematics Research Strategy for Algae in South Africa*. Available: www.Algaebase.org [2021, July 03].

Borrion, A.L., Khraisheh, M. & Benyahia, F. 2012. Environmental life cycle impact assessment of Gas-to-Liquid processes. *Proceedings of the 3rd Gas Processing Symposium*. (January, 1):71–77. DOI: 10.1016/B978-0-444-59496-9.50011-4.

Brand South Africa. 2013. *SA to blend biofuels from 2015 | Brand South Africa*. Available: https://www.brandsouthafrica.com/investments-immigration/business/trends/newbusiness/biofuels-011013 [2021, July 03].

Brennan, L. & Owende, P. 2010. Biofuels from microalgae-A review of technologies for production, processing, and extractions of biofuels and co-products. *Renewable and Sustainable Energy Reviews*. 14(2):557–577. DOI: 10.1016/j.rser.2009.10.009.

Burk, C. 2018. Techno-Economic Analysis for New Technology Development. *Chemical Engineering Progress*. 43–52.

Burnley, S., Wagland, S. & Longhurst, P. 2019. Using life cycle assessment in environmental engineering education. *Higher Education Pedagogies*. 4(1):64–79. DOI: 10.1080/23752696.2019.1627672.

Bušić, A., Marđetko, N., Kundas, S., Morzak, G., Belskaya, H., Šantek, M.I., Komes, D., Novak, S., et al. 2018. Bioethanol Production from Renewable Raw Materials and Its Separation and Purification: A Review. *Food Technology & Biotechnology*. 56(3). DOI: 10.17113/ftb.56.03.18.5546.

Chen, P.H. & Quinn, J.C. 2021. Microalgae to biofuels through hydrothermal liquefaction: Open-source techno-economic analysis and life cycle assessment. *Applied Energy*. 289. DOI: 10.1016/j.apenergy.2021.116613.

Chen, H., Fu, Q., Liao, Q., Zhang, H., Huang, Y., Xia, A. & Zhu, X. 2018. Rheological properties of microalgae slurry for application in hydrothermal pretreatment systems. *Bioresource Technology*. 249:599–604. DOI: 10.1016/J.BIORTECH.2017.10.051.

Chen, W., Lin, B., Lin, Y., Chu, Y., Ubando, A.T., Loke, P., Chyuan, H., Chang, J., et al. 2021. Progress in biomass torrefaction : Principles , applications and challenges. 82. DOI: 10.1016/j.pecs.2020.100887.

Chen, W.H., Lin, B.J., Huang, M.Y. & Chang, J.S. 2015. Thermochemical conversion of microalgal biomass into biofuels: A review. *Bioresource Technology*. 184:314–327. DOI: 10.1016/j.biortech.2014.11.050.

Connelly, R. 2014. Second-Generation Biofuel from High-Efficiency Algal-Derived Biocrude. In *Bioenergy Research: Advances and Applications*. Elsevier Inc. 153–170. DOI: 10.1016/B978-0-444-59561-4.00010-3.

Curran, M.A. 2006. *Life Cycle Assessment: Principles and Practice*.

Danquah, M., Liu, B. & Harun, R. 2011. Analysis of process configurations for bioethanol production from microalgal biomass. *Progress in Biomass and Bioenergy Production*. (July, 27). DOI: 10.5772/17468.

Dasan, Y.K., Lam, M.K., Yusup, S., Lim, J.W. & Lee, K.T. 2019. Life cycle evaluation of microalgae biofuels production: Effect of cultivation system on energy, carbon emission and cost balance analysis. *Science of the Total Environment*. 688. DOI: 10.1016/j.scitotenv.2019.06.181.

Davis, R., Kinchin, C., Markham, J., Tan, E.C.D. & Laurens, L.M.L. 2014. *Process Design and Economics for the Conversion of Algal Biomass to Biofuels : Algal Biomass Fractionation to Lipid-Products Process Design and Economics for the Conversion of Algal Biomass to Biofuels : Algal Biomass Fractionation to Lipid- and Carbohyd*.

Demirbas, A. & Fatih Demirbas, M. 2011. Importance of algae oil as a source of biodiesel. In *Energy Conversion and Management*. V. 52. DOI: 10.1016/j.enconman.2010.06.055.

Demirbaş, A. 2006. Oily products from mosses and algae via pyrolysis. *Energy Sources, Part A: Recovery, Utilization and Environmental Effects*. 28(10). DOI: 10.1080/009083190910389.

Demırbas, A. 2017. The social, economic, and environmental importance of biofuels in the future. *Energy Sources, Part B: Economics, Planning and Policy*. 12(1):47–55. DOI: 10.1080/15567249.2014.966926.

Dilia, P. & Leila, K. 2018. Fatty Acids From Microalgae Botryococcus braunii For Raw Material of Biodiesel. *J. Phys*. 12010. DOI: 10.1088/1742-6596/1095/1/012010.

Dolganyuk, V., Belova, D., Babich, O., Prosekov, A., Ivanova, S., Katserov, D., Patyukov, N. & Sukhikh, S. 2020. Microalgae: A Promising Source of Valuable Bioproducts. *Biomolecules 2020, Vol. 10, Page 1153*. 10(8):1153. DOI: 10.3390/BIOM10081153.

Dote, Y., Sawayama, S., Inoue, S., Minowa, T. & Yokoyama, S. ya. 1994. Recovery of liquid fuel from hydrocarbon-rich microalgae by thermochemical liquefaction. *Fuel*. 73(12):1855–1857. DOI: 10.1016/0016-2361(94)90211-9.

Duan, P. & Savage, P.E. 2010. Hydrothermal Liquefaction of a Microalga with Heterogeneous Catalysts. *Industrial and Engineering Chemistry Research*. 50(1):52–61. DOI: 10.1021/IE100758S.

Dutta, S., Neto, F. & Coelho, M.C. 2016. Microalgae biofuels : A comparative study on techno-economic analysis & life-cycle assessment. *ALGAL*. 20:44–52. DOI: 10.1016/j.algal.2016.09.018.

EduPristine. 2018. *Sensitivity Analysis: Meaning, Uses, Methods of measurement*. Available: https://www.edupristine.com/blog/all-about-sensitivity-analysis [2022, March 15].

El-Mekkawi, S.A., Abdo, S.M., Samhan, F.A. & Ali, G.H. 2019. Optimization of some fermentation conditions for bioethanol production from microalgae using response surface method. *Bulletin of the National Research Centre*. 43(164). DOI: 10.1186/s42269-019-0205-8.

Enerdata. 2019. *South Africa Energy Information | Enerdata*. Available: https://www.enerdata.net/estore/energy-market/south-africa/ [2021, July 07].

ExchangeRates. 2022. *US Dollar to South African Rand Spot Exchange Rates for 2021*. Available: https://www.exchangerates.org.uk/USD-ZAR-spot-exchange-rates-history-2021.html [2022, March

31].

Fakruddin, M., Quayum, M.A., Ahmed, M.M. & Choudhury, N. 2012. Analysis of key factors affecting ethanol production by Saccharomyces cerevisiae IFST-072011. *Biotechnology*. 11(4). DOI: 10.3923/biotech.2012.248.252.

Fasahati, P., Woo, H.C. & Liu, J.J. 2015. Industrial-scale bioethanol production from brown algae: Effects of pretreatment processes on plant economics. *Applied Energy*. 139:175–187. DOI: 10.1016/J.APENERGY.2014.11.032.

Fawthrop, A. 2019. *Coal to remain a "significant" part of South Africa energy mix before 2030*. Available: https://www.nsenergybusiness.com/news/south-africa-energy-mix-2030/ [2021, July 07].

Fernando, J. 2022. *Internal Rate of Return (IRR) Definition*. Available: https://www.investopedia.com/terms/i/irr.asp [2022, March 15].

Gao, G., Burgess, J.G., Wu, M., Wang, S. & Gao, K. 2020. Using macroalgae as biofuel: current opportunities and challenges. *Botanica Marina*. 63(4):355–370. DOI: 10.1515/BOT-2019-0065.

Gheewala, S.H., Damen, B. & Shi, X. 2013. Biofuels: Economic, environmental and social benefits and costs for developing countries in Asia. *Wiley Interdisciplinary Reviews: Climate Change*. 4(6):497–511. DOI: 10.1002/wcc.241.

Gnansounou, E. & Kenthorai Raman, J. 2016. Life cycle assessment of algae biodiesel and its co-products. *Applied Energy*. 161. DOI: 10.1016/j.apenergy.2015.10.043.

Gouveia, J.D., Ruiz, J., van den Broek, L.A.M., Hesselink, T., Peters, S., Kleinegris, D.M.M., Smith, A.G., van der Veen, D., et al. 2017. Botryococcus braunii strains compared for biomass productivity, hydrocarbon and carbohydrate content. *Journal of Biotechnology*. 248:77–86. DOI: 10.1016/J.JBIOTEC.2017.03.008.

Gouveia, J.D., Moers, A., Griekspoor, Y., Van Den Broek, L.A.M., Springer, J., Sijtsma, L., Sipkema, D., Wijffels, R.H., et al. 2019. Effect of removal of bacteria on the biomass and extracellular carbohydrate productivity of Botryococcus braunii. *Journal of Applied Phycology*. DOI: 10.1007/s10811-019-01847-0.

GSCTanks. 2018. *7 Types of Industrial Storage Tanks Explained - GSC Tanks*. Available: https://www.gsctanks.com/industrial-storage-tanks/ [2022, March 02].

Gu, X., Yu, L., Pang, N., Martinez-Fernandez, J.S., Fu, X. & Chen, S. 2020. Comparative techno-economic analysis of algal biofuel production via hydrothermal liquefaction: One stage versus two stages. *Applied Energy*. 259(November 2019):114115. DOI: 10.1016/j.apenergy.2019.114115.

Gutiérrez Ortiz, F.J. 2020. DOI: 10.1016/j.supflu.2020.104788.

Henley, G. & Fundira, T. 2019. Policy and trade issues for a future regional biofuels market in Southern Africa. *Development Southern Africa*. 36(2):250–264. DOI: 10.1080/0376835X.2019.1605882.

Herbert Lee Stafford, W., Adrian Lotter, G., Paul von Maltitz, G. & Colin Brent, A. 2019. Biofuels technology development in Southern Africa. *Development Southern Africa*. 36(2):155–174. DOI: 10.1080/0376835X.2018.1481732.

Hertwich, E.G., Mateles, S.F., Pease, W.S. & McKone, T.E. 2001. Human toxicity potentials for life-cycle assessment and toxics release inventory risk screening. *Environmental Toxicology and Chemistry*. 20(4):928–39. Available: https://www.researchgate.net/publication/11992946_Human_toxicity_potentials_for_life-cycle_assessment_and_toxics_release_inventory_risk_screening [2022, March 01].

Hiloidhari, M., Banerjee, R. & Rao, A.B. 2021. Life cycle assessment of sugar and electricity production under different sugarcane cultivation and cogeneration scenarios in India. *Journal of Cleaner Production*. 290:125170. DOI: 10.1016/J.JCLEPRO.2020.125170.

Hong, Y., Chen, W., Luo, X., Pang, C., Lester, E. & Wu, T. 2017. Microwave-enhanced pyrolysis of macroalgae and microalgae for syngas production. *Bioresource Technology*. 237:47–56. DOI: 10.1016/J.BIORTECH.2017.02.006.

Hossain, S.M.Z., Razzak, S.A., Al-Shater, A.F., Moniruzzaman, M. & Hossain, M.M. 2020. Recent Advances in Enzymatic Conversion of Microalgal Lipids into Biodiesel. *Energy and Fuels*. 34(6):6735–6750. DOI: 10.1021/acs.energyfuels.0c01064.

Hou, J., Zhang, P., Yuan, X. & Zheng, Y. 2011. Life cycle assessment of biodiesel from soybean, jatropha and microalgae in China conditions. *Renewable and Sustainable Energy Reviews*. 15(9):5081–5091. DOI: 10.1016/J.RSER.2011.07.048.

Howard, D. 2016. *Net Present Value and Internal Rate of Return | Vertical Spaces Properties*. Available: https://www.verticalspaces.co.za/news/net-present-value-and-internal-rate-of-return/ [2022, March 15].

Humbird, D., Davis, R., Tao, L., Kinchin, C., Hsu, D., Aden, A., Schoen, P., Lukas, J., et al. 2011. Process design and economics for conversion of lignocellulosic biomass to ethanol. *NREL technical report NREL/TP-5100-51400*. 303(May 2011):275–3000. Available: http://www.nrel.gov/docs/fy11osti/51400.pdf%5Cnpapers2://publication/uuid/49A5007E-9A58-4E2B-AB4E-4A4428F6EA66.

Ilgin, M.A. & Gupta, S.M. 2010. Environmentally conscious manufacturing and product recovery (ECMPRO): A review of the state of the art. *Journal of Environmental Management*. 91(3):563–591. DOI: 10.1016/J.JENVMAN.2009.09.037.

Jafari, O. & Zilouei, H. 2016. Enhanced biohydrogen and subsequent biomethane production from sugarcane bagasse using nano-titanium dioxide pretreatment. *Bioresource Technology*. 214. DOI: 10.1016/j.biortech.2016.05.007.

Jahirul, M.I., Brown, J.R., Senadeera, W., Ashwath, N., Laing, C., Leski-Taylor, J. & Rasul, M.G. 2013. Optimisation of bio-oil extraction process from Beauty Leaf (Calophyllum inophyllum) oil seed as a second generation biodiesel source. In *Procedia Engineering*. V. 56. DOI: 10.1016/j.proeng.2013.03.168.

Jambo, S.A., Abdulla, R., Mohd Azhar, S.H., Marbawi, H., Gansau, J.A. & Ravindra, P. 2016. A review on third generation bioethanol feedstock. *Renewable and Sustainable Energy Reviews*. 65:756–769. DOI: 10.1016/J.RSER.2016.07.064.

Jazzar, S., Quesada-Medina, J., Olivares-Carrillo, P., Marzouki, M.N., Acién-Fernández, F.G., Fernández-Sevilla, J.M., Molina-Grima, E. & Smaali, I. 2015. A whole biodiesel conversion process combining isolation, cultivation and in situ supercritical methanol transesterification of native microalgae. *Bioresource Technology*. 190:281–288. DOI: 10.1016/J.BIORTECH.2015.04.097.

Jena, U. & Das, K.C. 2011. Comparative evaluation of thermochemical liquefaction and pyrolysis for bio-oil production from microalgae. *Energy and Fuels*. 25(11). DOI: 10.1021/ef201373m.

Jones, S. 2016. *Algae driving our bioeconomy*. Available: https://journals.co.za/doi/pdf/10.10520/EJC199197 [2021, July 03].

Jones, S. & Snowden-swan, L. 2021. *Microalgae Conversion to Biofuels and Biochemical via Sequential Hydrothermal Liquefaction (SEQHTL) and Bioprocessing : 2020 State of Technology*.

Jones, S., Zhu, Y., Anderson, D., Hallen, R.T. & Elliott, D.C. 2014. *Process Design and Economics for the Conversion of Algal Biomass to Hydrocarbons : Whole Algae Hydrothermal Liquefaction and Upgrading*. Available: http://www.pnnl.gov/main/publications/external/technical_reports/PNNL-23227.pdf.

Juneja, A. & Murthy, G.S. 2017. Evaluating the potential of renewable diesel production from algae cultured on wastewater: Techno-economic analysis and life cycle assessment. *AIMS Energy*. 5(2):239–257. DOI: 10.3934/energy.2017.2.239.

Kagan, J. 2021. *Modified Accelerated Cost Recovery System (MACRS) Definition*. Available: https://www.investopedia.com/terms/m/macrs.asp [2022, March 15].

Kapoore, R.V., Butler, T.O., Pandhal, J. & Vaidyanathan, S. 2018. DOI: 10.3390/biology7010018.

Kavitha, S., Gajendran, T., Saranya, K., Selvakumar, P. & Manivasagan, V. 2021. Study on consolidated bioprocessing of pre-treated Nannochloropsis gaditana biomass into ethanol under optimal

strategy. *Renewable Energy*. 172:440–452. DOI: 10.1016/J.RENENE.2021.03.015.

Kolmetz, K. & Sari, R.M. 2014. *General Process Plant Cost Estimating (Engineering Design Guideline)*. Available: www.klmtechgroup.com [2022, May 24].

Koohikamali, S., Tan, C.P. & Ling, T.C. 2012. Optimization of sunflower oil transesterification process using sodium methoxide. *The Scientific World Journal*. 2012. DOI: 10.1100/2012/475027.

Labriet, M. 2013. *ENERGY TECHNOLOGY SYSTEM ANALYSIS PROGRAMME IEA-ETSAP© Technology Brief P11-December 2013-www.etsap.org Biogas and Bio-syngas Production TECHNICAL HIGHLIGHTS*. Available: www.etsap.org [2021, July 01].

Lee, O.K. & Lee, E.Y. 2016. Sustainable production of bioethanol from renewable brown algae biomass. *Biomass and Bioenergy*. 92:70–75. DOI: 10.1016/J.BIOMBIOE.2016.03.038.

León, M., Silva, J., Carrasco, S. & Barrientos, N. 2020. Design, Cost Estimation and Sensitivity Analysis for a Production Process of Activated Carbon from Waste Nutshells by Physical Activation. *Processes 2020, Vol. 8, Page 945*. 8(8):945. DOI: 10.3390/PR8080945.

Levin, D.B., Verbeke, T.J., Munir, R., Islam, R., Ramachandran, U., Lal, S., Schellenberg, J. & Sparling, R. 2015. Omics Approaches for Designing Biofuel Producing Cocultures for Enhanced Microbial Conversion of Lignocellulosic Substrates. In *Direct Microbial Conversion of Biomass to Advanced Biofuels*. DOI: 10.1016/B978-0-444-59592-8.00017-8.

López-Gómez, J.P. & Pérez-Rivero, C. 2019. Cellular systems. In *Comprehensive Biotechnology*. Elsevier. 9–21. DOI: 10.1016/B978-0-444-64046-8.00067-7.

Marsolek, M.D., Kendall, E., Thompson, P.L. & Shuman, T.R. 2014. Thermal pretreatment of algae for anaerobic digestion. *Bioresource Technology*. 151:373–377. DOI: 10.1016/J.BIORTECH.2013.09.121.

Martinez-Fernandez, J.S. & Chen, S. 2017. Sequential Hydrothermal Liquefaction characterization and nutrient recovery assessment. *Algal Research*. 25. DOI: 10.1016/j.algal.2017.05.022.

Martinez-Guerra, E. & Gude, V.G. 2018. Energy analysis of extractive-transesterification of algal lipids for biocrude production. *Biofuels*. 9(2). DOI: 10.1080/17597269.2016.1195972.

Masoumi, S. & Dalai, A.K. 2021. Techno-economic and life cycle analysis of biofuel production via hydrothermal liquefaction of microalgae in a methanol-water system and catalytic hydrotreatment using hydrochar as a catalyst support. *Biomass and Bioenergy*. 151:106168. DOI: 10.1016/J.BIOMBIOE.2021.106168.

Math, M.C. & Chandrashekhara, K.N. 2016. Optimization of alkali catalyzed transesterification of safflower oil for production of biodiesel. *Journal of Engineering (United Kingdom)*. 2016. DOI: 10.1155/2016/8928673.

Mathiyazhagan, M. & Ganapathi, a. 2011. Factors Affecting Biodiesel Production. *Research in Plant Biology*. 1(2):1–5.

Matsui, T.O., Nishihara, A., Ueda, C., Ohtsuki, M., Ikenaga, N.O. & Suzuki, T. 1997. Liquefaction of micro-algae with iron catalyst. *Fuel*. 76(11):1043–1048. DOI: 10.1016/S0016-2361(97)00120-8.

Maxwell, C. 2022. *Cost Indices – Towering Skills*. Available: https://www.toweringskills.com/financial-analysis/cost-indices/ [2022, March 15].

Medipally, S.R., Yusoff, F.M., Banerjee, S. & Shariff, M. 2015. DOI: 10.1155/2015/519513.

Milano, J., Ong, H.C., Masjuki, H.H., Chong, W.T., Lam, M.K., Loh, P.K. & Vellayan, V. 2016. Microalgae biofuels as an alternative to fossil fuel for power generation. *Renewable and Sustainable Energy Reviews*. 58:180–197. DOI: 10.1016/J.RSER.2015.12.150.

Molino, A., Iovane, P. & Migliori, M. 2016. Biomethane production by biogas with polymeric membrane module. In *Membrane Technologies for Biorefining*. Elsevier Inc. 465–482. DOI: 10.1016/B978-0-08-100451-7.00018-9.

Monari, C., Righi, S. & Olsen, S.I. 2016. Greenhouse gas emissions and energy balance of biodiesel production from microalgae cultivated in photobioreactors in Denmark: A life-cycle modeling. *Journal of Cleaner Production*. 112. DOI: 10.1016/j.jclepro.2015.08.112.

Monteith, E.R., Mampuys, P., Summerton, L., Clark, J.H., Maes, B.U.W. & McElroy, C.R. 2020. Why we might be misusing process mass intensity (PMI) and a methodology to apply it effectively as a discovery level metric. *Green Chemistry*. 22(1):123–135. DOI: 10.1039/C9GC01537J.

Moradi-kheibari, N., Ahmadzadeh, H., Talebi, A.F., Hosseini, M. & Murry, M.A. 2019. Recent advances in lipid extraction for biodiesel production. In *Advances in Feedstock Conversion Technologies for Alternative Fuels and Bioproducts: New Technologies, Challenges and Opportunities*. DOI: 10.1016/B978-0-12-817937-6.00010-2.

Mu, D., Xin, C. & Zhou, W. 2019. Life cycle assessment and techno-economic analysis of algal biofuel production. In *Microalgae Cultivation for Biofuels Production*. DOI: 10.1016/B978-0-12-817536-1.00018-7.

Mujeeb, M.A., Vedamurthy, A.B. & Shivasharana, C.T. 2016. Current strategies and prospects of biodiesel production: A review. *Pelagia Research Library Advances in Applied Science Research*. 7(1).

Murthy, G.S. 2011. Overview and assessment of algal biofuels production technologies. In *Biofuels*. DOI: 10.1016/B978-0-12-385099-7.00019-X.

Nagaraja, Y.P., Biradar, C., Manasa, K.S. & Venkatesh, H.S. 2014. Production of biofuel by using micro algae (Botryococcus braunii) Sample collection. *Internatational Jornal of Current Micobiology*

and Applied Sciences. 3(4).

Neste. 2016. *4 reasons why the world needs biofuels | Neste*. Available: https://www.neste.com/4-reasons-why-world-needs-biofuels [2021, July 16].

Obeid, R., Lewis, D.M., Smith, N., Hall, T. & van Eyk, P. 2020. Reaction kinetics and characterisation of species in renewable crude from hydrothermal liquefaction of monomers to represent organic fractions of biomass feedstocks. *Chemical Engineering Journal*. 389(February):124397. DOI: 10.1016/j.cej.2020.124397.

Odoki, J.B., Stannard, E.E. & Kerali, H.R. 2006. Improvements Incorporated in the new HDM- 4 Version 2. In *Proceedings from the International Conference on Advances in Engineering and Technology*. DOI: 10.1016/b978-008045312-5/50003-0.

Okoronkwo, M.U., Galadima, A. & Leke, L. 2012. Advances in Biodiesel synthesis : from past to present. 43:6924–6945. Available: http://www.elixirpublishers.com/articles/1350731626_43 (2012) 6924-6945.pdf.

Özçimen, D. & İnan, B. 2015. An Overview of Bioethanol Production From Algae. *Biofuels - Status and Perspective*. (September, 30). DOI: 10.5772/59305.

Özçimen, D., Gülyurt, M.Ö. & İnan, B. 2013. Algal Biorefinery for Biodiesel Production. In *Biodiesel - Feedstocks, Production and Applications*. 26–48. Available: http://www.intechopen.com/books/trends-in-telecommunications-technologies/gps-total-electron-content-tec- prediction-at-ionosphere-layer-over-the-equatorial-region%0AInTec%0Ahttp://www.asociatiamhc.ro/wp-content/uploads/2013/11/Guide-to-Hydropower.pdf.

Pacheco, R., Ferreira, A.F., Pinto, T., Nobre, B.P., Loureiro, D., Moura, P., Gouveia, L. & Silva, C.M. 2015. The production of pigments & hydrogen through a Spirogyra sp. biorefinery. *Energy Conversion and Management*. 89. DOI: 10.1016/j.enconman.2014.10.040.

Pan, P., Hu, C., Yang, W., Li, Y., Dong, L., Zhu, L., Tong, D., Qing, R., et al. 2010. The direct pyrolysis and catalytic pyrolysis of Nannochloropsis sp. residue for renewable bio-oils. *Bioresource Technology*. 101(12). DOI: 10.1016/j.biortech.2010.01.070.

Pandey, A. 2008. *Handbook of plant-based biofuels*. DOI: 10.1201/9780789038746.

Papavinasam, S. 2014. Oil and Gas Industry Network. In *Corrosion Control in the Oil and Gas Industry*. Elsevier. 41–131. DOI: 10.1016/b978-0-12-397022-0.00002-9.

Parachin, N.S., Hahn-Hägerdal, B. & Bettiga, M. 2019. A microbial perspective on ethanolic lignocellulose fermentation. In *Comprehensive Biotechnology*. Elsevier. 510–518. DOI: 10.1016/B978-

0-444-64046-8.00379-7.

Payscale. 2019. *Food Manufacturing Hourly Rate in South Africa | PayScale*. Available: https://www.payscale.com/research/ZA/Industry=Food_Manufacturing/Hourly_Rate [2022, March 31].

Peralta-Ruiz, Y., Obregon, L.G. & González-Delgado, Á. 2018. Design of biodiesel and bioethanol production process from microalgae biomass using exergy analysis methodology. *Chemical Engineering Transactions*. 70. DOI: 10.3303/CET1870175.

Perry, S., Perry, R.H., Green, D.W. & Maloney, J.O. 1997. *Perry's Chemical Engineers' Handbook Seventh Edition*. V. 38.

Phillips, T. 2021. *South Africa tops G20 coal-reliance list in 2020, report finds - The Mail & Guardian*. Available: https://mg.co.za/business/2021-03-31-south-africa-tops-g20-coal-reliance-list-in-2020-report-finds/ [2021, July 07].

Piloni, R. V., Daga, I.C., Urcelay, C. & Moyano, E.L. 2021. Experimental investigation on fast pyrolysis of freshwater algae. Prospects for alternative bio-fuel production. *Algal Research*. 54. DOI: 10.1016/j.algal.2021.102206.

Pradhan, A. & Mbohwa, C. 2014. DOI: 10.1016/j.rser.2014.07.131.

Raheem, A., Wan Azlina, W.A.K.G., Taufiq Yap, Y.H., Danquah, M.K. & Harun, R. 2015. DOI: 10.1016/j.rser.2015.04.186.

Rajesh Banu, J., Kavitha, S., Gunasekaran, M. & Kumar, G. 2020. Microalgae based biorefinery promoting circular bioeconomy-techno economic and life-cycle analysis. DOI: 10.1016/j.biortech.2020.122822.

Ramos-Suárez, J.L. & Carreras, N. 2014. Use of microalgae residues for biogas production. *Chemical Engineering Journal*. 242:86–95. DOI: 10.1016/j.cej.2013.12.053.

Rawat, I., Ranjith Kumar, R., Mutanda, T. & Bux, F. 2013. Biodiesel from microalgae: A critical evaluation from laboratory to large scale production. *Applied Energy*. 103:444–467. DOI: 10.1016/j.apenergy.2012.10.004.

Ren, R., Han, X., Zhang, H., Lin, H., Zhao, J., Zheng, Y. & Wang, H. 2018. High yield bio-oil production by hydrothermal liquefaction of a hydrocarbon-rich microalgae and biocrude upgrading. *Carbon Resources Conversion*. 1(2):153–159. DOI: 10.1016/J.CRCON.2018.07.008.

Rodriguez, C., Alaswad, A., Mooney, J., Prescott, T. & Olabi, A.G. 2015. Pre-treatment techniques used for anaerobic digestion of algae. *Fuel Processing Technology*. 138:765–779. DOI: 10.1016/J.FUPROC.2015.06.027.

Saad, M.G., Dosoky, N.S., Zoromba, M.S. & Shafik, H.M. 2019. Algal biofuels: Current status and key challenges. *Energies*. 12(10). DOI: 10.3390/en12101920.

Sacramento-Rivero, J.C., Navarro-Pineda, F. & Vilchiz-Bravo, L.E. 2016. Evaluating the sustainability of biorefineries at the conceptual design stage. *Chemical Engineering Research and Design*. 107:167–180. DOI: 10.1016/J.CHERD.2015.10.017.

Salam, K.A., Velasquez-Orta, S.B. & Harvey, A.P. 2016. A sustainable integrated in situ transesterification of microalgae for biodiesel production and associated co-product-a review. *Renewable and Sustainable Energy Reviews*. 65:1179–1198. DOI: 10.1016/J.RSER.2016.07.068.

Salema, A.A. & Ani, F.N. 2012. Microwave-assisted pyrolysis of oil palm shell biomass using an overhead stirrer. *Journal of Analytical and Applied Pyrolysis*. 96. DOI: 10.1016/j.jaap.2012.03.018.

Saranya, G. & Ramachandra, T. V. 2020. Life cycle assessment of biodiesel from estuarine microalgae. *Energy Conversion and Management: X*. 8:100065. DOI: 10.1016/J.ECMX.2020.100065.

Saratale, G.D., Saratale, R.G., Banu, J.R. & Chang, J.-S. 2019. Biohydrogen Production From Renewable Biomass Resources. In *Biohydrogen*. Elsevier. 247–277. DOI: 10.1016/b978-0-444-64203-5.00010-1.

SARS. 2021. *Corporate Income Tax | South African Revenue Service*. Available: https://www.sars.gov.za/types-of-tax/corporate-income-tax/ [2022, March 15].

SGBiofuels. 2016. *6 Reasons Why We Need Biofuels | SG Bio Fuels*. Available: https://www.sgbiofuels.com/6-reasons-why-we-need-biofuels/ [2021, July 16].

Sharifzadeh, M., Sadeqzadeh, M., Guo, M., Borhani, T.N., Murthy Konda, N.V.S.N., Garcia, M.C., Wang, L., Hallett, J., et al. 2019. DOI: 10.1016/j.pecs.2018.10.006.

Show, K.-Y., Yan, Y. & Lee, D.-J. 2019. Bioreactor and Bioprocess Design for Biohydrogen Production. In *Biohydrogen*. Elsevier. 391–411. DOI: 10.1016/b978-0-444-64203-5.00016-2.

Sinnott, R.K. 2005. *Coulson and Richardson's chemical engineering. Vol. 6, Chemical engineering design*.

Sinnott, R. & Towler, G.P. 2013. *Chemical engineering design : principles, practice, and economics of plant and process design / Gavin Towler, Ray Sinnott.*

Skorupskaite, V., Makareviciene, V. & Gumbyte, M. 2016. Opportunities for simultaneous oil extraction and transesterification during biodiesel fuel production from microalgae: A review. *Fuel Processing Technology*. 150:78–87. DOI: 10.1016/J.FUPROC.2016.05.002.

Smetana, S., Sandmann, M., Rohn, S., Pleissner, D. & Heinz, V. 2017. Autotrophic and heterotrophic

microalgae and cyanobacteria cultivation for food and feed: life cycle assessment. *Bioresource Technology*. 245. DOI: 10.1016/j.biortech.2017.08.113.

Suali, E. & Sarbatly, R. 2012. DOI: 10.1016/j.rser.2012.03.047.

Tejada Carbajal, E.M., Martínez Hernández, E., Fernández Linares, L., Novelo Maldonado, E. & Limas Ballesteros, R. 2020. Techno-economic analysis of Scenedesmus dimorphus microalgae biorefinery scenarios for biodiesel production and glycerol valorization. *Bioresource Technology Reports*. 12:100605. DOI: 10.1016/J.BITEB.2020.100605.

Thomassen, G., Egiguren Vila, U., Van Dael, M., Lemmens, B. & Van Passel, S. 2016. A techno-economic assessment of an algal-based biorefinery. *Clean Technologies and Environmental Policy*. 18(6):1849–1862. DOI: 10.1007/s10098-016-1159-2.

Tibbetts, S.M., Milley, J.E. & Lall, S.P. 2014. Chemical composition and nutritional properties of freshwater and marine microalgal biomass cultured in photobioreactors. *Journal of Applied Phycology 2014 27:3*. 27(3):1109–1119. DOI: 10.1007/S10811-014-0428-X.

Tiwari, A. & Kiran, T. 2018. Biofuels from Microalgae. In *Advances in Biofuels and Bioenergy*. M. Nageswara-Rao & J. Soneji, Eds. Environmental Science. DOI: 10.5772/intechopen.70022.

Tran, T.T.A., Le, T.K.P., Mai, T.P. & Nguyen, D.Q. 2019. Bioethanol Production from Lignocellulosic Biomass. *Xiandai Huagong/Modern Chemical Industry*. 31(SUPPL. 2):40–44. DOI: 10.5772/INTECHOPEN.86437.

Tsavatopoulou, V.D., Aravantinou, A.F. & Manariotis, I.D. 2021. Biofuel conversion of Chlorococcum sp. and Scenedesmus sp. biomass by one- and two-step transesterification. *Biomass Conversion and Biorefinery*. 11(4). DOI: 10.1007/s13399-019-00541-y.

Turton, R. 2013. *Analysis, Synthesis, and Design of Chemical Processes Fourth Edition*. V. 53.

Turton, R., Bailie, R.C., Whiting, W.B. & Shaeiwitz, J.A. 2009. *Analysis, Design and Synthesis of Chemical Processes*.

UnitedNations. 2019. *Growing at a slower pace, world population is expected to reach 9.7 billion in 2050 and could peak at nearly 11 billion around 2100 | UN DESA | United Nations Department of Economic and Social Affairs*. Available: https://www.un.org/development/desa/en/news/population/world-population-prospects-2019.html [2021, July 16].

Urban, W. 2013. Biomethane injection into natural gas networks. In *The Biogas Handbook: Science, Production and Applications*. Elsevier Inc. 378–403. DOI: 10.1533/9780857097415.3.378.

Varanda, M.G., Pinto, G. & Martins, F. 2011. Life cycle analysis of biodiesel production. *Fuel*

Processing Technology. 92(5). DOI: 10.1016/j.fuproc.2011.01.003.

Veeramuthu, A. & Ngamcharussrivichai, C. 2021. Potential of Microalgal Biodiesel: Challenges and Applications. In *Renewable Energy - Technologies and Applications*. DOI: 10.5772/intechopen.91651.

Veillette, M., Chamoumi, M., Nikiema, J., Faucheux, N. & Heitz, M. 2012. Production of Biodiesel from Microalgae. *Advances in Chemical Engineering*. DOI: 10.5772/31368.

Viswanathan, B. 2017. Petroleum. In *Energy Sources*. Elsevier. 29–57. DOI: 10.1016/B978-0-444-56353-8.00002-2.

Waldron, K. 2014. *Advances in Biorefineries: Biomass and Waste Supply Chain Exploitation*. DOI: 10.1533/9780857097385.

Wang, Y. 2013. Microalgae as the Third Generation Biofuel Production, Usage, Challenges and Prospects.

Wankat, P.C. 2012. *Separation Process Engineering : Includes Mass Transfer Analysis*. V. 66.

WorldBank. 2021. *World Bank Global Economic Prospects*. Available: https://www.worldbank.org/en/news/press-release/2021/06/08/world-bank-global-economic-prospects-2021 [2021, July 16].

Wu, N., M. Moreira, C., Zhang, Y., Doan, N., Yang, S., J. Phlips, E., A. Svoronos, S. & C. Pullammanappallil, P. 2019. Techno-Economic Analysis of Biogas Production from Microalgae through Anaerobic Digestion. In *Anaerobic Digestion*. DOI: 10.5772/intechopen.86090.

Xin, C., Addy, M.M., Zhao, J., Cheng, Y., Cheng, S., Mu, D., Liu, Y., Ding, R., et al. 2016. Comprehensive techno-economic analysis of wastewater-based algal biofuel production: A case study. *Bioresource Technology*. 211:584–593. DOI: 10.1016/j.biortech.2016.03.102.

Yang, C., Li, R., Cui, C., Liu, S., Qiu, Q., Ding, Y., Wu, Y. & Zhang, B. 2016. DOI: 10.1039/c6gc01239f.

Yang, C., Wu, J., Deng, Z., Zhang, B., Cui, C. & Ding, Y. 2017. A Comparison of Energy Consumption in Hydrothermal Liquefaction and Pyrolysis of Microalgae. *Trends in Renewable Energy*. 3(1):76–85. DOI: 10.17737/tre.2017.3.1.0013.

Yang, Y.F., Feng, C.P., Inamori, Y. & Maekawa, T. 2004. Analysis of energy conversion characteristics in liquefaction of algae. *Resources, Conservation and Recycling*. 43(1):21–33. DOI: 10.1016/J.RESCONREC.2004.03.003.

Zabed, H.M., Akter, S., Yun, J., Zhang, G., Zhang, Y. & Qi, X. 2020. DOI: 10.1016/j.rser.2019.109503.

APPENDICES

Appendix A: Process Design Basis

A.1 Process simulation specifications

A.1.1 Thermochemical conversion

Table A-1 shows the yield specification used for model R-301. The specifications were sourced from (Jones *et al.*, 2014), (Chen & Quinn, 2021). The inert components were H_20, NH_4SO_4, and ash.

Table A-1: Specifications of model R-301.

Component	**Aspen Plus ID**	**Basis**	**Basis yield**
1-ethyl-2-pyrrolidinone	1E2PYDIN	Mass	0,0408
N-methylthiopyrrolidone	C5H9NS	Mass	0,0164
Ethylbenzene	ETHYLBEN	Mass	0,013
p-cresol	4M-PHENO	Mass	0,0261
p-ethylphenol	4E-PHENO	Mass	0,0261
Indole	INDOLE	Mass	0,0261
7-methylindole	7MINDOLE	Mass	0,0173
Myristamide	C14AMIDE	Mass	0,0173
Hexadecanamide / Palmitic amide	C16AMIDE	Mass	0,0779
Octadecamide	C18AMIDE	Mass	0,0347
cis-9-hexadecenoic acid	C16:1FA	Mass	0,0692
N-hexadecenoic acid	C16:0FA	Mass	0,0518
Oleic acid	C18FACID	Mass	0,0087
Naphthalene	NAPHTHAL	Mass	0,0261
Beta-cholesterol	CHOLESTE	Mass	0,0086
Aniline	ANILINE	Mass	0,0414
Phthalic acid	C30DICAD	Mass	0,0259
Methanol	METHANOL	Mass	0,0483
Ethanol	ETHANOL	Mass	0,0097
Acetone	ACETONE	Mass	0,0097
Formic acid	FORMIC	Mass	0,0964
Acetic acid	AACID	Mass	0,029
Carbon dioxide	CO2	Mass	0,1172
Ammonia	NH3	Mass	0,0299
3-hydroxypyridine	3-PYRDOL	Mass	0,0145
Carbon	C (CISOLID)	Mass	0,14
Carbon monoxide	CO	Mass	0,0024
Methane	CH4	Mass	0,0024
Nitrogen	N2	Mass	0,0024
Hydrogen	H2	Mass	0,0012
Glycerol	GLYCEROL	Mass	0,0097

Table A-2 shows the yield specifications used for the R-310Y reactor model for hydrotreating. The specification were sourced from (Jones *et al*., 2014), (Chen & Quinn, 2021).

Table A-2: Specifications for the R-310Y model used in hydrotreating.

Component	**Aspen Plus ID**	**Basis**	**Basis Yield**
HYDROGEN	H2	Mass	0,0767
WATER	H2O	Mass	0,1061
AMMONIA	NH3	Mass	0,0449
METHANE	CH4	Mass	0,0174
ETHANE	C2	Mass	0,0223
PROPANE	PROPANE	Mass	0,0126
N-BUTANE	C4	Mass	0,0066
N-PENTANE	C5	Mass	0,0052
N-HEXANE	HEXANE	Mass	0,0031
ETHYLBENZENE	ETHYLBEN	Mass	0,0156
2-METHYL-BUTANE	2MBUTAN	Mass	0,0031
2-METHYL-PENTANE	2MPENTAN	Mass	0,0031
2-METHYLHEXANE	2MHEXAN	Mass	0,0031
N-HEPTANE	C7	Mass	0,0031
METHYLCYCLOHEXANE	CC6-METH	Mass	0,0078
PIPERIDINE	PIPERDIN	Mass	0,0031
TOLUENE	TOLUENE	Mass	0,0078
3-METHYLHEPTANE	3MHEPTAN	Mass	0,0078
N-OCTANE	C8	Mass	0,0078
ETHYLCYCLOHEXANE	ETHCYC6	Mass	0,0031
O-XYLENE	O-XYLENE	Mass	0,0078
N-NONANE	C9	Mass	0,0031
N-PROPYLCYCLOHEXANE	PROCYC6	Mass	0,0031
N-PROPYLBENZENE	C3BENZ	Mass	0,0078
N-DECANE	C10	Mass	0,0016
N-BUTYLBENZENE	C4BENZ	Mass	0,0093
N-UNDECANE	C11	Mass	0,0156
BENZENE,-1-BUTENYL-	BENZE-01	Mass	0,0156
N-DODECANE	C12	Mass	0,0156
1,2,3,4-TETRAHYDRONAPHTHALENE	1234NA	Mass	0,0078
N-HEXYLBENZENE	C6BENZ	Mass	0,0156
6-METHYLTETRALIN	12346N	Mass	0,0156
N-HEPTYLBENZENE	C7BENZ	Mass	0,0156
N-OCTYLBENZENE	C8BENZ	Mass	0,0156
DIMETHYL-1,4-CYCLOHEXANEDICARBOX	C10H16O4	Mass	0,014
N-PENTADECANE	C15	Mass	0,0467
N-HEXADECANE	C16	Mass	0,14
N-HEPTADECANE	C17	Mass	0,0622

N-OCTADECANE	C18	Mass	0,0311
N-NONADECANE	C19	Mass	0,0311
N-HENEICOSANE	C21	Mass	0,0311
N-TRICOSANE	C23	Mass	0,0311
N-TRIACONTANE	C30	Mass	0,0016
C20H42-N2	PHYTANE	Mass	0,0778
DIISOOCTYL-PHTHALATE	C24H38O4	Mass	0,0062
HEPTYL-UNDECYL-PHTHALATE	C26H42O4	Mass	0,0078
AMMONIUM-CARBONATE	NH4SO4	Mass	0,0098

Table A-3 shows the yield specifications used to model the R-350Y hydrocracking reactor. The specification were sourced from (Jones *et al*., 2014), (Chen & Quinn, 2021).

Table A-3: Specifications of the R-350Y model used in hydrocracking.

Component	**Aspen Plus ID**	**Basis**	**Basis Yield**
HYDROGEN	H2	Mass	0,0442
CARBON DIOXIDE	CO2	Mass	0,095
METHANE	CH4	Mass	0,0217
HEXANE	HEXANE	Mass	0,0101
N-HEPTANE	C7	Mass	0,1023
N-OCTANE	C8	Mass	0,0716
N-NONANE	C9	Mass	0,0797
N-DECANE	C10	Mass	0,1029
N-UNDECANE	C11	Mass	0,1473
N-DODECANE	C12	Mass	0,1153
N-TRIDECANE	C13	Mass	0,0813
N-TETRADECANE	C14	Mass	0,0406
N-PENTADECANE	C15	Mass	0,0284
N-HEXADECANE	C16	Mass	0,0168
N-HEPTADECANE	C17	Mass	0,0038
N-OCTADECANE	C18	Mass	0,0009
N-NONADECANE	C19	Mass	0,0043
N-EICOSANE	C20	Mass	0,0001
PHYTANE	PHYTANE	Mass	0,0001
CYCLOHEXANE	CY6	Mass	0,0336

Table A-4 below summarises the specifications of the hydrotreating distillation columns.

Table A-4: Specifications for the distillation columns used in hydrotreating.

	Hydrotreating		
	T-310 Radfrac	**T-320 Radfrac**	**T-330 Radfrac**
No. of stages	5	5	5
Reboiler type	Kettle	Kettle	Kettle
Reflux ratio (mass)	1	0,869	0,126
Distillate:Feed (mass)	0,014	0,131	0,874
Condenser type	Partial vapor	Total	Total
Top stage P (bar)	3,31	1,72	1,29
Top stream	HTScrub	HTNaphtha	HTDiesel
Bottom stream	Biocrude	Biocrude	HTHeavy oil

Table A-5 summarizes the specifications of the hydrocracking distillation column.

Table A-5: Specifications for the distillation column model used for hydrocracking.

	Hydrocracking
	T-350 Radfrac
No. of stages	5
Reboiler type	Kettle
Reflux ratio (mass)	1
Distillate:Feed (mass)	0,68
Condenser type	Partial-Vapor-Liquid
Top stage P (bar)	1,38
Top stream	HCNaphtha
Bottom stream	HCDiesel

A.1.2 Biochemical Conversion

This section outlines the specifications used of specific models used in Aspen Plus for the process simulation of a biochemical conversion method.

A300: Purification

Table A-6 summarizes the specifications of the T-301.

Table A-6: Specification for the T-301 model.

No. of stages	32
Condenser type	Partial vapour
Reboiler type	Kettle
Distillate rate	6500

Reflux ratio	12
Top stage pressure (bar)	2,07
Stage 2	0,03
Column press drop	0,21

Table A-7 summarizes the specifications of the T-302.

Table A-7: Specification for the T-302 model.

No. of stages	45
Condenser type	Partial vapor
Reboiler type	Kettle
Reflux ratio	4.4
Bottoms:feed	0.1
Top stage Pressure (bar)	1.62

Table A-8 summarizes the specifications of the T-303.

Table A-8: Specification for the T-303 model.

No. of stage	4
Condenser	None
Reboiler	None
Top stage pressure (bar)	0,91

A 500: Anaerobic Digestion

Tables A-9 and A-10 summarize the specification of R-501 and 502 which represents anaerobic digestors.

Table A-9: Specification for the R-501 model.

Component	**Basis**	**Basis Yield**
CH4	Mass	0,45
CO2	Mass	0,9
H2O	Mass	1
NH3	Mass	0,017
H2S	Mass	0,014

Table A-10: Specification for the R-502 model.

Component	Basis	Basis Yield
BIOMASS (CISOLID)	Mass	1

Appendix B: Mass and Energy Balances

The general mass balance equation that can be used for any process stream is:

Mass Out = Mass In + Generation - Consumption – Accumulation

B.1 Thermochemical conversion balances

Overall Balance streams.

Table A-11: Overall balance streams

		Inlet Streams		Outlet Streams				
Stream Name	**Units**	**FEED**	**HYDROGEN**	**A100GAS**	**A100H2O**	**A100SOL**	**BIODIESL**	**NAPHTHA**
Temperature	**K**	298,15	298,15	368,96	353,06	751,72	519,53	338,66
Pressure	**bar**	1,01	1,01	1,38	3,79	205,19	1,29	1,38
Enthalpy Flow	**MW**	-283,82	47,87	-4,08	-273,43	-0,63	-1,73	-0,44
Mass Flows	**kg/hr**	75428,19	335,83	2272,40	65266,16	2312,32	4939,12	973,99

Overall balance = Input – Out = 75764,02 -75763,97 = 0,05 kg/hr.

Error % = [(75764,02 - 75763,98)/ 75764,02] x 100% = -6,06E-05 %.

Equipment energy summary

Table A-12: Equipment energy summary

Equipment	Duty (MW)	Equipment	Duty (MW)
A100.HC.H-352	0,02	**A100.HTL.V-301**	-2,27
A100.HC.H-381	-0,04	**A100.HC.P-350**	0,00
A100.HC.HX-380	-0,04	**A100.HT.P-310**	0,03
A100.HC.HX-381	-0,10	**A100.HTL.HTLPUMP**	0,79
A100.HT.E-310	-0,17	**A300.CWTOWER.COOLPUMP**	0,08
A100.HT.H-316	-0,53	**A300.CWTOWER.WARMPUMP**	0,01
A100.HT.HTLCOOL	-0,81	**A100.HC.C-350**	0,01
A100.HT.HX-320	-1,92	**A100.HC.C-351**	0,00
A100.HTL.E-304	7,45	**A100.HT.C-310**	0,32
A100.HTL.E-305	-0,58	**A100.HT.C-311**	0,09
A100.HTL.E-306	-2,86	**A300.AIRCOOL.ACFAN**	0,02
A300.AIRCOOL.COOLFAN	0,57	**A100.HC.T-350 (condenser)**	-0,05
A300.CWTOWER.CWHX	5,82	**reboiler**	0,09
A100.HC.H-351	0,06	**A100.HT.T-310 (condenser)**	0,00
A100.HT.H-311	0,56	**reboiler**	0,35

A100.HT.HX-318A	0,19	**A100.HT.T-320 (condenser)**	-0,19
A100.HTL.E-301	23,25	**reboiler**	0,44
A100.HC.V-351	0,00	**A100.HT.T-330 (condenser)**	-0,49
A100.HC.V-375	0,00	**reboiler**	0,46
A100.HT.V-311	0,00	**A300.CWTOWER.COOLTOW**	0,00
A100.HT.V-315	-0,16	**A100.HC.R-350Y**	-0,03
A100.HT.NH3SEP	0,01	**A100.HT.R-310Y**	-0,67
A100.HT.V-300	-0,11	**A100.HTL.R-301**	1,59
A100.HTL.C-301	-2,02	**A100.HTL.F-301**	0,00
Total	**29,19**		

Error % = [(-241541,36 - -267257,14)/ -241541,36] x 100% = 9,62 %

HTL

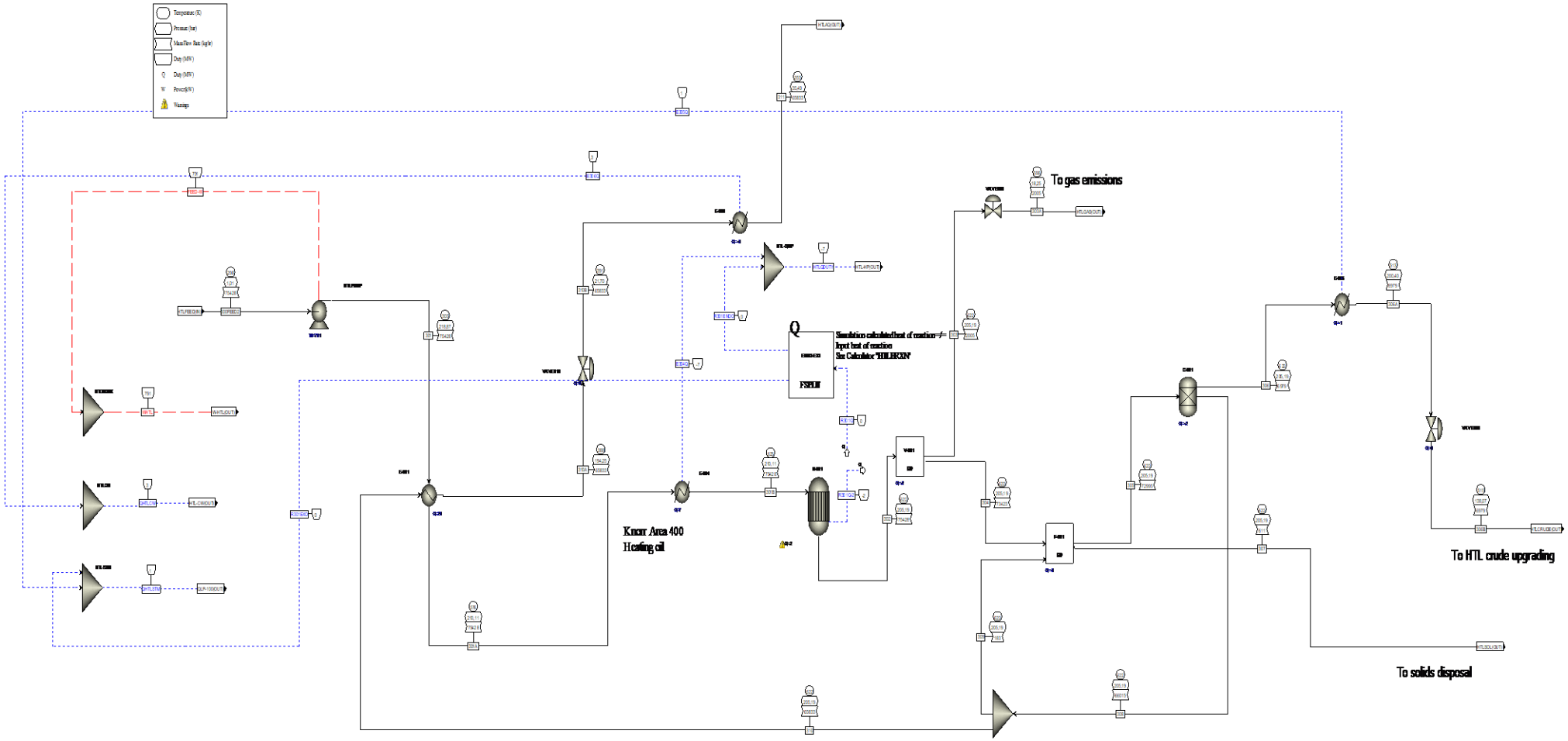

Figure A-1: HTL simulation.

Hydrotreating

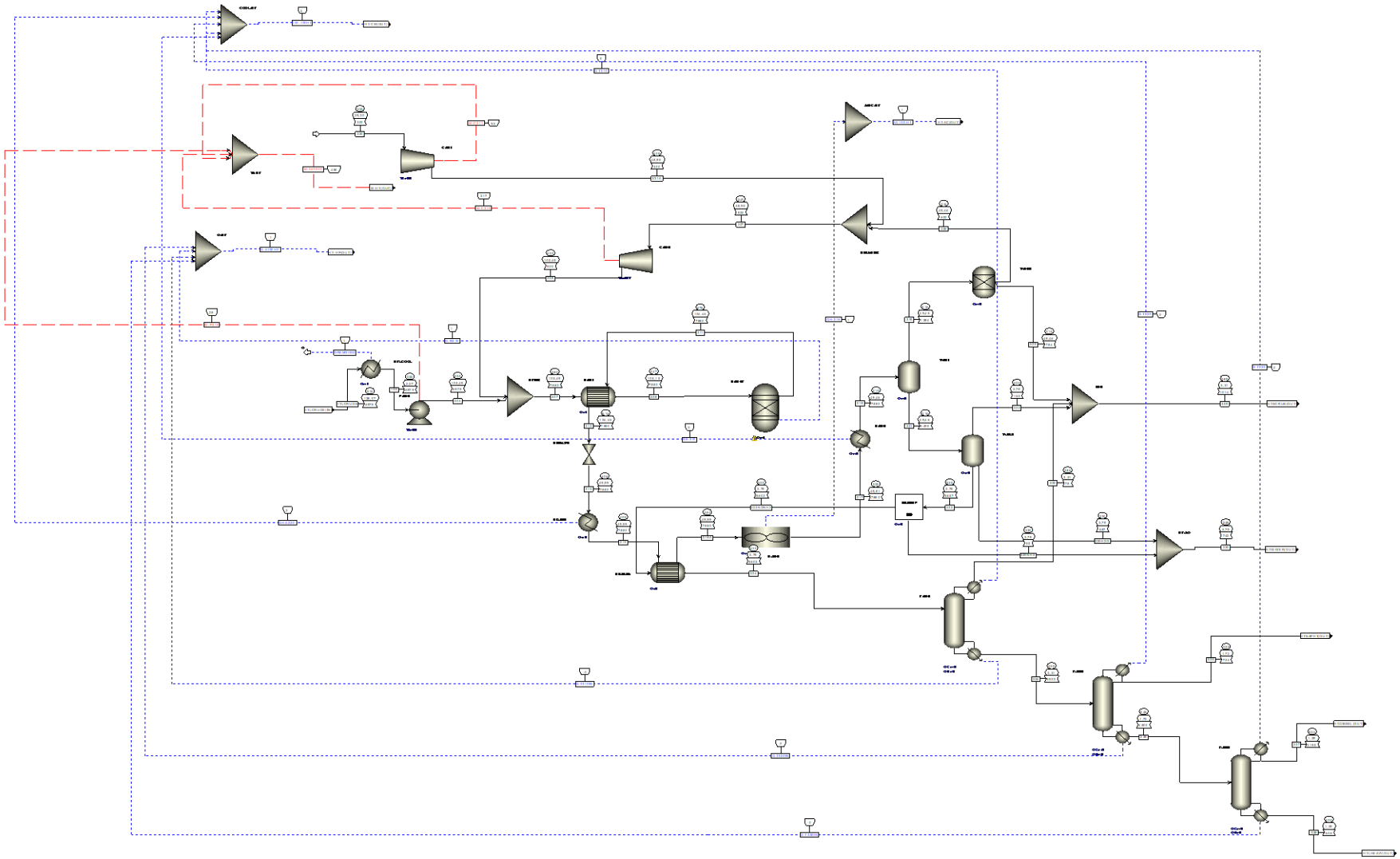

Figure A-2: Hydrotreating simulation.

Hydrocracking

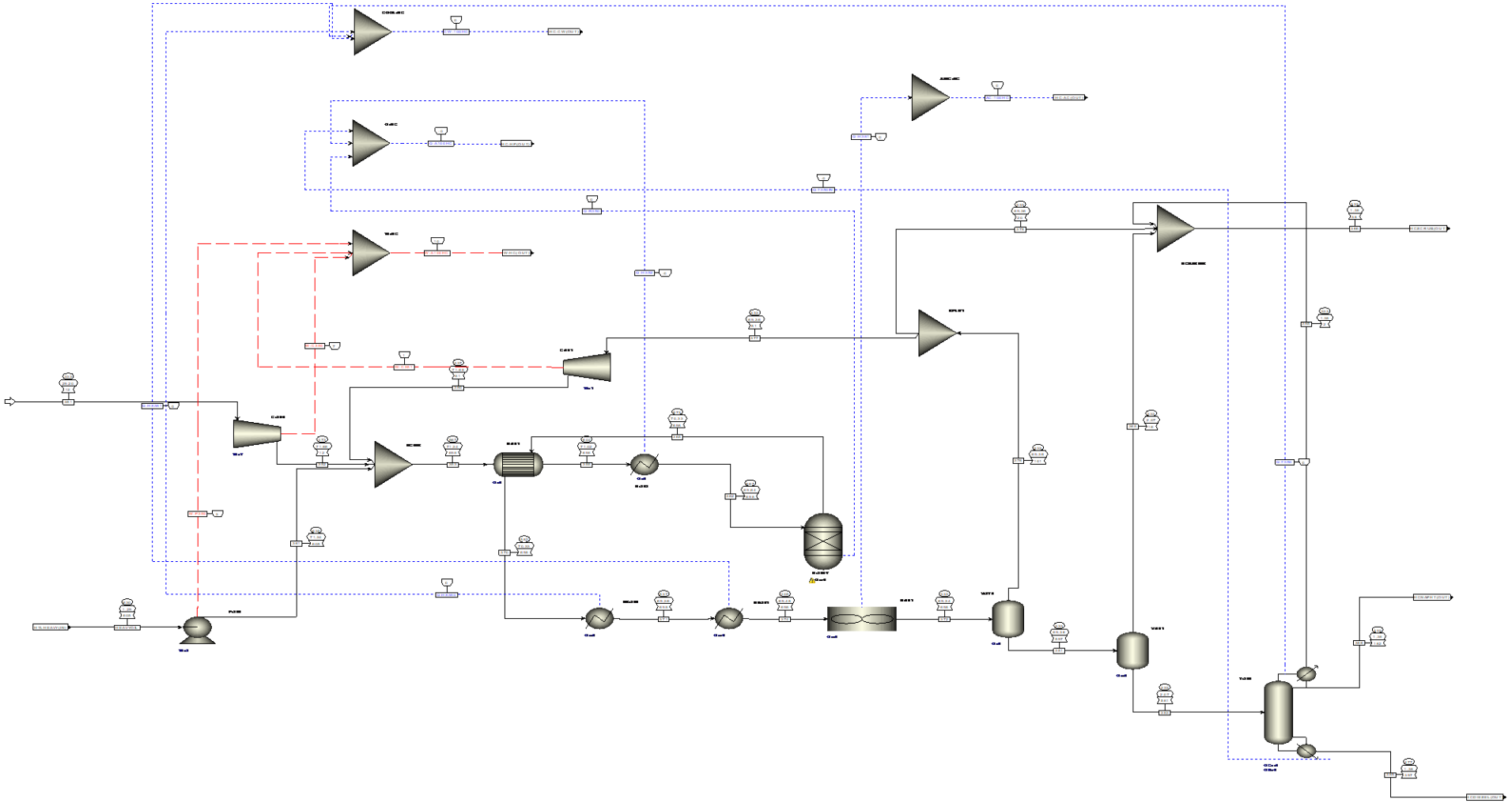

Figure A-3: Hydrocracking simulation.

B.2 Biochemical conversion balances

Overall balance

Table A-13: Overall balance streams.

Inlet Streams												
	Units	**DA**	**DAP**	**DAP2**	**H2O**	**NH3**	**S1**	**S3**	**S5**	**S8**	**S34**	**S110**
Temperature	**K**	298,15	293,15	293,15	306,15	293,15	298,15	443,65	298,15	443,65	298,15	301,35
Pressure	**bar**	1,01325	1,01	1,01	1,01	1,01	1,01	7,09	3,45	7,09	1,01	5,07
Enthalpy Flow	**MW**	-6,8E-21	-26,27	-31,27	-34,09	-0,83	-290,62	-73,04	-3,41	-127,83	-68,34	-8884,13
Mass Flows	**kg/hr**	1	10500	12500	7751	1100	75428,19	20000	1420	35000	15500	2017741
Outlet Streams												
	Units	**S121**	**WA**	**S75**	**S73**	**S54**	**S51**					
Temperature	**K**	301,15	311,15	311,7455	315,0311	308,15	311,15					
Pressure	**bar**	5,17	1,01	1,01	1,05	1,62	1,01					
Enthalpy Flow	**MW**	-8870,83	-0,44	-615,41	-20,86	-61,79	-8,57					
Mass Flows	**kg/hr**	2014614	101,73	140757,5	9668,50	26672,78	5133,58					

Table A-14: Equipment energy summary.

Equipment	Duty (MW)	Equipment	Duty (MW)
H-101	-7,6767	**P-101**	0,01665
HX-201	-9,979	**P-102**	0,00012
HX-101	-0,3817	**P-103**	-0,0043
HX-302	0,3877	**P-201**	0
H-201	0,0822	**P-202**	0,0043
HX-301	10,336	**P-301**	0,0381
HX-303	-83,883	**P-302**	0,0242
HX-305	-0,1155	**P-401**	0,0476
HX-306	-2,471	**P-402**	0,2760
HX-304	-2,875	**K-501**	0,0117
HX-307	-2,3591	**cond T-303**	0
HX-02	-19,012	**reboil T-303**	0
HX-501	-0,039	**cond T-302**	-395,26
HX-01	20,46	**reboil T-302**	486,49
B63	-23,54	**cond T-301**	-27,55
V-101	2,13014E-13	**reboiler T-301**	32,96
V-201	0	**R-202**	-0,83
V-202	0	**R-102**	-5,27
V-302	0,0566	**R-101**	-14,54
V-501	0	**R-201**	-0,22
V-401	2,2891	**R-502**	0,53
C-301	0	**R-501**	3,73
C-302	-0,0962		
C-01	-0,0088		
C-501	0,3149		
C-502	0,0008		
Total	**-38,06**		

A100 Pre-treatment

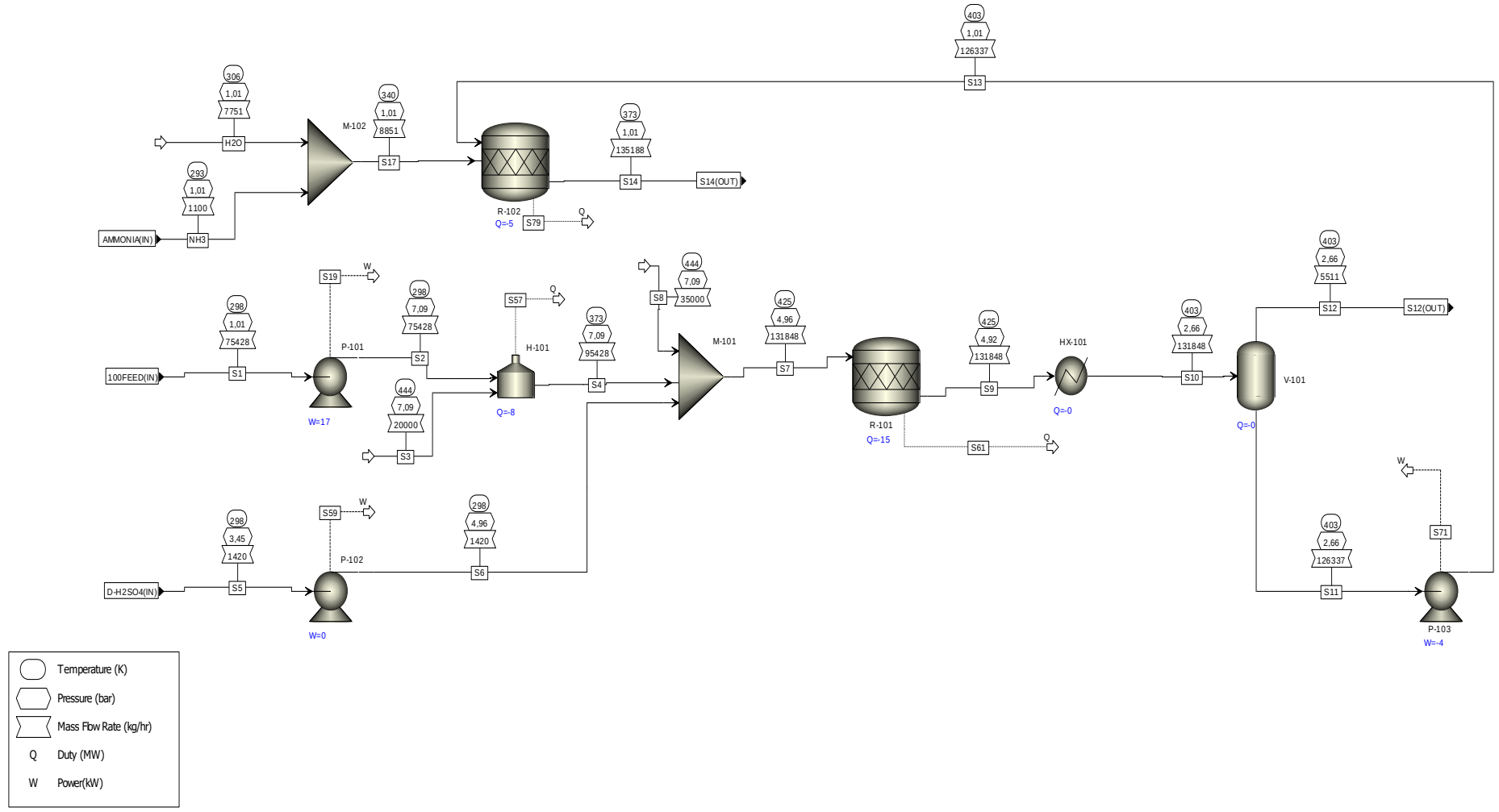

Figure 7-4: Pre-treatment simulation flowsheet.

A200 Fermentation

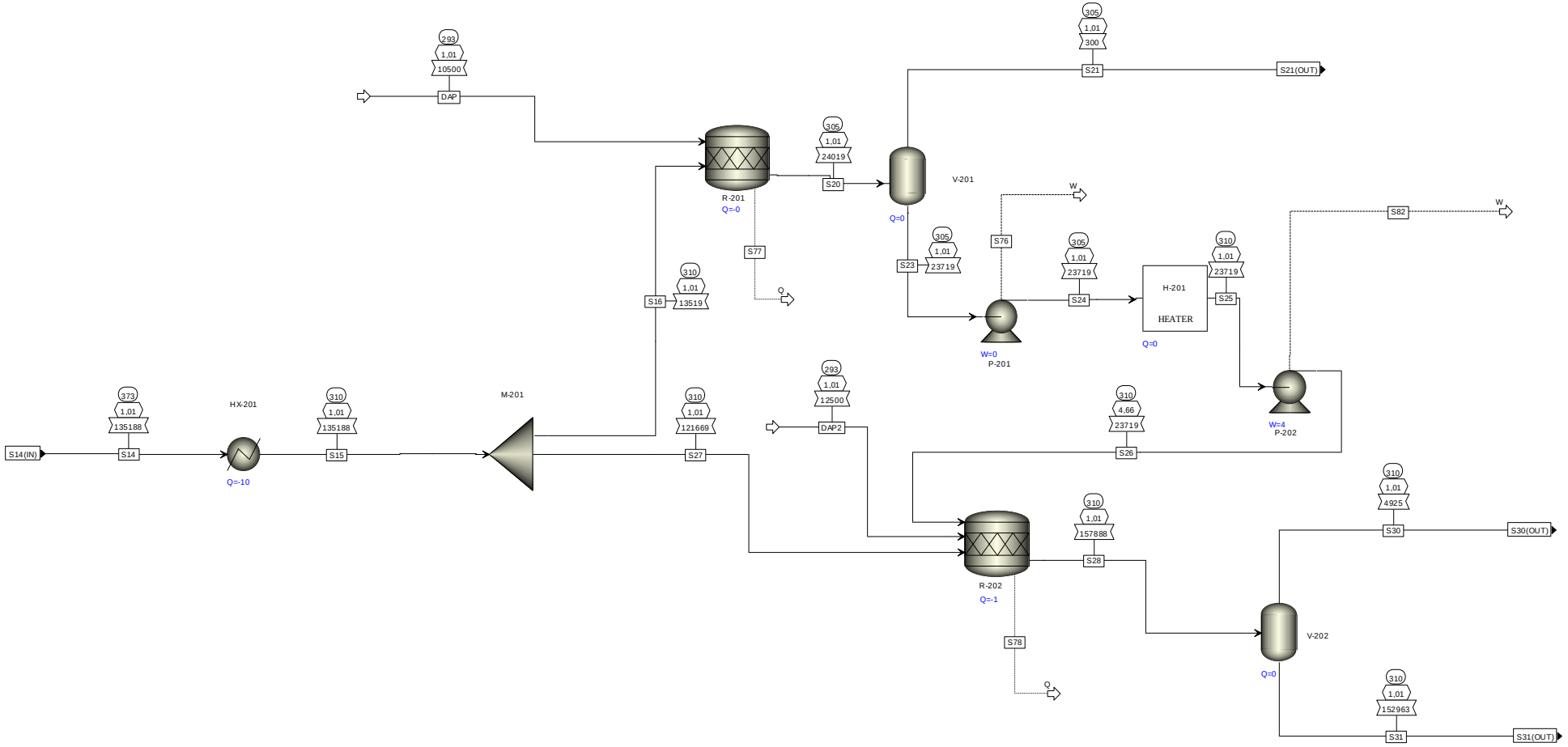

Figure 7-5: Fermentation simulation flowsheet.

A300 Purification

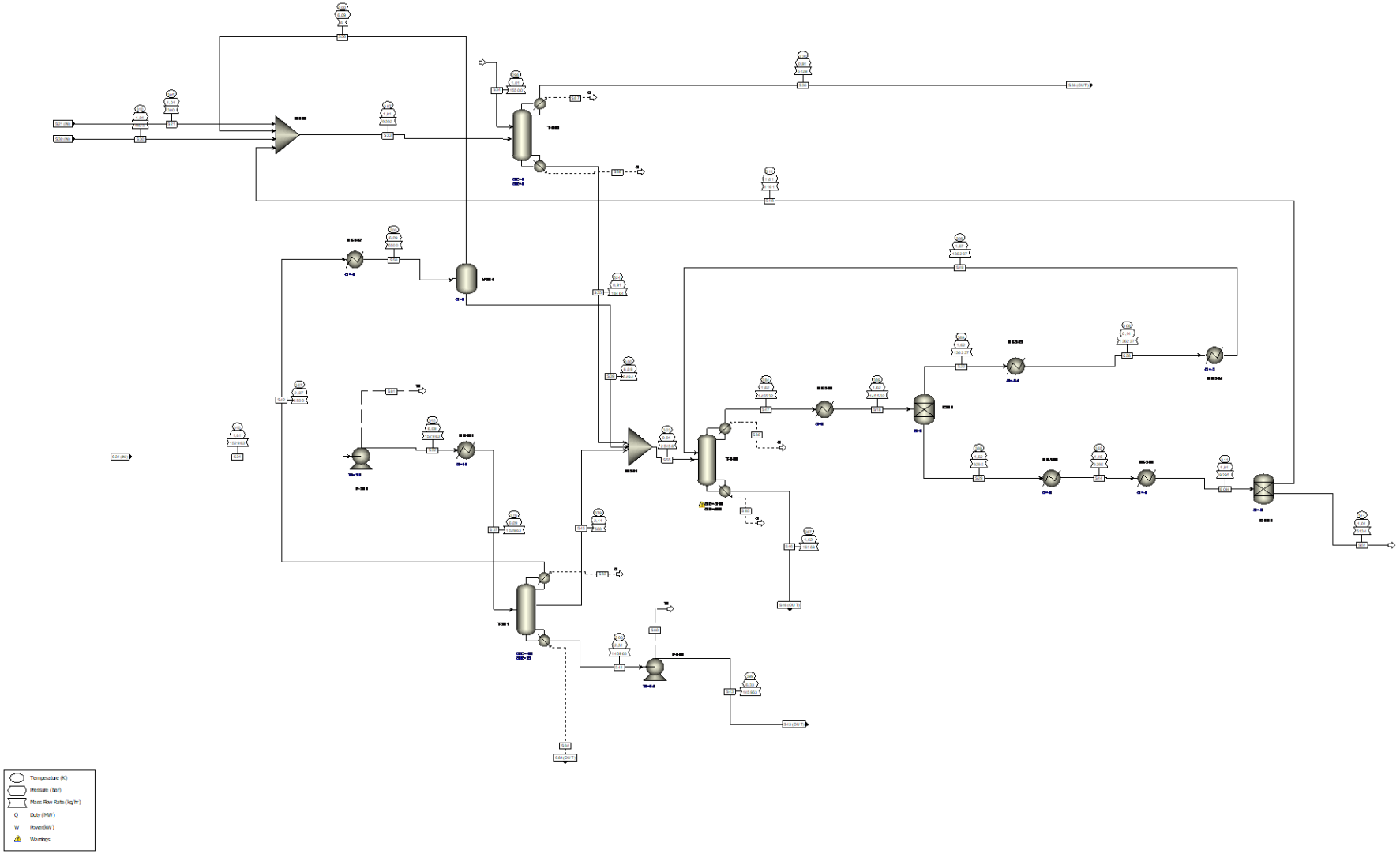

Figure 7-6: Purification simulation flowsheet.

A400 Utilities

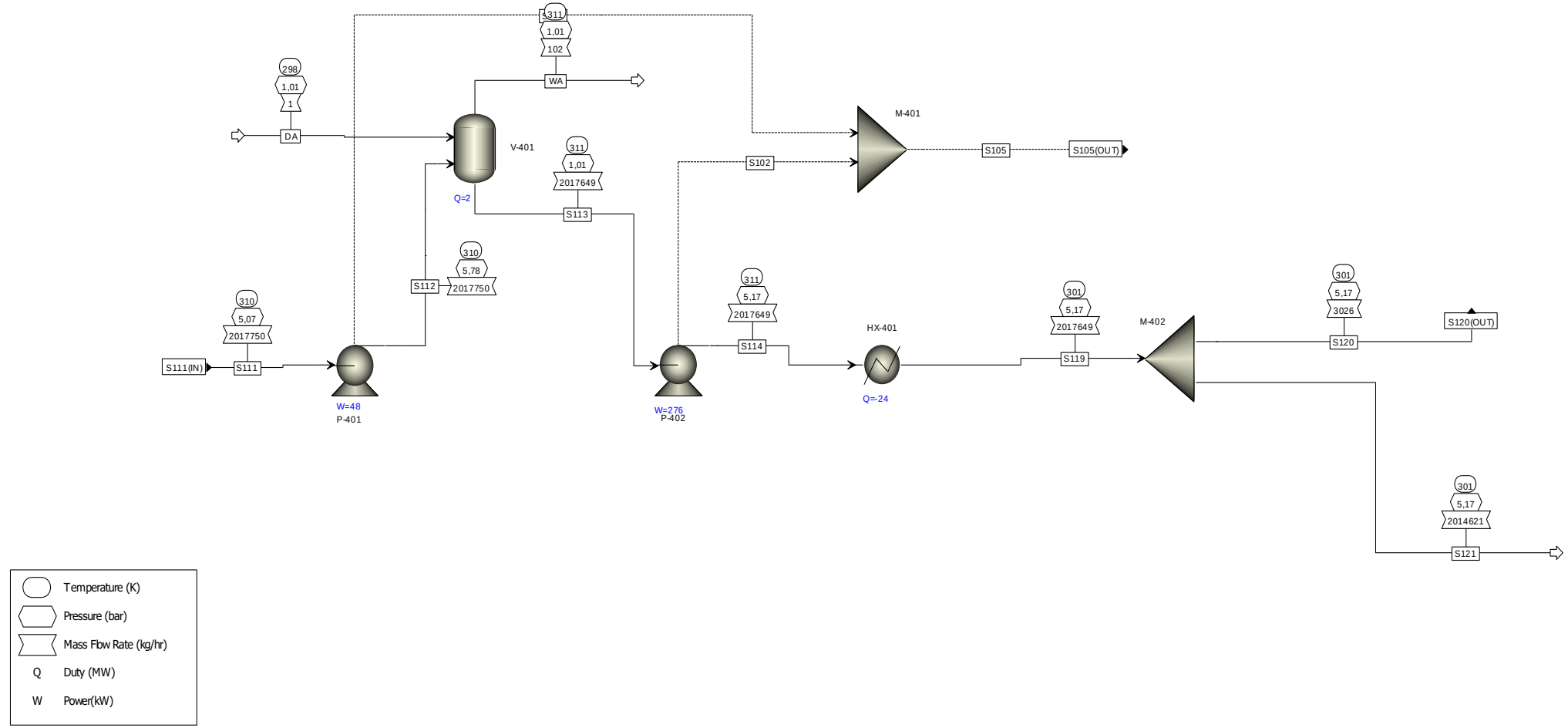

Figure A-7: Utilities simulation flowsheet.

A500 Anaerobic Digestion

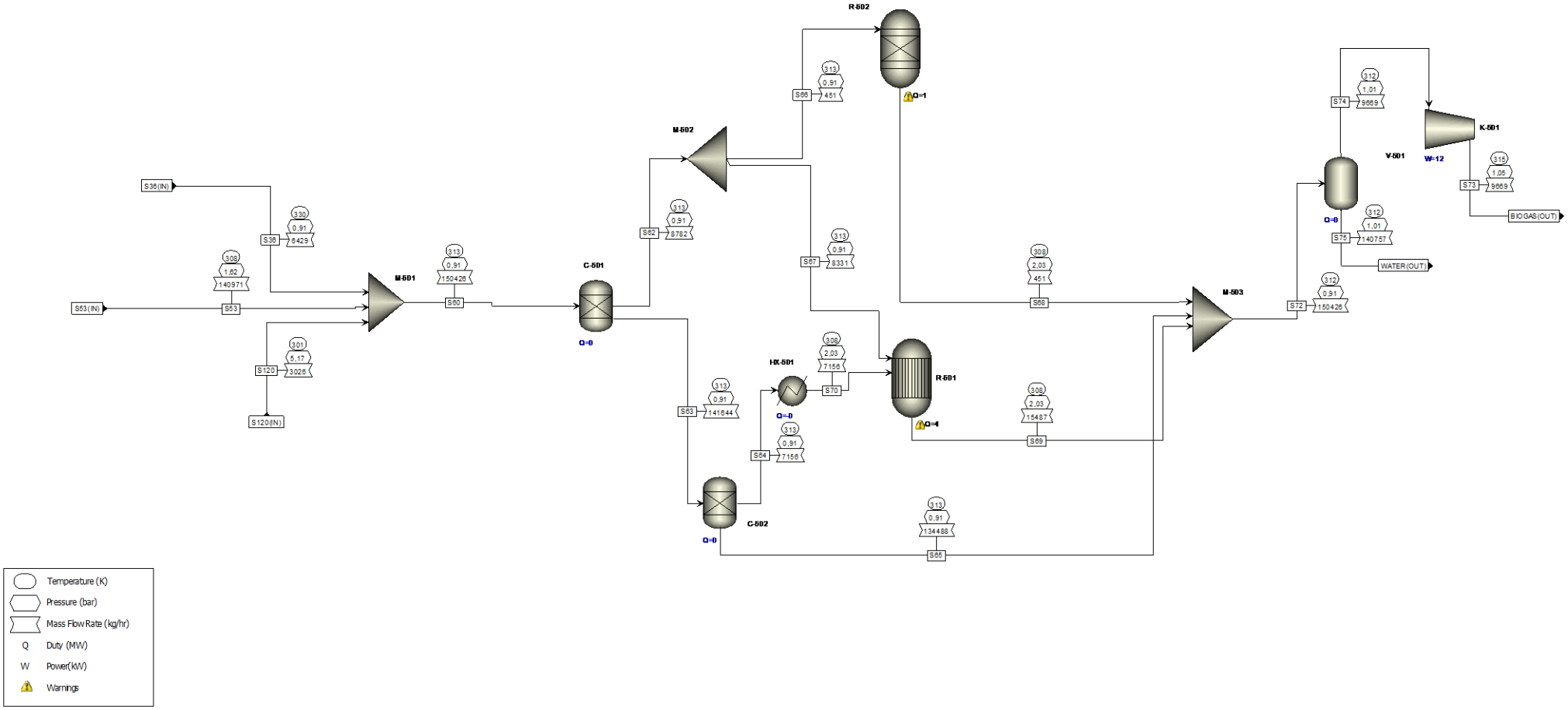

Figure 7-8: Anaerobic digestion simulation flowsheet.

Appendix C: Equipment Sizing

Most of the data for this section is from the Aspen Capital Cost Estimator. Only the flash drums were calculated. Below is the sample calculation for the flash drum.

Flash drum: calculation sample

These equations were used in unison with the data collected from Aspen Plus regarding the streams exiting the flash drum.

Calculating settling velocity:

$$u_t = 0.07\left[\frac{\rho_L - \rho_V}{\rho_V}\right]^{0.5} \quad \text{(C.1)}$$

Where u_t = Permissible vapour velocity (m/s)

ρ_v = Vapour density (kg/m³)

ρ_L = Liquid density (kg/m³)

Calculating the minimum column diameter:

$$D_V = \sqrt{\frac{4V_V}{\pi u_t}} \quad \text{(C.2)}$$

Where V_v = Vapour volumetric flowrate (m³/s)

D_v = Minimum vessel diameter (m)

Calculating the length of the column:

$$\frac{L}{D_V} = 3 \quad \text{(C.3)}$$

Table A-15: Data from Aspen.

Stream Number	**25**	**368**	**383**
Stream Type	Water	Organic Solvent	Light Gases
Phase	Liquid	Liquid	Vapour
Density (kg/m³)		703,80	1,97
Volumetric Flowrate (m³/hr)		0,83	7,88

Table A-16: Summary of calculation results.

Equipment		**FLASH-1**
Mean Density of Liquid Streams (kg/m³)	pv	703,8
Settling Velocity (m/s)	ut	1,3
Minimum Vessel Diameter (m)	Dv	2,8
Length (m)	L	8,3
Estimated Volume (m³)	V	49,3

Oversizing Factor (10%)		4,9
Actual Volume (m^3)	V	54,2

Sample calculation:

Settling velocity

$$u_t = 0.07\left[\frac{\rho_L - \rho_V}{\rho_V}\right]^{0.5} = 0.07\left[\frac{703{,}8 - 1{,}97}{1{,}97}\right]^{0.5} = 1{,}3$$

Minimum vessel diameter

$$D_V = \sqrt{\frac{4V_V}{\pi u_t}} = \sqrt{\frac{4 * (7{,}88)}{\pi(1{,}3)}} = 2{,}88$$

Appendix D: Heat Integration

This appendix provides additional details of the heat integration conducting for this project. Selected heat exchanger networks are presented to supplement the discussion.

D.1 Thermochemical conversion heat integration

Scenario 2 solutions for thermochemical conversion.

Table A-17: Scenario 2 solutions from Aspen for the thermochemical method.

	Energy Saving [%]	**New Area [sqm]**	**Extra Capital Cost [R]**	**Energy Cost Savings [R/Yr]**
Solution 1	23,56	21,25	3,15E+05	2,08E+06
Solution 2	17,18	263,6	1,88E+09	3,22E+10
Solution 3	23,52	397,9	1,12E+10	7,18E+10
Solution 4	21,31	354,6	1,52E+10	8,92E+10
Solution 5	0,02	0,2702	1,22E+09	2,85E+07

Scenario 3 solutions for thermochemical conversion.

Table A-18: Scenario 3 solutions from Aspen for the thermochemical method.

	Energy Saving [%]	**New Area [sqm]**	**Extra Capital Cost [R]**	**Energy Cost Savings [R/Yr]**
Solution 1	22,98	11,99	5,99E+04	1,97E+06
Solution 2	22,98	388,4	4,46E+08	4,07E+10
Solution 3	20,76	345,1	1,12E+10	8,49E+10
Solution 4	20,81	346,9	1,05E+10	7,71E+10

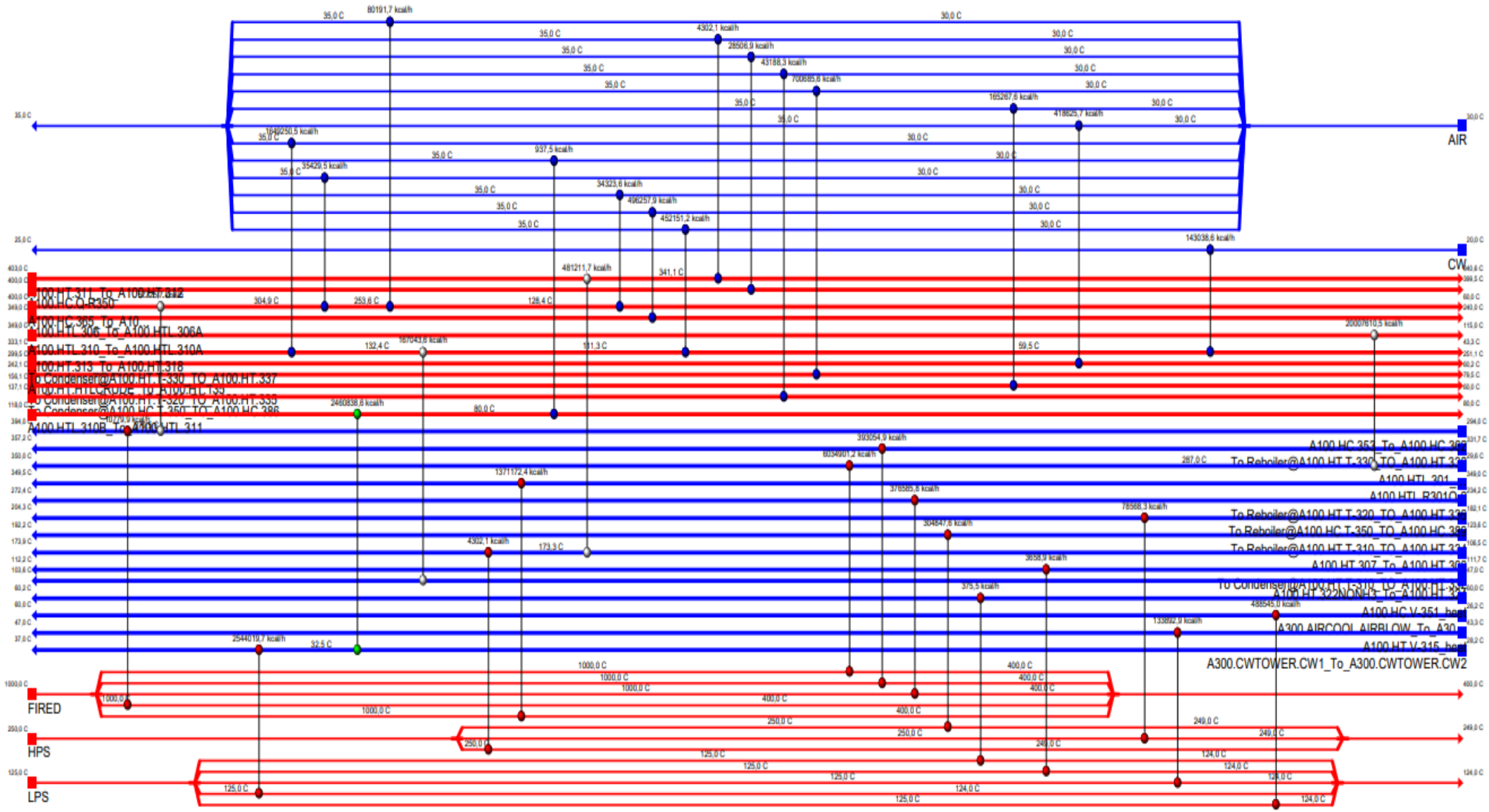

Figure A-9: HEN for the thermochemical method (scenario 2 solution 1).

C.2 Biochemical conversion heat integration

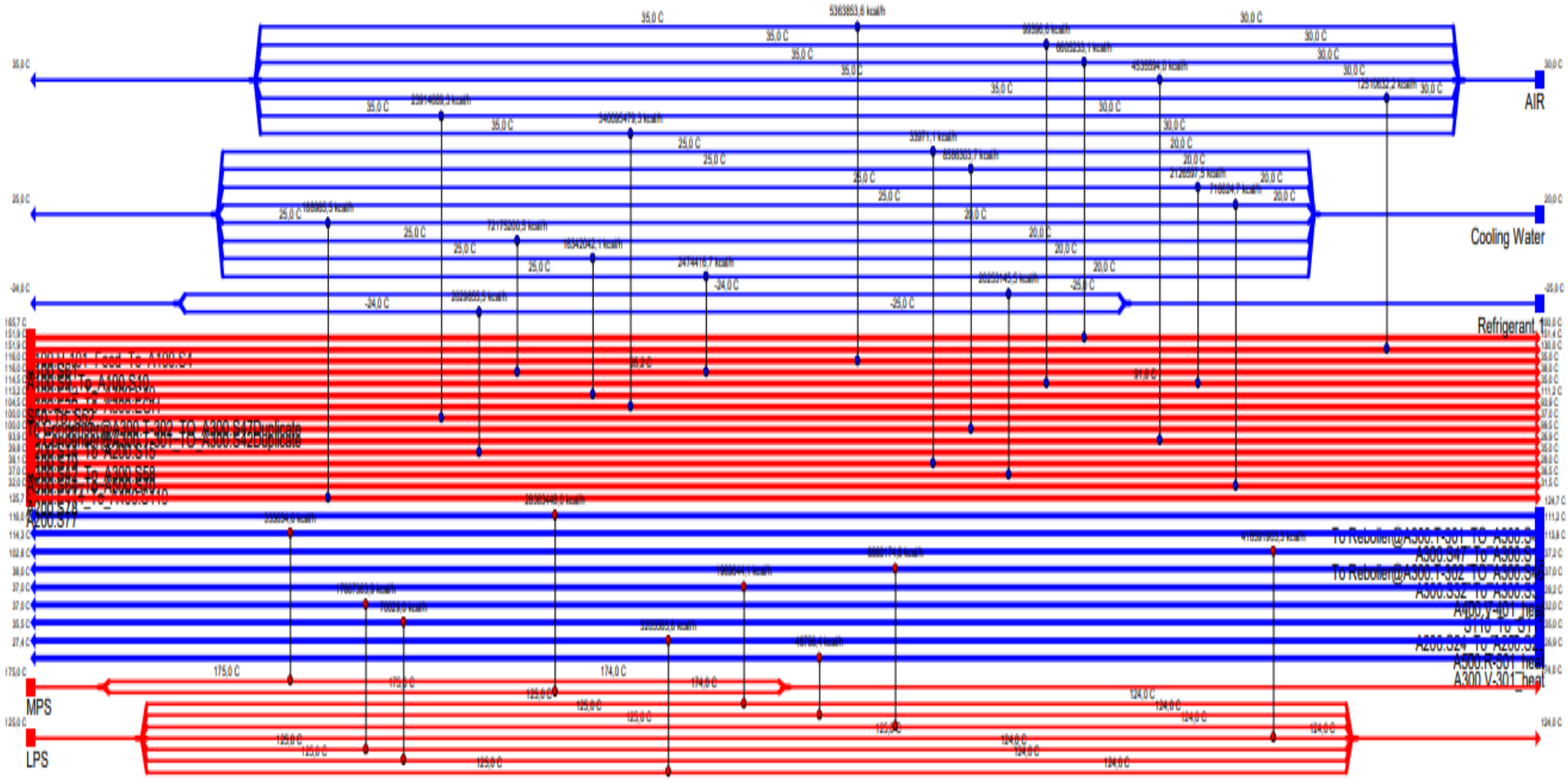

Figure 7-10: HEN for the biochemical method.

Appendix E: Economic Evaluation

E.1 Total Capital Investment Estimation Data

Table A-19: Purchase equipment cost data for furnaces, cooling towers and compressors (Sinnott & Towler, 2013).

Furnace data						
	Units	S_{lower}	S_{upper}	*a*	*b*	*n*
Cylindrical	MW	0.2	60	53000	69000	0.8
Compressor Data						
	Units	S_{lower}	S_{upper}	*a*	*b*	*n*
Centrifugal	Driver power (kW)	132	29000	8400	3100	0.6
Cooling tower Data						
	Units	S_{lower}	S_{upper}	*a*	*b*	*n*
Cooling tower	Flow (litres/s)	100	10000	61000	650	0.9

Table A-20: Heat Exchanger data (Sinnott & Towler, 2013).

Exchanger Type	**K_1**	**K_2**	**K_3**	**C_1**	**C_2**	**C_3**
Floating Head	4.8306	-0.8509	0.3187	0.03881	-0.1127	0.08183
	B_1	**B_2**	**A_{min} (m²)**	**A_{max}(m²)**	**P_{max}(barg)**	
	1.63	1.66	10.0	1000	140	
	K_1	**K_2**	**K_3**	**C_1**	**C_2**	**C_3**
Kettle Reboiler	4.4646	-0.5277	0.3955	0.03881	-0.1127	0.08183
	B_1	**B_2**	**A_{min} (m²)**	**A_{max}(m²)**	**P_{max}(barg)**	
	1.63	1.66	10.0	100	140	

Material Factor	
Material	**FM**
CS Shell/ SS Tube	1.8
CS shell/CS Tube	1.4

E.1.1. Base Purchase Cost

The purchased equipment cost was determined using the following equation (Turton *et al*., 2009):

$$log_{10}C_p^o = K_1 + K_2 log_{10}(A) + K_3[log_{10}(A)]^2 \quad \text{(E.1)}$$

Where K_1, K_2, K_3 = Equipment data

A = Capacity or size parameter for equipment

E.1.2. Bare Module Cost

The bare module cost for all equipment was determined using the following equation (Turton *et al*., 2009):

$$C_{BM} = C_P^o F_{BM} \quad \text{(E.2)}$$

Where C_{BM} = Bare module equipment cost

F_{BM} = Bare module cost factor

C_p° = Purchased cost for base condition

For heat exchangers (shell and tube), compressors, pumps (centrifugal), process vessels the bare module cost equation is expanded to be (Turton *et al*., 2009):

$$C_{BM} = C_P^o F_{BM} = C_P^o (B_1 + B_2 F_M F_P) \quad \text{(E.3)}$$

Where B_1, B_2 = B constants

F_M = Material of construction factor

F_P = Pressure factor

For the distillation column, the bare module cost equation is expanded to be (Turton *et al*., 2009):

$$C_{BM} = C_P^o F_{BM} N F_q \quad \text{(E.4)}$$

Where N = no of trays

For the cooling tower, the bare module cost equation becomes (Turton *et al*., 2009):

$$C_{BM} = C_P^o F_P F_M \quad \text{(E.5)}$$

The cost estimation for the cooling towers, furnaces, and compressors was determined using a slightly different equation obtained from (Sinnott & Towler, 2013) which is given below. This equation is used when not enough data can be accessed for specific equipment.

$$C_e = a + bS^n \quad \text{(E.6)}$$

Where C_e = purchased equipment cost

a, b = cost constants

S = capacity parameter, units depend on the equipment

n = exponent for that type of equipment

E.1.3. Pressure and Material Factors

To determine the pressure factor for most of the equipment the following equation was used:

$$log_{10} F_p = C_1 + C_2 log_{10} P + C_3 (log_{10} P)^2 \quad \text{(E.7)}$$

Where C_1, C_2, C_3 = pressure constants, which were obtained form (Turton *et al*., 2009).

E.1.4. Effect of Capacity

The cost exponent for various equipment, ranges from 0.3 – 0.9, but for most equipment, the cost exponent, n, used is 0.6 (Turton *et al*., 2009).

$$\frac{C_a}{C_b} = \left(\frac{A_a}{A_b}\right)^n \quad \text{(E.8)}$$

Where A_a = Equipment cost for the required

A_b = Equipment cost for the base

C_a = Purchased cost for the required

C_b = Purchased cost for the base

n = Cost exponent

E.1.5. Effect of Time

Using this expression is essential for accuracy as it takes into consideration the changing economic conditions or inflation.

$$C_2 = C_1 \left(\frac{I_2}{I_1}\right) \quad \text{(E.9)}$$

Where C_1 = Purchased cost for base time

C_2 = Purchased cost desired

I_1 = Cost index for base time

I_2 = Cost index for desired time

E.2. Total Module Cost

E.2.1. Grass Roots Cost

Grassroots costs refers to the costs for constructing a completely new plant in undeveloped land. To evaluate this the following equation was used (Turton *et al*., 2009).

$$C_{GR} = C_{TM} + 0.5 \sum_{i=1}^{n} C_{BM,i}^{o} \quad \text{(E.10)}$$

Where n = Total number of equipment

C_{BM}° = Bare module cost for base conditions

E.3. Purchase Equipment Cost Data

E3.1. Purchased equipment cost data and bare module cost results for Heat Exchangers.

Table A-21: Purchased cost for heat exchangers.

HX Name	Type	HX area	Material of Construction	Purchased cost (C_p^o)	Bare Module Cost C^o_{BM}	Bare Module Cost C_{BM}
		m^2		$	R	R
A100.HTL.E-304	Fixed tube	414,32	CS shell/CS Tube	44772,30	3 986 746,57	6 631 657,56
A100.HT.H-311 cold	Fixed tube	2,87	CS shell/CS Tube	16607,46	698 737,94	1 036 040,56
Reboiler@A100.HT.T-320	Kettle	27,38	CS Shell/ SS Tube	33359,61	2 970 504,26	4 275 505,79
Reboiler@A100.HT.T-330	Kettle	61,55	CS Shell/ SS Tube	61173,65	5447203,29	7 967 728,52
A100.HC.Q-R350_Exchanger	Fixed tube	1,26	CS shell/CS Tube	19749,78	508 416,52	714329,02
A100.HC.H-351 cold	Fixed tube	3,38	CS shell/CS Tube	16223,51	753 576,10	1 060 051,29
A100.HT.HX-318A cold	Fixed tube	5,19	CS shell/CS Tube	15545,19	933 569,52	1 123 475,77
A100.HTL.E-301 cold	Fixed tube	447,87	CS shell/CS Tube	46760,22	4 163 760,74	6 926 107,51
Condenser@A100.HC.T-350	U Tube	0,65	CS Shell/ SS Tube	24336,32	421 712,80	614 325,60
Condenser@A100.HT.T-320	U Tube	3,18	CS Shell/ SS Tube	16360,02	1 456 777,09	1 053 650,55
Condenser@A100.HT.T-310	U Tube	1,75	CS Shell/ SS Tube	18217,53	570842,78	804 049,80
Condenser@A100.HT.T-330	U Tube	2,70	CS Shell/ SS Tube	16760,82	680 950,91	996 039,93
A100.HC.HX-381	Fixed tube	0,50	CS shell/CS Tube	27011,26	397 468,65	557 617,76
A100.HT.HTLCOOL	Fixed tube	17,72	CS shell/CS Tube	15889,16	1 414 849,49	1 726 942,78
Reboiler@A100.HT.T-310	Kettle	6,84	CS Shell/ SS Tube	19940,07	1 413 685,85	1 991 220,45
Reboiler@A100.HC.T-350	Kettle	4,34	CS Shell/ SS Tube	19450,57	1 049 192,49	1 528 399,91
A300.CWTOWER.CWHX	Fixed tube	35,43	CS shell/CS Tube	17680,46	1 574 355,16	1 892 130,98
A100.HT.E-310	Fixed tube	9,85	CS shell/CS Tube	15309,10	1 350 781,91	1 823 632,13
A300.AIRCOOL.COOLFAN	Fixed tube	34,03	CS shell/CS Tube	17537,93	1561663,84	1978182,13
A100.HT.HX-320	Fixed tube	8,22	CS shell/CS Tube	15284,74	1 210 011,53	1 635 383,12
A100.HC.H-352	Fixed tube	1,01	CS shell/CS Tube	21050,58	473940,66	665 087,23
A100.HTL.E-306	Fixed tube	51,70	CS shell/CS Tube	19286,96	1 717 406,32	2 245 999,86
A100.HC.HX-380	Fixed tube	0,12	CS shell/CS Tube	54572,22	346 220,04	485 619,86
A100.HC.H-381	Fixed tube	0,87	CS shell/CS Tube	22 066,35	453 787,02	636 473,77
A100.HTL.E-305	Fixed tube	4,45	CS shell/CS Tube	15738,79	861 708,70	1 420 805,18
A100.HT.H-316	Fixed tube	12,40	CS shell/CS Tube	15443,51	1 375 166,49	1 857 898,75
A100.HTL.R301Q-2_Exchanger	Fixed tube	94,87	CS shell/CS Tube	23140,19	2 060 516,27	3 412 351,29

A100.HT.V-315_heat_Exchanger	Fixed tube	10,14	CS shell/CS Tube	15319,68	1 364 139,69	1 641 632,32
A100.HC.V-351_heat_Exchanger	Fixed tube	0,04	CS shell/CS Tube	129425,35	387 452,27	472 918,08
				41605144,9		**59 175 257,53**

E.3.3. Purchased equipment cost data and bare module cost results for reactors

A jacketed non-agitated reactor was assumed to behave like an adiabatic reactor.

Table A-22: Reactor data.

Reactor Type	**K_1**	**K_2**	**K_3**	**V_{min} (m^3)**	**V_{max} (m^3)**	**F_{BM}**
Jacketed Non-Agitated	3.3496	-0.2765	0.0025	5.00	45.00	4

Table A-23: Bare module cost for reactors.

Reactor name	**Volume**	**Purchased cost (C_P^o)**	**Bare Module Cost C_{BM}**
	m^3	$	R
A100.HC.R-350Y	9,96	1191,59	129003,325
A100.HT.R-310Y	98,85	642,60	111549,341
A100.HTL.R-301	110,55	623,73	115790,737
		3291,51	**356343,4**

E.3.4. Purchased equipment cost data and bare module cost results for vessels.

Table A-24: Vertical vessels.

Vertical Vessel					
K_1	**K_2**	**K_3**	**V_{min} (m^3)**	**V_{max} (m^3)**	**P_{max} (barg)**
3.4974	0.4485	0.1074	0.3	520	400
Materials of Construction					
$F_{BM,CS}$	**$F_{BM,SS}$**	**Vessel Type**		**B1**	**B2**
1.0	3.1	**Vertical**		2.25	1.82

Table A-25: Purchased cost for vessels.

Vessel unit tag	**Volume (m^3)**	**Minimum Thickness (t_w) (m)**	**Corrosion allowance ($t_{corrosion}$) (m)**	**Construction Material**	**Purchased cost (C_p°) ($)**	**Pressure factor (F_p)**
A100.HC.T-350	1,10	0.0063	0.004	Carbon Steel	3282,52	1.63
A100.HT.T-310	0,49	0.0063	0.004	Carbon Steel	2335,79	1.63
A100.HT.T-320	1,96	0.0063	0.004	Carbon Steel	4337,22	1.63
A100.HT.T-330	3,06	0.0063	0.004	Carbon Steel	5499,28	1.63

A300.CWTOWER.COOLTOW	152,14	0.0063	0.004	Carbon Steel	97186,69	1.63
					112641,48	

Table A-26: Bare module cost for vessels.

Vessel unit tag	**C_{BM}° (2001) ($)**	**C_{BM}° (2019) ($)**	**C_{BM}° (2019) (R)**	**Bare Module Cost (C_{BM}) 2001 ($)**	**Bare Module Cost (C_{BM}) 2019 ($)**	**Bare Module Cost (C_{BM}) (R)**
A100.HC.T-350	13359,84	24448,17	361588,36	17152,97	31389,50	464250,63
A100.HT.T-310	9506,65	17396,93	257300,58	12205,78	22336,27	330353,43
A100.HT.T-320	17652,48	32303,59	477770,06	22664,37	41475,23	613418,67
A100.HT.T-330	22382,06	40958,61	605777,91	28736,79	52587,60	777770,54
A300.CWTOWER.COOLTOW	395549,81	723846,20	10705685,26	507854,43	929360,82	13745246,46
			12408122,17			**15931039,74**

E.3.5. Purchased equipment cost data and bare module cost results for sieve trays.

Table A-27: Sieve trays F_q.

Tray Type	**K_1**	**K_2**	**K_3**	**A_{min} (m²)**	**A_{max} (m²)**
Sieve Tray	2.9949	0.4465	0.3961	0.07	12.3

Table A-28:Sieve trays F_{BM}.

Material of Construction	**Sieve Tray**
Carbon Steel	1.0
Stainless Steel	1.8

Table A-29: Purchased cost for trays.

Tray unit tag	**Area (m²)**	**Number of trays**	**Construction Material**	**Type of tray**	**Purchased cost (C_p°) ($)**	**Purchased cost (C_p°) applying six-tenths rule ($)**
A100.HC.T-350	0,16	5	Carbon Steel	Sieve	773,52	
A100.HT.T-310	0,07	5	Carbon Steel	Sieve	998,48	
A100.HT.T-320	0,29	5	Carbon Steel	Sieve	740,28	
A100.HT.T-330	0,46	5	Carbon Steel	Sieve	773,86	
A300.CWTOWER.COOLTOW	27,73	3	Carbon Steel	Sieve	29102,40	142196,27
						145482,41

Table A-30: Bare module cost for trays.

Tray unit tag	**F_q (m)**	**F_{BM}**	**Bare Module Cost (C_{BM}) 2001 ($)**	**Bare Module Cost (C_{BM}) 2019 ($)**	**Bare Module Cost (C_{BM}) (R)**
A100.HC.T-350	1	1.0	773,52	1415,52	20935,49
A100.HT.T-310	1	1.0	998,48	1827,20	27024,28
A100.HT.T-320	1	1.0	740,28	1354,69	20035,89
A100.HT.T-330	1	1.0	773,86	1416,15	20944,83
A300.CWTOWER.COOLTOW	1	1.0	142196,27	260215,60	3848588,67
					3937529,16

E.3.6. Purchased equipment cost data and bare module cost results for storage tanks.

Table A-31: Storage tanks.

Tank Type	**K_1**	**K_2**	**K_3**	**B_1**	**B_2**	**V_{min} (m³/s)**	**V_{max} (m³/s)**
Fixed Roof	4.8509	-0.3973	0.1445	1.10	0	90	30000

Table A-32: Purchased cost for storage tanks.

Storage Tank unit tag	**Volume (m³)**	**Material Construction**	**Number of tanks**	**Minimum Thickness (t_w) (m)**	**Corrosion allowance ($t_{corrosion}$) (m)**	**Purchased cost (C_p°) ($)**
100FEED	110	Stainless Steel	165	0.0063	0.004	438558,20
Biodiesel	110	Stainless Steel	31	0.0063	0.004	438558,20
Naphtha	110	Stainless Steel	36	0.0063	0.004	438558,20
						1315674,61

Table A7-33: Purchased cost for storage tanks.

Storage tank unit tag	**Pressure factor (F_p)**	**F_{BM}**	**F_{BM}°**	**C_{BM}° (2001) ($)**	**C_{BM}° (2019) ($)**	**Bare Module Cost (C_{BM}) (R)**
100FEED	1.63	1.1	1.10	482414,0225	882805,5096	13056693,49
Biodiesel	1.63	1.1	1.10	482414,0225	882805,5096	13056693,49
Naphtha	1.63	1.1	1.10	482414,0225	882805,5096	13056693,49
					2648416,529	**39170080,46**

E.4. Exchange rate and Chemical Engineering Plant Cost Index results

Table A-34: Exchange rate and CEPCI for 2022.

CEPCI 2019	
2001	397

2020	596,2
May-22	686,7
Jun-22	701,4
Jul-22	720,2
Aug-22	735,2
Sep-22	754
Oct-22	761,5
Average	726,5
Exchange rate (R/$) for the past 12 months	
Low	13,42
High	16,28
Midpoint	14,79

E.5. Total Other Direct Costs Heuristics

E.5.1. Instrumentation and controls

The cost of instrumentation and controls refers to both instrumentations and all the auxiliaries in the whole plant. Since the plant has extensive controls, the cost was estimated to be 30 % of the purchased equipment cost (Kolmetz & Sari, 2014).

E.5.2. Insulation

Insulation costs are necessary for plants with high temperatures. The cost estimation is usually 8 % of the purchased equipment cost. The estimation includes the cost for the labour and materials required for insulating equipment and piping (Kolmetz & Sari, 2014). The cost was assumed to be 8 % of the purchase equipment cost, as this is a new plant it will be more demanding.

E.5.3. Electrical Installation

Electrical installation costs for a plant include costs for power wiring, transformation and service, lightning, and instrument and control wiring. The costs are normally 10 to 15% of the purchase equipment (Kolmetz & Sari, 2014). Since this is a new plant, the cost was estimated to be 12 % of the purchased equipment cost.

E.5.4. Buildings

All buildings in the plant will have to be built from the ground up, as it will be a new plant. The costs for this are estimated to be 45 % of the purchased equipment cost (Kolmetz & Sari, 2014), for plants that primarily process fluids.

E.5.5. Yard Improvement

Yard improvement costs refers to the costs for the construction for fencing, grading, roads, landscaping, sidewalks, and railway sidings. This cost is usually between 10 to 20 % of the purchased equipment cost (Kolmetz & Sari, 2014). For this process, the cost was estimated to be 15 % of the purchased cost.

E.5.6. Service facilities

Service facilities refers to utilities for supplying power, water, steam, compressed air, and fuel. It also includes fire protection, waste disposal, and miscellaneous service items (Kolmetz & Sari, 2014).. The services cost was assumed to be 75% of the purchased equipment costs as these are completely new facilities.

E.5.7. Equipment Installation

Equipment installation involves the cost of installing foundations, platforms and supports, and erection of equipment. It also considers the cost of labour and material required for installation. The estimation is usually about 43 % of the purchased equipment cost (Kolmetz & Sari, 2014). For this process, the cost of equipment installation was assumed to be 43 % of the purchased equipment cost.

E.5.8. Piping

Pipe costing involves labour, fittings, valves, pipe, supports etc. The estimation for a fluid-based process is normally 66 % of the purchased equipment value (Kolmetz & Sari, 2014).

E.5.9. Land

The cost of land was found during site selection, in the previous chapter.

E.6. Total Indirect Cost Heuristics

E.6.1. Engineering and supervision

This refers to the costs of detailed design, construction and cost engineering drafting etc. Typically, this cost is about 30 % of the purchased equipment cost (Kolmetz & Sari, 2014). For this process, the cost was assumed to be 30 % of the purchased equipment cost.

E.6.2. Construction expense

Construction expenses consists of temporary construction and operating, home office personnel located at the construction site, travel and living, taxes and insurance, construction payroll, and other construction overhead (Kolmetz & Sari, 2014). Usually, the cost ranges from 8 to 10 % of the direct cost. The costs were assumed to be 10 % of the direct cost, which is a reasonable assumption for an average chemical plant.

E.6.3. Contractor’s fee

The contractor’s fees are added to the total capital cost and usually range from 2 to 8 % of the direct costs (Sinnott, 2005).These fees depend on the complexity, location and the size of the plant (Kolmetz & Sari, 2014). A suitable percentage for this process was chosen to be 6 % due to the size of the plant.

E.6.4. Contingency allowance

Contingency allowance accounts for unforeseen circumstances the plant might face such as, labour disputes, design errors, and adverse weather (Sinnott, 2005). Generally, this ranges from 10 to 25 % of

the direct costs (Kolmetz & Sari, 2014). For this process, 25 % was chosen as a suitable percentage for a detailed process such as this.

E.7. Total Manufacturing Costs

Once the cost of raw materials, utilities, waste treatment and operating labour as well as the fixed capital cost were determined, it was possible to calculate the total cost of manufacturing (COM) with the use of the following equation:

$$COM = 0.280FCI + 2.73C_{OL} + 1.23(C_{UT} + C_{WT} + C_{RM}) \quad \text{(E.11)}$$

Where COM = Total manufacturing cost
FCI = Fixed capital investment (R/year)
C_{OL} = Operating labour cost (R/year)
C_{UT} = Cost of utilities (R/year)
C_{WT} = Cost of waste treatment (R/year)
C_{RM} = Cost of raw materials (R/year)

However, if the value of the depreciation was unknown then the following equation could be utilised:

$$COM_d = 0.180FCI + 2.73C_{OL} + 1.23(C_{UT} + C_{WT} + C_{RM}) \quad \text{(E.12)}$$

Where COM_d = Total manufacturing cost without depreciation (R/year)

E.7.1. Cost of Operating Labour

The cost of operating labour refers to the cost involved in paying the employees directly involved in the manufacturing of the desired work. These employees include the plant workers responsible for the handling of plant equipment.

In the calculation of the cost of operating labour, the number of operators required per single shift was initially calculated using the following equation:

$$N_{OL} = \left(6.29 + 31.7P^2 + 0.23N_{np}\right)^{0.5} \quad \text{(E.13)}$$

Where N_{OL} = Number of operators required per single shift
P = Number of particulate processes
N_{np} = Number of non-particulate processes

The numbers of particulate and non-particulate processes present in the plant are tabulated below:

Table A-35: Number of particulate and non-particulate processes.

Data required to calculate the number of operators per single shift	
Number of particulate processes (P)	0
Number of non-particulate processes (N_{np})	28

It should be noted that this method can be used to estimate the number of operators required for a single shift because the number of non-particulate processes is greater than the particulate processes present in the plant (Turton *et al*., 2009).

After substituting in the values for P and N_{np}, Equation E.13 becomes:

$N_{OL} = \left(6.29 + 31.7(0)^2 + 0.23(28)\right)^{0.5} = 3.57$

After the calculation of the number of operators required per single shift was completed, the number of operators required for all shifts per year could be determined. Since there are multiple working shifts i.e. day shift and night shift, more than one operator will be hired to perform the same job however during different shifts of the day.

Before the calculation could be performed, it was necessary to collect information regarding the average working times of a chemical plant operator. Table A-36 below provides this information.

Table A-36: Average working times of a chemical plant operator and the operation times.

Data regarding the working times of the operators and operation times of the plant	
Average weeks worked by a single operator	49
Shifts per week	5
Shifts per day	2
Chemical Plant operating hours (hours/day)	24
Days plant is in operation per year	343

With the use of the information in Table 8.36 above, the number of operators required for all shifts per year was calculated.

Number of shifts per an operator per year = $49\frac{weeks}{operator} x\ 5\frac{shifts}{week} = 245\frac{shifts}{operator}$

Total number of shifts per year = $2\frac{shifts}{day}\ x\ 343\frac{days}{year} = 686\frac{shifts}{year}$

Number of operators required for all the shifts per year = $686\frac{shifts}{year}\ \div 245\frac{shifts}{operator}$

Number of operators required for all the shifts per year = 2.8 operators/year

Now the operating labour could be calculated by multiplying the number of operators required per a single shift and the number of operators required for all the shifts per year.

Therefore, operating labour = 2.8 x 3.57 = 9.99 ≈ 10.

Lastly, the cost of operating labour was determined using the average hourly chemical plant operator rate, which is currently R52.82 (Payscale, 2019), in unison with the operating labour. Both values were

multiplied to obtain the value of the cost of operating labour. Table A-37 below gives a summary of the average hourly rate and the yearly salary of a chemical plant operator.

Table A-37: Summary of average hourly rate and yearly salary of an operator.

Data regarding the average hourly rate of a chemical plant working	
Average hourly chemical plant operator rate (R/hour)	52.82
Average yearly chemical plant operator salary (R/year)	434 814.24

Cost of operating labour = (Operating labour) (Average yearly salary)

Cost of operating labour = (10) (R 434 814.24)

The cost of operating labour was calculated to be R4 348 142.40 per year.

E.8. Cost of Raw Materials

Tables 8-38 and 8-39 below provide this information. The required quantity for each raw material was collected from Aspen Plus.

Table A-38: Cost prices of all species contributing to the cost of raw material.

Species	**Cost Prices of Pure Chemicals in 2019 ($/kg)**	**Cost Prices of Pure Chemicals in 2019 (R/kg)**
Microalgae (2022)	0,58	8,5
Biodiesel	3,56	60,5
Naphtha	18,07	267,3
Activated Carbon	2,7	39,9
Cost of electricity	0,15	2,2
AD digestate cake	0,50	7,4
CO2 gas	0,03	0,5
Steam	0,023017376	0,3

Table A-39: Cost of raw material.

Raw materials	**Quantity Used (kg/hr)**	**Quantity used (kg/year)**	**Cost of raw material (R/year)**
Microalgae (2022)	75428,19	620924889,6	R5 280 500 492,61
Total Raw Material Cost	-	-	R5 280 500 492,61

Revenue sample calculation

All input and output stream flowrates were multiplied with the cost of materials.

Biodiesel cost:

Quantity used = 4 939,12 kg/hr = 40 658 803,54 kg/yr

Cost price of biodiesel = R60,50/kg

Biodiesel cost = Quantity used (kg/yr) * Cost price of biodiesel (R/kg) = R2 461 445 878,79

All input and output streams followed the same calculation.

E.9. Cost of Wastewater Treatment

To calculate the wastewater treatment cost it was necessary to determine the average cost of treating wastewater. From research, the wastewater treatment cost was found to be $0.006/gal however when converted to R/m³, it becomes R 23,44/m³.

The quantity of wastewater produced from the plant was then obtained from Aspen Plus and tabulated in Table A-40 below.

Table A-40: Quantity of wastewater produced.

Volumetric flowrate of wastewater in the plant	
Wastewater production rate (m³/h)	324,33
Wastewater production rate (m³/year)	2669847,44

Now the cost of wastewater treatment could be calculated by multiplying the volumetric flowrate of wastewater produced per year with the cost of treating wastewater. The cost of wastewater treatment was calculated to be R 62 588 269,76.

E.10. Profitability Analysis

Table A-41: Discounted cash flow 1 of 2.

			Finished Constrution						
	0	1	2	3	4	5	6	7	8
Investment (Cost)	R 22 772 482	R 2 344 388 111	R 473 432 118		R 0	R 0	R 0	R 0	R 0
Revenue				R 8 000 039 881	R 8 000 039 881	R 8 000 039 881	R 8 000 039 881	R 8 000 039 881	R 8 000 039 881
Cost of Sales				R 6 635 796 393	R 6 635 796 393	R 6 635 796 393	R 6 635 796 393	R 6 635 796 393	R 6 635 796 393
Depreciation				R 1 518 165	R 1 518 165	R 1 518 165	R 1 518 165	R 1 518 165	R 1 518 165
Profit before tax				R 1 362 725 322	R 1 362 725 322	R 1 362 725 322	R 1 362 725 322	R 1 362 725 322	R 1 362 725 322
Tax				R 381 563 090	R 381 563 090	R 381 563 090	R 381 563 090	R 381 563 090	R 381 563 090
PAT+Depr				R 982 680 398	R 982 680 398	R 982 680 398	R 982 680 398	R 982 680 398	R 982 680 398
Cash Flow (Future value)	-R 22 772 482	-R 2 344 388 111	-R 473 432 118	R 982 680 398	R 982 680 398	R 982 680 398	R 982 680 398	R 982 680 398	R 982 680 398
Discount Factor (1/((1+i)^n))	1,0000	0,8511	0,7243	0,6164	0,5246	0,4465	0,3800	0,3234	0,2752
Discounted Cash Flows	-R 22 772 481,82	-R 1 995 223 923,86	-R 342 911 448,42	R 605 757 350,92	R 515 538 171,00	R 438 755 890,21	R 373 409 268,26	R 317 795 121,93	R 270 463 933,55
Cumulative discounted CF	-R 22 772 482	-R 2 017 996 406	-R 2 360 907 854	-R 1 755 150 503	-R 1 239 612 332	-R 800 856 442	-R 427 447 174	-R 109 652 052	R 160 811 882

Table A-42: Discounted cash flow 2 of 2.

	9	10	11	12	13	14	15	16	17
Investment (Cost)	R 0	R 0	R 0	R 0	R 0	R 0	R 0	R 0	R 0
Revenue	R 8 000 039 881	R 8 000 039 881	R 8 000 039 881	R 8 000 039 881	R 8 000 039 881	R 8 000 039 881	R 8 000 039 881	R 8 000 039 881	R 8 000 039 881
Cost of Sales	R 6 635 796 393	R 6 635 796 393	R 6 635 796 393	R 6 635 796 393	R 6 635 796 393	R 6 635 796 393	R 6 635 796 393	R 6 635 796 393	R 6 635 796 393
Depreciation	R 1 518 165	R 1 518 165	R 1 518 165	R 1 518 165	R 1 518 165	R 1 518 165	R 1 518 165	R 1 518 165	R 1 518 165
Profit before tax	R 1 362 725 322	R 1 362 725 322	R 1 362 725 322	R 1 362 725 322	R 1 362 725 322	R 1 362 725 322	R 1 362 725 322	R 1 362 725 322	R 1 362 725 322
Tax	R 381 563 090	R 381 563 090	R 381 563 090	R 381 563 090	R 381 563 090	R 381 563 090	R 381 563 090	R 381 563 090	R 381 563 090
PAT+Depr	R 982 680 398	R 982 680 398	R 982 680 398	R 982 680 398	R 982 680 398	R 982 680 398	R 982 680 398	R 982 680 398	R 982 680 398
Cash Flow (Future value)	R 982 680 398	R 982 680 398	R 982 680 398	R 982 680 398	R 982 680 398	R 982 680 398	R 982 680 398	R 982 680 398	R 982 680 398
Discount Factor (1/((1+i)^n))	0,2342	0,1994	0,1697	0,1444	0,1229	0,1046	0,0890	0,0758	0,0645
Discounted Cash Flows	R 230 182 071,11	R 195 899 634,99	R 166 723 093,61	R 141 891 994,56	R 120 759 144,31	R 102 773 739,83	R 87 467 012,62	R 74 440 010,74	R 63 353 200,63
Cumulative discounted CF	R 390 993 953	R 586 893 588	R 753 616 681	R 895 508 676	R 1 016 267 820	R 1 119 041 560	R 1 206 508 573	R 1 280 948 584	R 1 344 301 784

Appendix F: Life Cycle Assessment

Supply chain of the thermochemical conversion

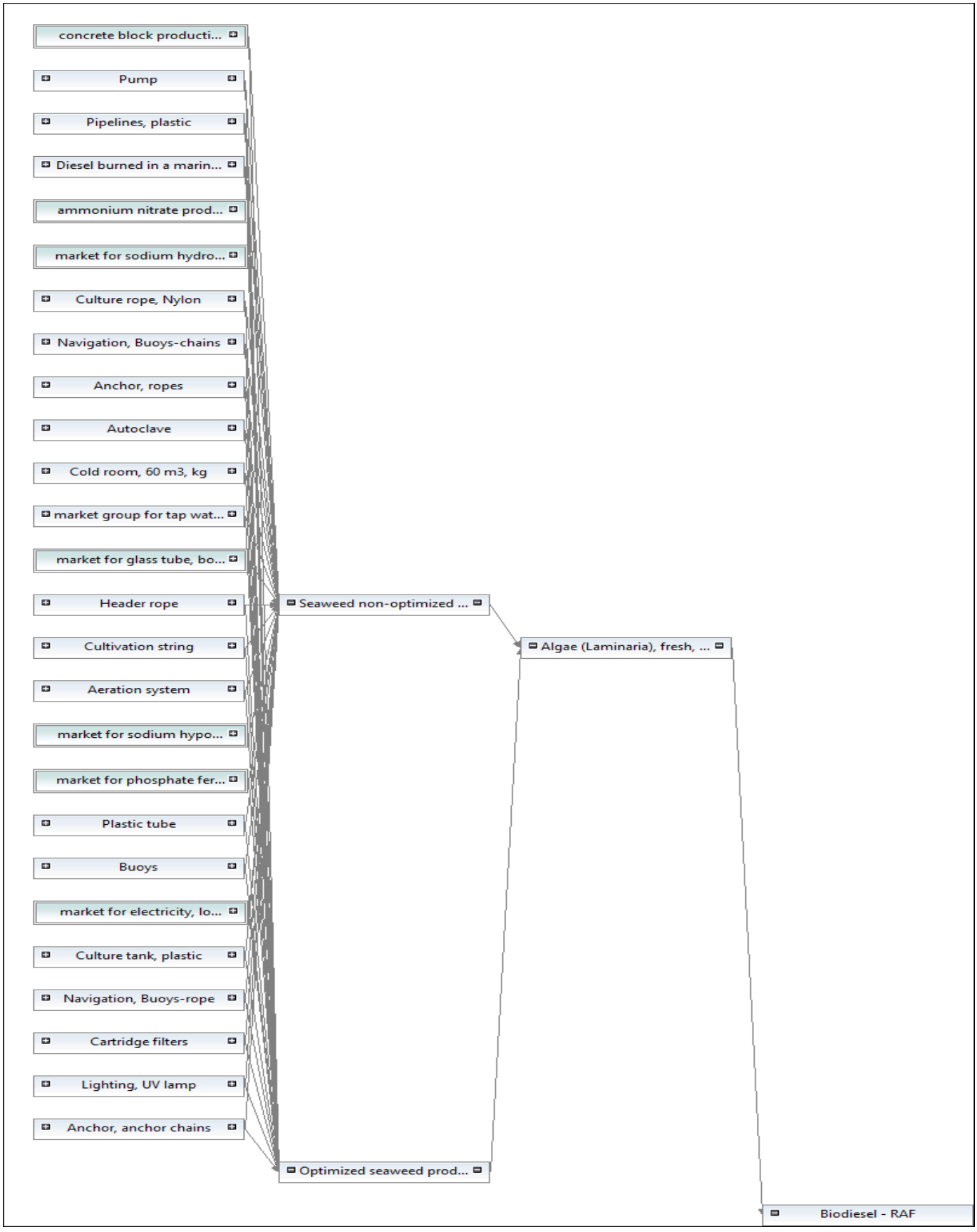

Figure 7-11: Supply chain for the thermochemical conversion method.

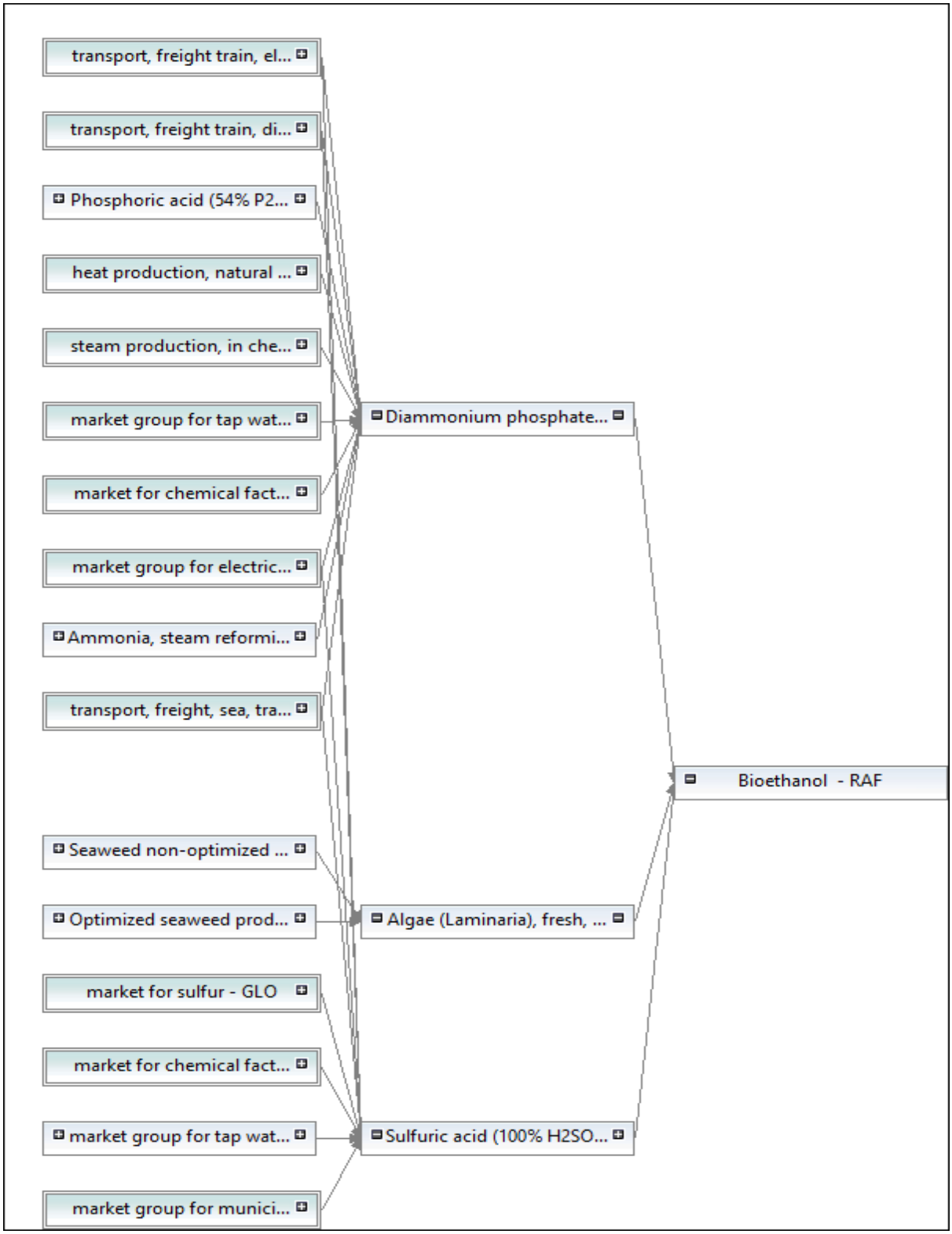

Figure 7-12: Supply chain for the biochemical conversion method.